The discovery and biological mechanisms of a widespread phenazine's oxidation

Thesis by

Lev Maximovich Tsypin

In Partial Fulfillment of the Requirements for the Degree of

Doctor of Philosophy

CALIFORNIA INSTITUTE OF TECHNOLOGY

Pasadena, California

2023

(Defended January 5th, 2023)

Lev Maximovich Tsypin
ORCID: 0000-0002-0642-8468

To my grandparents and great-grandparents.

ACKNOWLEDGEMENTS

I have been thinking about these acknowledgements since way before my thesis was near completion. In fact, I probably started composing them when I was not sure that my dissertation would ever *be* completed. I do not think that "acknowledgement" is quite apt to express what I wish to the people I appreciate and love, so I will return to them in the next section, Gratitudes. Here, though, I do have a few *things* to acknowledge.

I did this work during a time that felt unrelenting. As I came into my own as an adult and a scientist, so seemed to mature the newest manifestations of fascism, racism, and mass misinformation. When the COVID-19 pandemic struck, I felt undone: I could not bear the uncertainty of research compounded with the uncertainty of the world. And, as I looked to institutions around me, ones that I had respected—and perhaps, deep down, revered—I saw them fail me and my dearest people, many of whom I address in the next section. And I learned what has been said by others before, that institutions will not, *cannot*, love you back. Since then, I have been carrying a tension with me: what does it mean when I do not trust an institution but love the people who constitute it?

I found a way back out of the dark pits that I had been in, and I found a way to regain myself, my interests, and even my joy. I know that a lot of people call this kind of overcoming resiliency, and a lot of messaging within the University focuses on cultivating resilience, but I loathe this usage of the term. To praise someone for being resilient feels like an invocation of survivorship bias. Is resiliency really something that can be learned, or do we just define the people who survive as resilient? The way I see it, actual resiliency is having access to the resources we need, recognizing that we have access to them, and exercising that access. At every step, there is an opportunity for others to help or hinder us. And, while it is true that we can learn about these resources or get better at recognizing when we need them, it is ultimately the people and systems around us that determine the outcome.

The focus on resiliency as a personal quality frustrates me because it casts those who left Caltech/academia as failures. But this is not the case: getting out for the sake of your wellbeing is also resiliency. I am proud that I was able to complete to my dissertation despite managing acute mental and physical illness at various points during my graduate studies, but I do not want any reader of this dissertation to see my completion of my thesis as a favorable reflection of my personality. It is not a metric to use against the personalities of those who did not complete theirs.

Instead, I want to invite you to join me in my appreciation of the people who helped me do what I wanted to do as I address them in the next section.

GRATITUDES

I always worry that I have not thanked people enough or have forgotten someone I should thank. For the sake of keeping this section manageable, I will address the people who I feel contributed directly to my thesis and PhD experience. I am sure that I will fail to remember someone because my thesis has been shaped by so many people: I might not have recognized when someone helped me or perhaps thought that something was a matter of happenstance, when it was in fact a deliberate act. If you find that I missed something or someone in this section, please let me know, and I will reach out to thank you and them directly.

* * *

Aaron Turkewitz, I trace every thread of myself as a biologist (at least every thread of which I am proud) to what I learned from you and from working in your lab. Joining your group was one of the greatest strokes of serendipity in my life. Thank you for taking me on. Thank you for reminding me to enjoy pastries and gelato. Thank you for encouraging my exploration of challah recipes. Thank you for supporting me through my leave of absence during graduate school. Thank you for teaching me my scientific sense. There are few things that would make me as happy as some future student thinking of me as I think of you.

* * *

Dianne Newman, thank you for being so attuned to my needs and interests. I came to Caltech bubbling over with ideas and self-assuredness, and I appreciate how you helped me find a path to develop my work and self-conception as a scientist. You are a wonderful mentor for me. And, whenever I reached a peak of distress, you were able to hear me and attend to my vision for what a healthier life would be. I also deeply appreciate your hearing me when I expressed that I simply cannot do more experiments. For this, and for many other things, I'll always be grateful.

John Ciemniecki, thank you for sharing this stage of our careers with me, both inside the lab and out. I always think fondly about how we got to know each other during our grad school interview tour, meeting on different campuses to continue our conversation about life and science. I feel that conversation is still ongoing, and I hope that it stays with us. Your friendship has made my time here easier and better.

Elise Tookmanian, you were one of the first people in the lab I felt I could talk to about my struggles. Thank you. Thank you also for starting our antiracism discussion group with me.

Kyle Costa, thank you for taking me on as a rotation student in the Newman lab. You helped me have a smooth entry into graduate research. Being able to start with a sense of competency and security shaped the rest of my time at Caltech very positively.

Scott Saunders, your advice for how to pursue my project always proved correct. I appreciate that I could always rely on your instincts and experience no matter how off course I felt my experiments took me. Thank you for your work at the inception of what was to become my thesis project. Thank you for sharing the tools that you have developed.

Elena Perry, I have tried to emulate you and your work probably more than you realize, from your clarity of thinking to your style of presentation. Thank you for giving me this guidance.

Georgia Squyres, when I think about what I want to bring to my next lab as a postdoc, I think of what you have brought to the Newman lab. I so appreciate the care with which you help the people around you, and I hope that I can invoke the same kind of rigor and enjoyment for the work that I have felt coming from you.

Darcy McRose, in helping me with some of my writing and applications, you have helped me more than you might know. By pushing me to think and write with an intentional positivity, you helped me exercise skills that atrophied during the pandemic. It was a real turning point for me, and it enabled me to take the next step in regaining my mental health. Thank you.

Steven Wilbert, I always look up to how you cultivate your talents. Over the years, your research, cooking, and plant care have helped me remember to try to foster my interests. Even when I was depressed, I was able to vicariously enjoy and appreciate things through you. Thank you.

Chelsey VanDrisse, you have always helped me keep my priorities straight, be it in the work or outside of it. Thank you.

Rei Alcalde, I hope that I will learn to advocate for change and improvement as effectively as you do. I really appreciate the depth of your thinking about community engagement.

Avi Flamholz, thank you for your generosity. You have always welcomed me, both scientifically and personally, and this has really helped me. I really appreciate the time, advice, and tools that you have given me.

Shannon Park, the Newman lab would not run without you. Thank you for your time and care in answering my questions and helping all of us lab members.

Kristy Nguyen, thank you for everything you do behind the scenes. CEMI is a wonderful program, and one of the reasons why I chose to come to Caltech. Your work has really enriched my time here.

Kurt Dahlstrom, I am so grateful for your company: your way of thinking is invigorating, and our conversations have helped me mature in my worldview.

Melanie Spero, you were one of the people who really helped me learn which experimental details to stress over and which to not. You helped me loosen my grip when I was clenching too tightly, and that allowed me to move forward. Thank you.

Daniel Dar, you provided me with an important example of someone who can roll with the punches of academic work while providing a happy childhood for their kids. As someone who wants children, I will carry these memories with me, and I thank you for them.

Lucas Meirelles, in addition to your generosity in helping me in the lab, you helped hone my aesthetic sense. I (and everyone who likes my figures and slides) thank you.

Megan Bergkessel, I learned so much just from listening in on your conversations with other lab members, not to mention through our own discussions. Thank you for your insights and care.

Brittany Belin, I deeply appreciate your feedback on my writing, your insights into the inner workings of academic organizations, and your scientific sense. Talking with you has helped me clarify what I would and would not put up with in my career, and I think that is one of the most important things that I can realize.

Will DePas, I still have the "Microbiology" banner you taped to my bench one day, and I have passed it on to someone else in the lab. This little thing made a lot of moments at the bench easier. Thank you.

Yinon Bar-On, you set the seed that allowed my dissertation to crystallize around it. Thank you.

* * *

Citrobacter portucalensis MBL, I don't think I could have dreamt up a more amenable environmental isolate to work with. Thank you.

* * *

To my thesis advisory committee: thank you all for your understanding and for helping me navigate my leave of absence. It was absolutely crucial. Thank you also for your constant support for and curiosity in my work.

Justin Bois, thank you for your teaching. Your instructional program was the tipping point in my choice to come to Caltech. I appreciate the classes of yours that I have taken and those that I have TAed for.

Victoria Orphan, I deeply appreciate the atmosphere you create in our conversations, and your work always sparks my imagination. I aspire to learn some of your intellectual daring. Thank you for making more of biology possible to study.

Joe Parker, I feel that we share the same sense for the sublime in biology. Thank you for taking me on as one of your first rotation students and for always making the time when I wanted or needed to talk with you.

Jared Leadbetter, I leave each of our conversations with a deep gratitude for your depth (and breadth) of knowledge and care. I hope that I am able to share even a fraction of your insight with my future students and trainees.

* * *

Liz Ayala, Raina Beeven, and Lauren Breeyear: You are the pillars on which our Division rests. Thank you for all your wisdom and advice over the years. Thank you for planning and organizing the events that bring people together.

* * *

Aditi Narayanan, talking with you over the years has helped me mold my humanistic priorities and values. It has always been a great comfort to know that we find the same things missing or wrong at Caltech—that I am not insane. You helped me not gaslight myself. Thank you for being here.

Julian Wagner, I am so grateful for the time we have spent together. Many of our conversations feel special in that they do not stop at the point of mutual understanding: we hear each other's feelings, opinions, and beliefs and then take steps to understand something new about the world. Thank you.

Tom Naragon, I often catch myself yearning to be more like you. Thank you for showing me ways in which I can be more curious, more engaged, goofier, broader in my interests. I hope that I can provide people the same sort of comfort that you have provided me.

David Miller, you often gave me a feeling of clarity—that it is actually possible to know what I want out of life and, moreover, to pursue it without compunction. Thank you.

Prashant Bhat, through our friendship and your example, I have learned a lot about how to right wrongs and improve relationships with grace. Thank you for your camaraderie.

Hannah Weller, it was so wonderful to have our friendship deepen during the pandemic. Perhaps you do not realize all of them, but you have thrown me many lifelines over the years. Back at UChicago, it was thanks to you that I took Stefano Allesina's class (thank you, Stefano), which directly led to me being accepted to PhD programs. During the pandemic, you first reminded me how to learn mindfulness, which helped me through some forms of darkness, and then invited me to play ttRPGs with your friends (now also my friends), which helped me through other forms of it. I will be forever grateful to you for this and more.

David Rokhinson, every so often, I remember how unusual it is that we have been talking on the phone (sometimes several times a week) since we were eight years old, but it feels so natural that I often forget how special it is. I hope you know how much I appreciate you and our friendship. Thank you for always being there to remind me that I should consider cheering up.

* * *

Fayth Tan and Krystal Vasquez, thank you for undertaking difficult work with me. We somehow managed to write a hell of a report on Caltech's COVID-19 response, get the Graduate Student Council and other campus organizations on board, and spur positive changes in institutional policies. It came at a very high personal cost, and I am forever grateful for your advocacy and activism in this effort and all the others that you pursue. You helped me form a core belief that I am empowered to make academic environments better.

Sarah Sam, your work to improve the campus environment at Caltech has dramatically affected me. Thank you for showing me and others what we can achieve and how.

Jessica Foss, being able to talk regularly and openly with you about my experiences during graduate school, both in my personal life and in my work and advocacy, has been critical for my ability to cultivate my mental health (and to begin to regain it whenever it had fallen apart). Thank you for listening and for your advice.

* * *

To my parents: I am endlessly grateful for the life that you provided me. Your emigration from Russia in 2000 was courageous and painful. It is easy for me to see it as simply positive, but I know that it was not. I am proud that I have been able to lead my life in a way that often reflects your hopes and values, and I appreciate that you trust me enough to understand and be proud of me when I lead my life in a way that is different from how you imagined it might be. Thank you for supporting me in my interests, sometimes before I even realized I had them. I also always appreciate being able to ask you for scientific advice: you have helped me countless times with my questions in biology, chemistry, math, and physics from grade school until now, and I recognize how special that is.

Ilya, there is nothing quite like an older brother, and some of the most important decisions that I have made have been to follow in your footsteps. At many junctures in my life, I have turned to you for your advice, experience, and help, and I will continue to do so. Thank you.

Nelli, Feliks, and Donna, the uncertainty of graduate research is unmooring, and moving to a new city, away from friends and family, is isolating. Thank you for welcoming me so fully into your home and for always reaching out to help when I was unwell. Even the small things made all the difference.

Willow and Wilbur, you are rapscallions who have done nothing but be cute, fuzzy, rude, and a great comfort. You are my most beloved kittens. Thank you.

Yana, you do the impossible: how can it be that a single person embodies all that I wrote above and more? And yet, all those facets of gratitude, all the ineffable cores of my feeling, are rightfully directed to you. I love you. And I cannot wait for our wedding.

BRIEF ABSTRACT

During the 2017 Microbial Diversity course at the Marine Biological Laboratory in Woods Hole, MA, Scott Saunders and Yinon Bar-On started enrichment cultures in hopes of discovering biological oxidation of phenazine-1-carboxylic acid (PCA). I took these enrichment cultures and described their PCA oxidation activity. From one of the mixed cultures, I isolated a bacterial strain that recapitulated the behavior of the enrichment. I identified it as a strain of *Citrobacter portucalensis* via a whole-genome analysis and called the strain "MBL" in reference to the Marine Biological Laboratory. Using a combination of analytical chemistry, quantitative fluorescence measurements, and genetic engineering, I showed that *C. portucalensis* MBL couples PCA oxidation to each mode of anaerobic respiration it employs with nitrate, fumarate, dimethyl sulfoxide (DMSO), and trimethylamine-N-oxide (TMAO) as terminal electron acceptors (TEAs). I further found that most of the PCA oxidation activity depends on electron flux through the quinone/quinol pool but can be driven by certain terminal reductase complexes when no quinones are available, particularly in the case of nitrate reductases. Every bacterial strain I tested catalyzed PCA oxidation when provided the appropriate TEA. My described mechanism for bacterial PCA oxidation is generalizable and implies that this previously undocumented phenomenon should occur wherever PCA is produced in rhizosphere environments.

NARRATIVE ABSTRACT

Laboratory conditions are optimized to grow bacteria fast to maximize cell density, protein production, and nucleic acid yields, or else just to save researchers' time. In nature, however, bacteria experience stresses that limit their growth, such as starvation due to environmental constraints and competition. Thus, the predominant mode of bacterial growth in the environment is slow, and the usual lab approaches to microbiology do not lend themselves to studying bacteria in an environmentally relevant way. An underlying aim of my PhD was to take a step toward resolving this discrepancy.

When starving, bacteria are forced to glean energy from metabolic scraps—biochemical reactions that are at once efficient and measured so that the cells do not outgrow their means. One such metabolism involves phenazines: small, secreted metabolites used by microbes in myriad ways. Depending on the context, phenazines regulate gene expression, act as antibiotics, or promote survival under starvation. All these functions are made possible by the phenazines' ability to accept electrons from cells (phenazines being reduced): for example, phenazines can substitute for oxygen under anoxic conditions. These functions have been extensively studied, but, prior to my dissertation, the counterpart role of phenazines donating electrons to cells (phenazines being oxidized) was overlooked. Consequently, little was known about what happens to phenazines once they are reduced by cells and what ramifications this may have for other members of the microbial community.

Members of the Newman lab hypothesized that phenazine oxidation should occur in soils during anaerobic respiration: oxygen abiotically oxidizes phenazines, but soils become anoxic at shallow depths and contain various alternative compounds that microbes can respire. In my PhD thesis, I was able to enrich for and isolate a soil bacterium that oxidizes phenazine-1-carboxylic acid (PCA). PCA is the most commonly produced phenazine in nature, and this was the first observation of its biological oxidation. I then sequenced, assembled, and annotated the isolate's genome, identified it as a strain of *Citrobacter portucalensis* (first discovered in 2017), and developed protocols for studying its physiology. Intriguingly, although *C. portucalensis* readily oxidizes PCA, it does not have the genes to synthesize it, implying a role in cross-species metabolite interactions. I discovered that *C. portucalensis* is not unique: *Escherichia coli*, *Pseudogulbenkiania* sp., *Pseudomonas aeruginosa*, *Pseudomonas chlororaphis*, and *Pseudomonas aureofaciens* all oxidize PCA while

respiring terminal electron acceptors alternative to oxygen. In the case of *C. portucalensis*, I found that it can oxidize PCA while respiring nitrate, fumarate, dimethyl sulfoxide, and trimethylamine-N-oxide. In the case of nitrate, I found that PCA oxidation increased the rate of nitrate reduction. This is a significant finding because relative nitrate content is a determinant of soil fertility.

The fact that any mode of anaerobic respiration across bacterial phyla could drive PCA oxidation implied that a general mechanism for this process might exist within the bacterial electron transport chain (ETC). I developed the first methods for genetically engineering *C. portucalensis* and systematically knocked out genes essential for different branches of the ETC. Sure enough, the cells lost the ability to oxidize PCA, given the appropriate terminal electron acceptor, when I knocked out the genes required for nitrate, fumarate, dimethyl sulfoxide, or trimethylamine-N-oxide respiration, respectively. To test whether there is a general mechanism for PCA oxidation, I knocked out the quinones, which are membrane-bound shuttles that convey electrons within the ETC. In this genetic background, I found that PCA oxidation activity is lost during fumarate, dimethyl sulfoxide, and trimethylamine-N-oxide respiration and mostly lost during nitrate respiration. Concurrently, another member of the Newman lab, John Ciemniecki, showed that quinones non-enzymatically oxidize PCA in solution. Altogether, these findings indicate that: 1) Any organism that utilizes quinones during anaerobic respiration will oxidize PCA, and potentially other phenazines; and 2) PCA can replace quinones as an electron shuttle for certain enzymes, such as the respiratory nitrate reductase. Hence, my discovery is generalizable to many organisms and environments.

My dissertation contributes to the fields of microbial physiology and ecology in several ways. Conceptually, it demonstrates that we are now able to predict a metabolic process from first principles, to discover and isolate an organism that performs it, and to develop the genetic tools to reveal the mechanism, all over the course of several years. Practically, we now have a better understanding of the fate of phenazines in the environment: by not relying on standard model organisms and fast growth, I was able to design an experimental system to study an environmentally relevant process that had not been previously appreciated.

PUBLISHED CONTENT AND CONTRIBUTIONS

Tsypin, L.M., Bar-On, Y., Saunders, S.H., Leadbetter, J.R., Newman, D., 2020a. Phenzine Oxidizer Enrichment and Isolation. protocols.io. http://dx.doi.org/10.17504/protocols.io.bh4tj8wn (Tsypin et al., 2020a)

L.M.T. compiled and standardized the protocols as initially developed by Y.B.-O. and S.H.S. This work is adapted in Chapter 2.

Tsypin LM, Saunders SH, Bar-On Y, Leadbetter JR, Newman DK. Draft genome sequence of the redox-active enteric bacterium *Citrobacter portucalensis* strain MBL. Cameron Thrash J, ed. *Microbiol Resour Announc*. 2020;9(32):e00695-20. doi:10.1128/MRA.00695-20 (Tsypin et al., 2020b)

L.M.T. isolated *C. portucalensis* MBL from the enrichment cultures generated by Y.B.-O. and S.H.S. L.M.T. extracted and sequenced its DNA, annotated its genome, and performed the phylogenetic analysis. L.M.T. wrote the paper drafts and edited them according to the co-authors' feedback. The published article is © 2020 Tsypin et al. distributed under a CC BY 4.0 license. This work is adapted in Chapters 1 and 2.

Tsypin LM, Newman DK. Nitrate reduction stimulates and is stimulated by phenazine-1-carboxylic acid oxidation by *Citrobacter portucalensis* MBL. Lovley DR, ed. *mBio*. 2021;12(4):e02265-21. doi:10.1128/mBio.02265-21(Tsypin and Newman, 2021)

L.M.T. conceived and performed all experiments and analysis under the guidance of D.K.N. L.M.T. wrote the paper drafts and edited them according to D.K.N.'s feedback. The published article is © 2021 Tsypin and Newman distributed under a CC BY 4.0 license. This work is adapted in Chapters 1 and 3.

TABLE OF CONTENTS

Acknowledgements iv

Gratitudes v

Brief Abstract xi

Narrative Abstract xii

Published Content and Contributions xiv

List of Figures xviii

List of Tables xix

Nomenclature xx

Chapter 1: INTRODUCTION AND BACKGROUND 1

Biology as a predictive science and microbial infallibility 1

Microbial slow growth and survival 2

Phenazines 5

The principle of microbial infallibility and biological phenazine oxidation 7

Chapter 2: ENRICHMENT FOR AND ISOLATION OF A PHENAZINE OXIDIZER 13

Abstract 13

Narrative 13

Materials and Methods 14
Stock solutions and media for enrichment and isolation 14
Sampling and Inoculation 16
Electrochemical PCA oxidation assays 16
Plate reader PCA oxidation assays 17
Isolation 18
DNA extraction and sequencing 19
Genomic sequence processing, assembly, and annotation 20
Plasmid sequencing 21

Results 22

Discussion 30

Chapter 3: THE PHENOMENOLOGY OF PCA OXIDATION 33

Abstract 33

Narrative 33

Materials and Methods *34*
Strains and media 34
Cell preparation for plate reader experiments 35
PCA redox plate reader measurements and nitrogen oxide concentration measurements 35
Electrochemistry survival experiments 36

Results *36*

Discussion *47*

Chapter 4: THE GENETIC MECHANISMS OF PCA OXIDATION **51**

Abstract *51*

Narrative *51*

Materials and methods *56*
Strains, media, and plate reader assays 56
Designing and engineering mutant strains 58

Results *62*

Discussion *76*

Chapter 5: CONCLUDING REMARKS **80**

Appendix I: DETAILED PROTOCOLS AS USED IN CHAPTERS 2–4 **86**

Chapter 2 *86*
Anoxic enrichment medium 86
Agar isolation medium 86
Electrode chamber assay medium 86
Plate reader assay medium 87
Plate reader assay 87

Chapter 3 *88*
Plate reader PCA oxidation assay medium 88
Electrode chamber PCA oxidation assay medium 88
Ion chromatography assay medium 88
Ion chromatography assay 89
Greiss colorimetry for nitrate and nitrite concentrations 89
Electrode chamber assays 90

Chapter 4 *93*
PCA oxidation assay basal medium 93
Preparation of electrocompetent cells for electroporating plasmids (E. coli and C. portucalensis MBL) 93
Designing and implementing translational knockouts 94
Gene deletions via homologous recombination 98
Cloning complementation vectors 99
Plate reader PCA oxidation assay 101

Computational analyses *102*

Appendix II: BLUE SOYMILK SIDE PROJECT **103**

Bibliography **105**

LIST OF FIGURES

Number *Page*

1. The logical outcome of exponential growth by bacteria 3
2. Canonical model of phenazine redox cycle in a biofilm 7
3. The two basal natural phenazines 9
4. The redox cycle of phenazine-1-carboxylic acid 11
5. Enrichment strategy 16
6. Electrochemical assay setup 19
7. Photos of enrichment cultures over the course of a week 21
8. Initial electrochemical assays of PCA oxidation 24
9. Colony morphologies of isolates from a PCA oxidizing enrichment 25
10. Spiral colony waves 25
11. PCA oxidation by enrichments, isolates, and lab strains 26
12. Quantification of maximum PCA oxidation from Figure 10 27
13. MLSA phylogeny identifying the *Citrobacter* isolate 28
14. A model for phenazine redox cycling in a biofilm 31
15. Possible models of PCA oxidation 34
16. A more rigorous comparison of PCA oxidation activities 38
17. PCA oxidation in direct response to nitrate addition 41
18. *C. portucalensis* MBL stops at nitrite 41
19. Duration of PCA oxidation in electrode chambers 43
20. Nitrite concentrations during PCA oxidation in electrode chambers 44
21. Bulk ATP content during PCA oxidation in electrode chambers 45
22. CFU counts during PCA oxidation in electrode chambers 46
23. A model of a PCA redox cycle driven by a single cell 48
24. How PCA oxidation may be coupled to anaerobic respiration 55
25. Comparison of nitrate reductase deletions and translational knockouts . 63
26. Nitrate reductase knockout phenotypes after standing pre-growth 64
27. Nitrate reductase knockout phenotypes after standing with nitrate 65
28. Nitrate reductase knockout phenotypes after shaking pre-growth 66

29. Fumarate, DMSO, and TMAO knockout phenotypes 67
30. PCA oxidation phenotypes of quinone knockouts 68
31. Complementation of nitrate-driven PCA oxidation phenotypes 70
32. Complementation of fumarate-driven PCA oxidation phenotypes 71
33. Complementation of DMSO-driven PCA oxidation phenotypes 72
34. Complementation of TMAO-driven PCA oxidation phenotypes 73
35. PCA oxidation phenotypes of pseudomonad strains 74
36. Pre-growth comparisons of PA14 phenotypes 75
37. Blue soymilk strains and a spontaneous colorless mutant 102
38. Soymilk phytoestrogens 103

LIST OF TABLES

Number *Page*

1. Recipe for the 100x freshwater salts stock solution 15
2. Recipe for the 1000x trace elements stock solution 15
3. Recipe for the 1000x 13-vitamin stock solution 15
4. Whole genome comparisons used to identify *C. portucalensis* MBL 29
5. Condition matrix for assessing physiological effects of PCA oxidation .. 41
6. Genotypes of *C. portucalensis* MBL mutants used 57
7. Oligos used for oligo-mediated recombineering 59
8. Oligos used for knocking out genes by homologous recombination 60
9. Oligos used for cloning complementation vectors 61
10. Plasmids used for knockouts and complementation 62

NOMENCLATURE

Anaerobiosis. Anaerobiosis describes life without oxygen. A metabolism or metabolic process (see below) under anaerobiosis is called "anaerobic."

Anoxia. Anoxia is a condition without oxygen. For example, an environment such as soil can become anoxic at shallow depths after rainfall or irrigation.

Bacterium. A bacterium is a microbe that falls into one of the broadest evolutionary groups of life on Earth (the Bacteria). Bacteria are typically characterized by their relatively small size (most are on the order of 1 μm long) and metabolic plasticity (while we can only breathe oxygen, there are bacteria out there that can breathe anything from nitrate to uranium). Our definition of what a bacterium is, or how to identify a specific one, has grown increasingly complex over time, especially after we came to recognize that there is a distinct, but analogously broad and diverse, group of organisms that are roughly the same size as bacteria—the Archaea. There are various laboratory techniques to identify different species of bacteria, but the least ambiguous approach, especially when working with a new organism, is to determine its DNA sequence (see below) and how it compares to previously identified sequences. The convention is to write species names as *Genus species* the first time they are mentioned and as *G. species* thereafter.

Biofilm. This is a metaphorical description for an aggregated lifestyle of microbes. A biofilm may be thin or thick, smooth or rugose, clonal or polymicrobial, exposed to air or immersed in liquid. While there is no strict visual definition for a biofilm, they are characterized by a developmental framework, which begins with an initial cell attaching to a surface and changing its gene regulatory program. This cell and its daughters then grow into a microcolony (see below), and the different cells in the nascent biofilm begin to take on distinct roles. For example, a subpopulation of the biofilm may die in order to provide a necessary extracellular matrix for the rest of the biofilm to thrive. The end of a biofilm may be disaggregation, when, in response to a signal, the individual cells disperse and swim away to other environments.

Colonies and colony-forming units. When working with bacteria, we often prefer to work with clonal or isogenic populations of cells. A direct way to derive a clonal population is to grow it from a single bacterial cell. It would be very difficult to isolate a single cell in liquid culture without specialized equipment due to the small size of the cells, but it is relatively easy to do on solid agar media: by sufficiently diluting a bacterial culture and gently letting the cells settle on the smooth, flat, solid medium, we can get good separation between individual cells. After an incubation at a favorable temperature, those single cells grow into "colonies." Because we cannot formally declare that each of the colonies arose from a single cell (what if it was a pair that were stuck together?), we often refer to "colony-forming units" (CFUs) as a more precise term for

the number of viable cells in the originating culture. A colony may also be thought of as a biofilm (see above).

DNA. This is an initialism for deoxyribonucleic acid. DNA "encodes" information inside living cells. The metaphor of "code" is apt because DNA comprises a long continuous string of four different nucleotides, which function like four letters (A for adenine, T for thymine, C for cytosine, and G for guanine) that can be arranged in various orders. The order of these letters determines the activity of a given stretch of DNA. In the context of this dissertation, there are two main ways in which DNA is studied or used. First, by determining the DNA sequence—meaning, the order of As, Ts, Cs, and Gs throughout a genome (the total collection of unique DNA in an organism), we can derive the evolutionary relationship (phylogeny) of a given organism to other species. Second, by manipulating genes (units of DNA that encode a specific function in the cell), we can ascertain how a cellular process works.

Enrichment. When trying to grow organisms or strains (see below) that carry a desired trait, while not knowing how to select (see below) for them out of a mixed culture (a culture that has multiple different organisms/strains), you can design an enrichment. Enrichment is an experimental framework in which the researcher predicts which conditions might be favorable for the desired organisms/strains, such that they increase in proportion relative to the undesired organisms/strains in the mixed culture. This approach is particularly useful for discovering species that perform a new metabolic process: you can take environmental samples, put them under conditions that would favor the theoretical metabolism, and wait to see which organisms grow in relative number over time.

Enzyme. An enzyme is a protein (see below) that serves to catalyze a chemical reaction. In other words, an enzyme enables a chemical reaction to proceed at a biologically useful rate when it would have been too slow on its own. Typically, enzyme names try to be descriptive of their function and end in the suffix -ase. Enzymes often do not work alone but instead form complexes of multiple different proteins.

Electron shuttle. An electron shuttle is a diffusible molecule that can acquire and donate electrons without losing its integrity or undergoing irreversible molecular modifications. In other words, electron shuttles can be reversibly reduced and oxidized. In considering what is and is not an electron shuttle, we quickly arrive at some edge-cases for which the answer becomes philosophical. For instance, should we consider molecular hydrogen as an electron shuttle? My inclination is to say no, as the oxidation of molecular hydrogen leads to two naked protons, and thus the loss of the original molecule. But if all protons are interchangeable, then maybe it does not matter? Regardless, for the purposes of this dissertation, electron shuttles are considered in the sphere of redox-active metabolites, meaning molecules that are synthesized by living cells

during their metabolism, which also act as electron shuttles. Of these, I focus on phenazines (see below)

Electron transport chain. The electron transport chain (ETC) is a feature of cells that perform respiration (see below). The ETC comprises multiple enzymes and electron shuttles (see above)—molecules that can carry electrons from one enzyme to another. The function of the ETC resembles that of a battery-powered circuit: the flow of electrons performs work for the cell by traveling along a path that couples the current to necessary cellular processes.

Fluorescence. Most of the materials we interact with are reflective, meaning that they absorb some wavelengths of light and reflect others, granting them the color(s) that we perceive. Some materials have the property of being fluorescent, meaning that they absorb certain wavelengths of light and *emit* light of a different wavelength. In other words, under certain illumination, they shine of their own accord. This is a very useful property for microbiological research because it enables us to perceive minute processes under the microscope: if something shines in the darkness, we can see it even if it is minute.

Knockouts and Complementation. In genetics, there is a gold standard for demonstrating that you know how an organismal process works: first, you disrupt or break (knockout) a gene and show that the organism can no longer perform the function that you are studying; second, you reintroduce the unbroken form of a gene (complement) and show that the function returns. There are many ways of knocking out or complementing genes.

Metabolism. Metabolism is a very broad concept for the set of typically internal processes that allow living organisms to move, grow, reproduce, and manipulate their external environment. Some metabolic processes function to conserve energy from food and respiration (see below). Some build cellular components, such as nucleotides for synthesizing DNA (see above). Yet others can serve different functions depending on the organismal need. Molecules that are produced during metabolic processes are often called "metabolites."

Midpoint potential. Redox reactions (see below) occur in the context of the potential energy of the reaction and the concentrations of the reacting compounds. The midpoint potential of a compound is a relative quantitative property that defines the propensity of the compound to donate or accept electrons. The midpoint potential is usually determined relative to a standard hydrogen electrode at a standard temperature of 25 ºC, a standard pressure of one atmosphere, a standard concentration of reactant and products of 1 M, and a standard pH (see below) of seven. It is a value that is characteristic of a reduction reaction relating the oxidized and reduced forms of a compound (a redox pair), say of molecular oxygen being reduced to water. In this way, the midpoint potential describes a half-reaction because a complete chemical reaction is balanced for all factors, including electrons. The convention is that a compound with a more

negative potential (say, -320 mV) will donate electrons to a compound with a more positive potential (say, +820 mV). The greater the difference between the two midpoint potentials (here, 1.14 V), the greater the energy that may be conceivably conserved from the reaction. The convention for writing a standard midpoint potential is in the form $E^{o'}_{1/2}$ = -320, where E is the symbol for potential, ½ indicates the midpoint, ° indicates standard conditions (1 atmosphere of pressure at 25 ºC with 1 M concentrations of each reactant and product), and ' indicates pH = 7 (see below). A more negative midpoint potential means that the given redox pair tends to more easily donate electrons, and a more positive potential means that the given redox pair tends to more easily accept electrons. Thus, if you see that one redox pair has a midpoint potential of -320 mV and another has +820 mV, you can expect that the thermodynamically favorable reaction will constitute the oxidation of the former and the reduction of the latter.

Nucleic acid. A nucleic acid is a chain of nucleotides, each of which comprising a phosphate, a five-carbon sugar, and a nucleobase. The two predominant nucleic acids in living organisms are DNA (see above) and RNA (see below).

pH and pKa. The pH is a measure of the concentration of protons (hydrogen ions) in a solution. The prefix p- represents a negative base 10 logarithm. Thus, the pH is calculated as $pH = -\log_{10}([H^+])$. pKa is a measure of the equilibrium acid dissociation constant, defined as $pKa = -\log_{10}([H^+][A^-]/[HA])$ at equilibrium.

Phenazines. These are specific molecules characterized by three aromatic carbon rings (aromatic meaning that some of the bonds between carbon atoms are ambiguously positioned, which is often the case for smelly compounds) with two central nitrogen atoms in the middle ring. Many microbes make various derivatives of phenazines, which are distinguished by the molecular decorations added to the core phenazine structure. Phenazines are examples of electron shuttles and redox-active metabolites.

Plasmid. A plasmid is a circular molecule of DNA that is maintained and replicated separately from the chromosome(s) of an organism. Thus, it carries accessory genomic information that is usually not essential for life, at least under favorable conditions. Due to this property, researchers can relatively easily engineer plasmids to carry genes that are useful for research without harming the organism being studied. Many wild bacteria carry native plasmids of various and sundry functions.

Polymerase chain reaction. Polymerase chain reaction (PCR) is a method for generating many identical copies of a DNA sequence. If you are reading this circa 2023, you might be most familiar with PCR as a means of getting tested for COVID-19: in these tests, the RNA of the SARS-CoV-2 virus is first processed into DNA, and then the DNA is amplified via PCR. If this

results in a bunch of copies of SARS-CoV-2 sequences, you have tested positive for carrying the virus.

Protein. A protein is a chain of amino acids (also called a polypeptide chain), which are small, stereotyped molecules defined by a carboxylic acid group, an amine group, and a decorative sidechain in between them. This sidechain determines the unique properties of each amino acid. In most organisms, 20 distinct amino acids are used. Much like DNA and RNA, the sequence and identities of amino acids determine the structure and function of a protein. Moreover, it is the fact that DNA, RNA, and proteins are all linear sequences of unambiguous subunits that allows DNA to encode information that is transcribed into messenger RNA (see above), which is then translated into protein. Proteins constitute the bulk of the "machinery" in living cells. In bacteriology, the convention is that protein names are written as the corresponding gene name but not italicized (e.g., NapA).

Rhizosphere. The biome associated with plant roots. For example, bacteria associated with plant roots are in the rhizosphere. Depending on the plant, the rhizosphere may be restricted to topsoil or extend very deep into the ground.

RNA. RNA is an initialism for ribonucleic acid. RNA differs from DNA (see above) in several important ways: 1) while DNA comprises a sequence of As, Ts, Cs, and Gs, RNA replaces thymine (T) with uracil (U); 2) DNA is almost always in the form of a double helix—antiparallel strands in which every A is paired with a T, and every C is paired with a G—but RNA is typically a single strand that can form myriad structures by way of folding onto itself, this folding being influenced by the given nucleotide sequence; 3) DNA predominantly serves to encode information, but RNA can have its own catalytic activity, support the functions of enzymes, or convey the "message" that DNA encodes. In this latter case, a given messenger RNA (mRNA) carries the information required to synthesize a particular protein (see above).

Screen. Like enrichments (see above), screens are counterposed to selections (see below). A screen is a census for whether a set of strains (see below) carries a desired trait. During a screen, each candidate has to be assayed individually.

Selection. Selection is an experimental approach that kills all organisms or strains (see below) except for the one(s) that the researcher wants to keep. Most commonly, we use antibiotics to maintain a strain that has been engineered to be resistant to the compound without it becoming contaminated by other organisms or strains. This is the most useful when you couple the attainment of antibiotic resistance to a desired genomic manipulation. When this is possible, you can use a selection instead of a screen to find the strains that were genetically engineered correctly, for example.

Strain. A strain is a specific variant of a species. For example, a bacterial species isolated from the environment would be called a "wildtype" strain. A strain in which a specific gene has been disrupted would be called a knockout strain for that gene. In bacteriology, the convention is that "wildtype" is abbreviated WT, WT gene names are written in italics with the first letter capitalized (e.g., *NapA*), and mutated gene names are written in italics with the first letter lowercase (e.g., *napA*).

Quinones/-ols. Quinones are important electron shuttles in the electron transport chain (see above). There are various derivatives that different species employ. In this dissertation, I will discuss ubiquinone, menaquinone, and demethylmenaquinone. These variants are distinguished by certain molecular details that determine from which donor (and to which recipient) the quinone can transfer electrons. This characteristic is often described through the midpoint potential (see above). When quinones are reduced, they are called quinols.

Redox reactions. This is an abbreviation of reduction-oxidation reactions. Reduction is the process of donating electrons; oxidation is the process of taking electrons away. Redox is very confusing to learn or talk about because reduction and oxidation always happen concurrently: the electron donor is oxidized as the electron acceptor is reduced. It is often helpful to focus on either 1) the flow of electrons and to ignore the compounds that are reduced or oxidized or 2) whether a particular compound is reduced or oxidized over time. This dissertation focuses on the oxidation of a particular phenazine (phenazine-1-carboxylic acid or PCA), and I am able to detect whether PCA is in its oxidized or reduced form because it is fluorescent (see above) only when reduced.

Respiration. Respiration is typically what we think about when we think about "burning calories." Respiration is the main form of metabolism that allows for energy conservation by coupling the chemical breakdown of food to the reduction of terminal electron acceptors (see below) such as oxygen.

Terminal electron acceptor. This is a molecule that can be respired by an organism. For example, in canonical human respiration, the terminal electron acceptor (TEA) is oxygen. This dissertation will include a discussion of alternative TEAs that can be respired by bacteria anaerobically (see above). Specifically, these will include nitrate (NO_3^-, the second-most favorable compound to respire after oxygen), fumarate (Fum^{2-}, an organic compound that is also a metabolic byproduct of respiration), dimethylsulfoxide (DMSO, a commonly used laboratory solvent and important component of marine metabolisms), and trimethylamine-N-oxide (TMAO, an important marine metabolic compound and major constituent of fishy odors). To bring together some of the definitions above, during respiration, food is oxidized and the electrons that are stripped from it are conveyed through the electron transport chain by electron shuttles, including

the quinones/-ols. These electrons ultimately arrive at enzyme complexes (oxido-reductases) that oxidize the electron shuttles and reduce the terminal electron acceptors such as oxygen.

CHAPTER 1: INTRODUCTION AND BACKGROUND

There are two types of dichotomy: True dichotomies, false dichotomies, and surprise trichotomies.
—Randall Munroe, xkcd #2592, alt-text

BIOLOGY AS A PREDICTIVE SCIENCE AND MICROBIAL INFALLIBILITY

As is wont to happen, there are turf wars in science, particularly when people want to flex that their area of research is "harder": more quantitative, more predictive, more macho. All of this is nonsensical and often damaging. As with any sophistry, the arguments can be effective because they are clever. For example, when learning biology, everyone bumps into the obstacle that it requires an enormous amount of memorization, as compared to mathematics or physics because those sciences have a theoretical framework that is much more quickly accessible. Does it stand to reason, then, that biology is worse off as a field of study?

No. Like physics, biology has branches that are firmly grounded in theory, complete with mathematical frameworks, though internalizing them takes both the legwork of memorizing biological phenomena *and* learning the underlying mathematics and physics that explains them. In the context of microbial chemical ecology and physiology, the relevant theoretical framework is called the "Principle of Microbial Infallibility," which states that, wherever there is a thermodynamically favorable chemical reaction that can be catalyzed, there will be a microbe that uses it in its metabolism to derive energy (Gale, 1951; O'Malley and Walsh, 2021).

Already, we can see the promise and complexity of the premise: if we have sufficient fluency in our knowledge of chemistry and thermodynamics, we can imagine new forms of life, predict where in the world they would be, and then go out and find them. The significance of being able to do this is manifold: 1) microbes are extremely efficient chemists because they often have to work with very low concentrations of substrates, so if there is a chemical reaction that humanity needs, such as degrading plastic, it is often more effective to find a microbe that does it than to develop a new chemical pipeline from scratch; 2) these principles are generalizable throughout time and space, meaning that they can be used to examine how life emerged on Earth and how it might emerge or manifest itself on other worlds; 3) we can begin to

understand how our biosphere is shaped by the interplay of geological and biological processes. Nonetheless, the bars for "sufficient fluency", imagination, and going out and finding microbes are very high and requires a collaborative, cross-disciplinary effort by many people.

Three of the most prominent discoveries within the framework of microbial infallibility are the anaerobic oxidation of ammonia (Kuenen, 2008; Strous et al., 1999), anaerobic oxidation of methane (Boetius et al., 2000), and chemolithoautotrophy via manganese oxidation (Yu and Leadbetter, 2020). These are examples of what might be termed "primary metabolism": metabolic processes that allow the microbes to grow and reproduce. Consequently, they were discovered via enrichment, meaning that environmental samples were incubated under conditions that would allow only these metabolisms to proceed, and whatever managed to grow was isolated. This work was incredibly difficult to do, which is why the discoveries were made decades after the metabolisms were postulated, but the conceptual approach for how to pursue them is relatively simple: force the desired bugs to grow. However, the metabolic and biochemical capabilities of microbes, as predicted by thermodynamic and "infallible" principles, extend much farther than just what is necessary for their growth. This raises the question of how we might discover new biochemistries and metabolisms that may be important but decoupled from growth. As ever, the answer depends on the exact biological context that interests us.

MICROBIAL SLOW GROWTH AND SURVIVAL

Microbes are difficult to study because they are so small. Uncovering how they work requires a combination of experimental cleverness and sheer biomass. Consequently, the majority of what we know about microbes comes from experiments that have them grow as quickly as possible to attain enough material to work with. This sort of work has carried microbiology very far, but we are beginning to increasingly appreciate that there is much more to learn from cells that are growing slowly, or not at all, because this is more reflective of what we observe in nature. In natural environments, microbes are usually under stress due to nutrient limitation (starvation), competition (which can be an active process when microbes secrete antibiotic compounds to kill competitors or a passive one when they simply compete for nutrients), and predation (viral, microbial, or macrobial). These stresses all limit the rate of growth far below

what is typically encouraged in labs. One way to illustrate this point is to consider the alternative: if a single bacterium unrestrictedly divided every thirty minutes, which is a reasonable rate for most of the bacteria used in rapid-growth experiments, the bacterial culture would have the same mass as several sugar cubes in around a day, as the Earth within four days, and as the observable universe within a week (Figure 1). In other words, to learn about bacteria as they actually are in the world, we need to focus on studying their activity when they are growing slowly or surviving in a non-growing state.

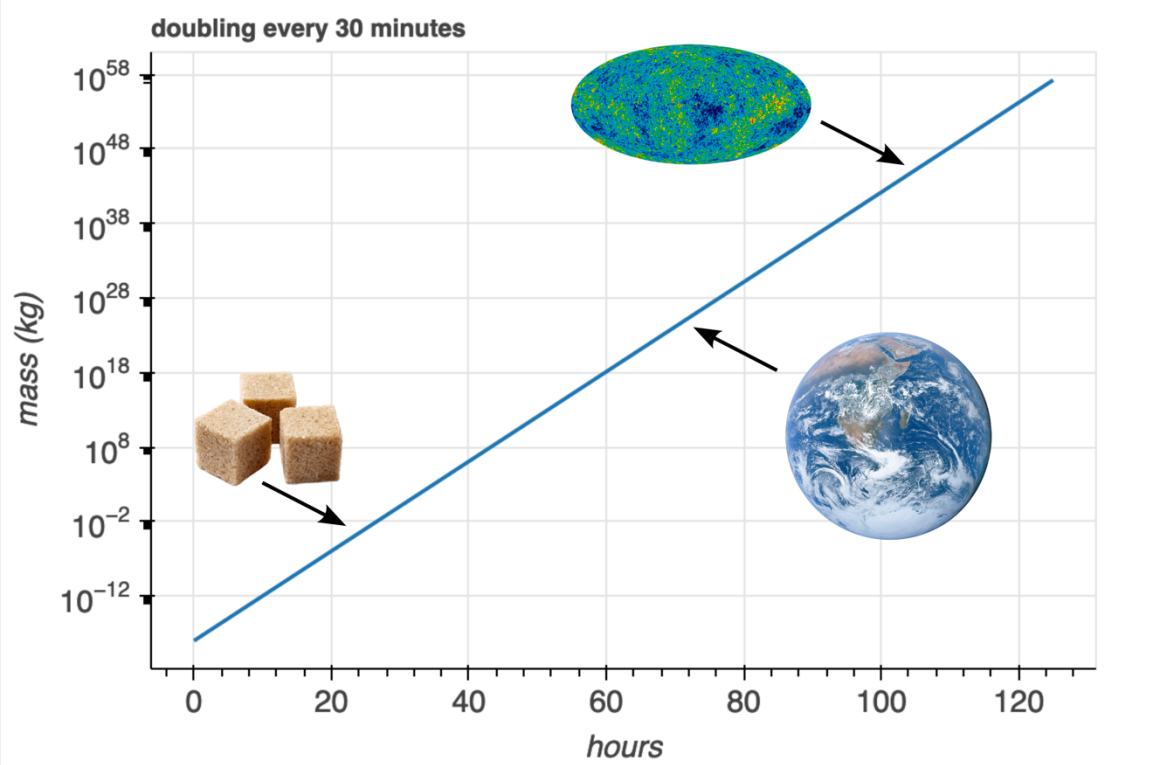

Figure 1. The logical outcome of unrestricted exponential growth by bacteria. Here, exponential growth appears linear because the y-axis is on a logarithmic scale.

When some of these slow-growth or non-growth studies were first being conducted, it was surprising to discover that the cells are not in a kind of stasis. Rather, they maintain a basal metabolic activity (Bergkessel et al., 2016; Teal et al., 2006), dynamically regulate gene expression (Bergkessel, 2021), and produce compounds that supported their survival or allow for an advantage over competing cells (Boedicker et al., 2009; Page and Peti, 2016). These processes are sometimes grouped under the umbrella term "secondary metabolism" because they were discovered as separate from those involved in rapid-growth or "primary" metabolism.

Secondary metabolites are extraordinarily diverse. Based on environmental DNA sequencing, there may be hundreds of thousands to millions of different microbial species on Earth, of which we have identified relatively few (Louca et al., 2019; Zhang et al., 2020). Each of those species has evolved to occupy certain niches in the environment, tuning its metabolism and molecular toolkit to interact with its neighbors and abiotic milieu. Thus, the myriad species produce and utilize myriad primary and secondary metabolites. Once the metabolites leave the cells due to export or diffusion, they become common goods or evils, benefitting or harming the surrounding cells and changing the physicochemical environment. Because this fractal tapestry of interwoven species, metabolisms, and interactions quickly becomes overwhelming to consider, I will now limit the scope of the discussion for this dissertation to bacteria and outline some principles.

While there are many different bacterial metabolisms, they all exist in the same chemical and thermodynamic framework, which is akin to how we use electricity. We understand (a very generalized) metabolism to comprise several key nodes that convey electrons from food to a final waste product. These nodes comprise a terminal electron donor, a carbon source, a terminal electron acceptor, enzymes to catalyze chemical conversions, and electron shuttles. When talking about human metabolism, for example, we often invoke the metaphor of "burning calories." Taken literally, this would mean setting fire to sugar. In this case, the sugar is both the carbon source and terminal electron donor, the oxygen is the terminal electron acceptor, and there are no intervening enzymes or electron shuttles—the sugar reduces molecular oxygen to water directly. The resultant fire releases energy (calories). The fact that sugar burns demonstrates that the reaction is thermodynamically favorable; it just does not happen at an appreciable rate unless the reaction is initiated by a first spark. The task of human metabolism is to make a middle path possible: make the sugar react with oxygen fast enough to be useful and capture the released energy rather than let it all dissipate as heat. So, we have enzymes instead of a spark, and we use intermediate electron shuttles rather than let the sugar react with oxygen directly. We could call this a tightly controlled burn.

Bacterial metabolism is much more modular than that of humans. For instance, the model bacterium *Escherichia coli* can use tens of different carbon sources (Tong et al., 2020) and six different terminal electron acceptors (Unden and Bongaerts, 1997), meaning that it can make use of dozens of different permutations for respiration.[1] Every metabolic combination produces characteristic waste or incidental byproducts, which ultimately play into biogeochemical cycles. For example, when respiring oxygen, *E. coli* contributes to the oxygen, water, and carbon cycles; when respiring nitrate, *E. coli* contributes to the nitrogen, water, and carbon cycles. Thus, depending on which metabolism bacteria employ in response to their environmental constraints, they affect their surroundings and neighbors in different ways.

With the above in mind, what might a bacterium do when it needs to respire, but its preferred terminal electron acceptors are unavailable? Explicitly, this is a stressful condition because without a sink for electrons, the bacterium will steadily become choked with waste, which is both toxic and stalls its metabolic activity. To resolve this, the bacterium may change its physiology to use less favorable terminal electron acceptors. If there are none available, the bacterium may migrate to improve its access to terminal electron acceptors. If this is impossible or ineffectual, the bacterium may synthesize its own terminal electron acceptor from scratch. This last case is a prime example of the utilization of secondary metabolites under survival conditions, and it is particularly interesting as an instance of a microbe actively shaping its environment in spite of stress or starvation. To me, this demonstration of microbial agency is sublime, deft like sleight of hand, and so I was delighted to learn about how phenazines can mediate this process when I joined the Newman lab.

PHENAZINES

Phenazines are secreted secondary metabolites that microbes use in diverse ways, from quorum sensing (Dietrich et al., 2006) to antimicrobial warfare (Baron et al., 1989; Meirelles and Newman, 2018; Thomashow and Weller, 1988) to energy conservation under anoxia

[1] *E. coli* can also ferment instead of respiring, meaning that it can use a carbon source as both an electron donor and acceptor (Clark, 1989), but this is beyond the scope of this dissertation.

(Glasser et al., 2014). Phenazines are able to contribute to these activities due to their redox activity, specifically by accepting electron acceptors from cells, a process that has been studied for over 120 years. Reduction of phenazines by bacteria was first proposed in the nineteenth century as an indicator for the presence of enteric bacteria in water supplies (Rothberger, 1898). Several decades later, pyocyanin, one of the phenazines produced by *Pseudomonas aeruginosa*, was described as an "accessory respiratory pigment" that increased the rate of oxygen consumption by *Staphylococcus*, *Pneumococcus*, and erythrocytes by shuttling electrons from the cells to oxygen (Friedheim and Michaelis, 1931). Once it became apparent that phenazines can have cytotoxic effects, they were characterized as antimicrobial compounds that destructively abstract electrons from the transport chain (Baron et al., 1989). It was then discovered that phenazine reduction can greatly benefit *P. aeruginosa* by 1) regulating gene expression during quorum sensing by oxidizing a transcription factor; 2) acting as alternative terminal electron acceptors to promote anoxic survival; and 3) facilitating iron acquisition (Dietrich et al., 2006; Dietrich and Kiley, 2011; Glasser et al., 2014; Gu and Imlay, 2011). These reports paint a complex picture of the multifarious effects phenazines can have, but in each case, the conceptual model ends with the cell reducing the phenazine. Because phenazines require energy and resources to synthesize, which are limited under the conditions in which the phenazines confer a survival advantage, they would be much more effective if they could be recycled (re-oxidized) and reused.

Reduced phenazines can be re-oxidized by inorganic electron acceptors like oxygen and ferric iron, and this abiotic process has been invoked to explain redox cycling of phenazines in biofilms (Saunders et al., 2020; Wang et al., 2011) (Figure 2). However, bacteria may be in environments where these electron acceptors are unavailable. In this situation, biological oxidation of reduced phenazines could close the redox cycle by regenerating oxidized phenazines. This

had not been observed for natural phenazines or any other natural organic compound[2], and my dissertation aimed to show that this process is possible and occurs.

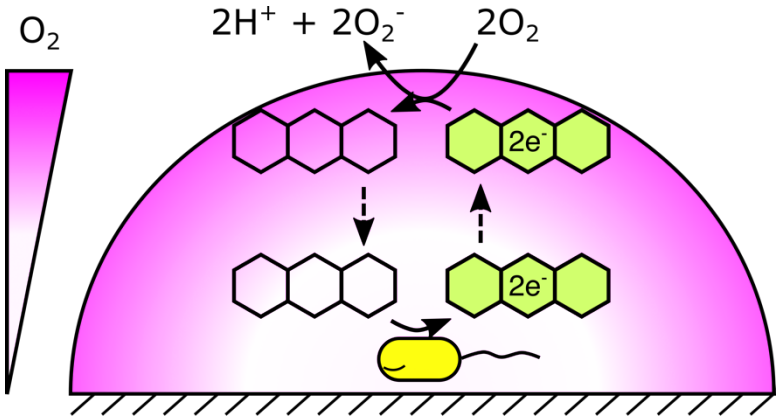

Figure 2. Canonical model of phenazine redox cycle in a biofilm. Bacterial biofilms become rapidly anoxic, when populated with oxygen-respiring microbes, because the surface cells consume the oxygen faster than it can diffuse inside. Thus, an oxygen gradient forms, and cells experience anoxia at depths as shallow as 50 μm (Dietrich et al., 2013). A bacterium that needs to respire oxygen, finding itself at the anoxic core of the biofilm, resorts to reducing a phenazine (depicted as a tricyclic molecule) as a TEA. The reduced phenazine can then convey electrons to a zone of the biofilm by a diffusive process (Saunders et al., 2020). The abiotic reaction between reduced phenazines and oxygen produces superoxide, which is highly toxic to cells. Thus, the oxygen gradient has a corollary effect that the cells that benefit from phenazine reduction are also protected from reactive oxygen species that are generated as part of the phenazine redox cycle.

THE PRINCIPLE OF MICROBIAL INFALLIBILITY AND BIOLOGICAL PHENAZINE OXIDATION

Given that phenazines are abiotically oxidized by compounds like ferric iron and oxygen, and that this can already be beneficial for the bacteria that reduce phenazines (Glasser et al., 2014; McRose and Newman, 2021), it is not immediately obvious how to distinguish this from a biological oxidation because any environmental measurement may be confounded by abiotic processes. Thus, to find bacteria that biologically oxidize phenazines, we need to identify conditions under which this process would be favorable and separable from the spurious oxidation reactions, which we can do by applying the principle of microbial infallibility. In this

[2] Examples of reduction-oxidation cycles of inorganic or anthropogenic compounds include the intracellular sulfur cycle for *Beggiatoa alba* (Schmidt et al., 1987), extracellular cycling of anthraquinone-2,6-disulfonate (Lovley et al., 1999), and extracellular cycling of neutral red, a synthetic phenazine derivative (Harrington et al., 2015).

scheme, the phenazine would be the electron donor, but not the carbon source (we want to distinguish bacteria non-destructively oxidizing the phenazine from bacteria eating it), so we should consider situations in which it would be thermodynamically favorable for the phenazine to donate electrons to some molecule that does not abiotically react with it. Moreover, if we want to grow bacteria that perform this phenazine oxidation, we need to provide them a separate carbon source to use as food.

In terms of a terminal electron acceptor that is abiotically inert, a good candidate is nitrate. It is a relatively favorable compound to respire after oxygen (nitrate reduction to nitrite has $E^{o'}_{1/2}$ = +433 mV and oxygen reduction to water has $E^{o'}_{1/2}$ = +818 mV (Thauer et al., 1977)). So, for bacteria to be able to oxidize a phenazine while reducing nitrate, the midpoint potential for the phenazine must be more negative than +433 mV. Now, the true midpoint potential in the relevant environment will not be under standard conditions, but this can be addressed later. Let us first choose a phenazine to nail down our target.

There is a grand diversity of phenazines, but their biosynthesis pathway is such that most of the diversity arises from decorating a basal phenazine in different ways. There are two basal phenazines, phenazine-1-carboxylic acid (PCA)[3] and phenazine-1,6-dicarboxylic acid (PDC) (Figure 3), which are synthesized by the same enzymatic pathway, meaning that any organism that produces phenazines will produce both PCA and PDC (Blankenfeldt and Parsons, 2014). However, one of the PDC intermediates during biosynthesis is unstable, so PCA always appears as the dominant product over PDC: either the PDC is not used and contributes a smaller fraction to the phenazine pool or it is further derivatized into other phenazines, further depleting it (Blankenfeldt and Parsons, 2014). Whether an organism can synthesize other phenazines can be predicted from the organism's genome, and metagenomic analyses reveal that PCA/PDC producers are phylogenetically diverse across the Proteobacteria (recently renamed

[3] Not to be confused with Principal Component Analysis, a commonly used approach for analyzing high-dimensional data. To make things simpler, I will say right now that I do not use principal component analysis anywhere in my dissertation.

Pseudomonadota) and Actinobacteria (recently renamed Actinomycetota), and these produc-

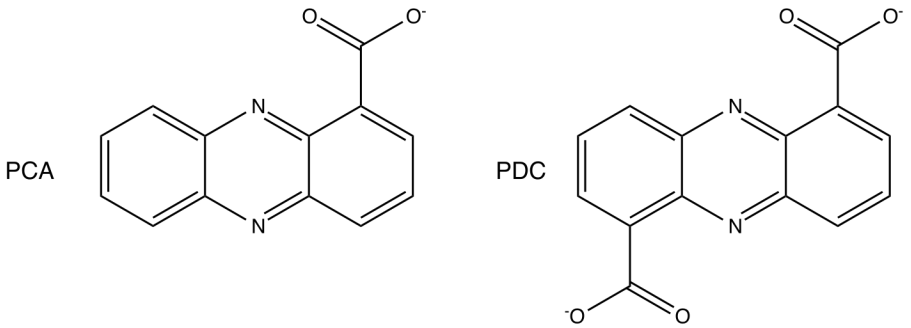

ers tend to be enriched in plant root-associated (rhizosphere) environment (Dar et al., 2020). Furthermore, PCA has a standard midpoint potential of -116 mV (Wang and Newman, 2008), making it a viable partner for nitrate respiration. Altogether, it is a priori reasonable to expect that PCA will be present in soils with vegetation and that bacteria that would be oxidizing PCA might be found there.

Figure 3. The two basal natural phenazines. Left: phenazine-1-carboxylic acid (PCA). Right: phenazine-1,6-dicarboxyclic acid (PDC). Note: the carboxylic acids are depicted as deprotonated because their pKa's (equilibrium acid dissociation constants) are circa 4.24, which is well below circumneutral pH (Brisbane et al., 1987).

Lending credence to this expectation, PCA is indeed found in the rhizosphere: it can be detected at concentrations of ~1 μg/g soil in the wheat rhizosphere and has an estimated half-life of 3.4 days in that environment, implying that it must be continually synthesized and secreted to maintain that concentration (Thomashow, 2013). PCA is also bioactive in the rhizosphere, providing one of the only direct examples of antibiotics being utilized by microbes in the environment (Thomashow and Weller, 1988). PCA producers are even used as commercially-available biocontrol agents in the Russian Federation, sold as Pseudobacterin-2 (Popov et al., 2018; Remali et al., 2017; Thomashow, 2013). Thus, we can be confident that the place to look for phenazine oxidizers will be in rhizospheres, and that PCA is a solid candidate phenazine to start with. To derive a workable concentration of PCA that could be oxidized, we can turn to the thermodynamics.

Whether a reaction is thermodynamically favorable is determined by the value of its Gibbs free energy, denoted ΔG. If ΔG is negative, then the reaction spontaneously proceeds (though

the rate of the reaction may be arbitrarily slow without catalysis, like in the case of glucose reacting with oxygen). However, because life does not occur under "standard conditions," we cannot rely on the ΔG under standard conditions to predict whether a biological process is thermodynamically feasible. The ΔG of a given reaction, ΔG_r is related to the ΔG under standard conditions ($\Delta G^{o'}$) by the equation $\Delta G_r = \Delta G^{o'} + RT\ln(Q_r)$, where Q_r is the quotient of the activities of reactants and products, T is the temperature in Kelvin (K), and R is the ideal gas constant 8.314 J K^{-1} mol^{-1}. To derive the ΔG from midpoint potentials, we invoke the following equation: $\Delta G^{\circ\prime}_r = -nFE^{\circ\prime}_r$, where n is the number of electrons exchanged, F is the Faraday constant (96,485 J mol^{-1} V^{-1}), and $E^{o'}$ is the standard potential of the reaction. In the case of PCA and nitrate, we then have:

1) $PCA_{oxidized} + 2e^- + 2H^+ \rightarrow PCA_{reduced}$ (Figure 4) $E^{o'}_{1/2} = -0.116$ V
2) $NO_3^- + 2e^- + 2H^+ \rightarrow NO_2^- + H_2O$ $E^{o'}_{1/2} = +0.433$ V
3) $PCA_{reduced} + NO_3^- \rightarrow PCA_{oxidized} + NO_2^- + H_2O$ $E^{o'} = +0.549$ V
4) $\Delta G^{o'} = -2 \times 96{,}485 \times 0.549$ J $mol^{-1} = -116$ kJ mol^{-1}

Now, for the sake of argument, consider a situation in which a bacterium finds itself in conditions with 9 mM nitrate, 1 mM nitrite, 150 μM reduced PCA, and 50 μM oxidized PCA:[4]

5) $\Delta G_r = -116$ kJ $mol^{-1} + RT\ln(\frac{[PCAox]\times[NO_2^-]}{[PCAred]\times[NO_3^-]}) = -116$ kJ $mol^{-1} + RT\ln(\frac{50\times1\times10^{-9}M}{150\times9\times10^{-9}M}) =$
   -116 kJ $mol^{-1} + 8.314 \times 298 \times \ln(0.037)$ J $mol^{-1} = -124$ kJ mol^{-1}.

Under these conditions, the reaction is thermodynamically feasible! This gives us an indication for what kind of cultivation medium composition would work for enriching for and isolating PCA oxidizing organisms. Furthermore, depending on the intracellular pH, the energy required for synthesizing ATP is 40-50 kJ mol^{-1} (Thauer et al., 1977). So, conceivably, this reaction could even power cellular metabolism.

[4] You will find that these numbers represent realistic values based on my experiments in Chapter 2.

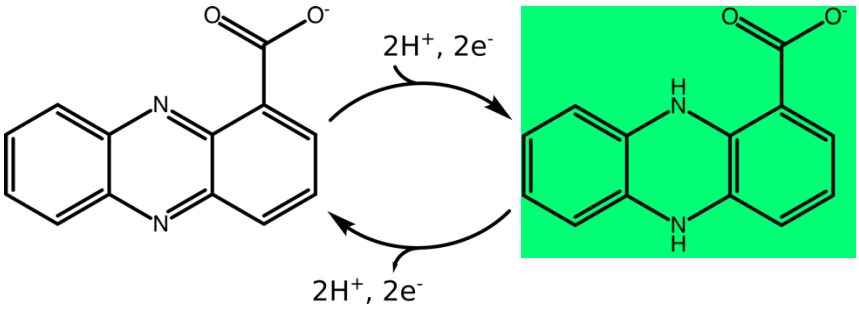

We can push the logic a bit further and ask under what conditions the reaction would cease to be viable—in other words, when ΔG_r ceases to be negative. This will occur when the value of $RT\ln(Q_r)$ is at least +116 kJ mol^{-1}:

6) $Q_r \geq e^{\frac{116\times10^3}{8.314\times298}} = 2.1 \times 10^{20}$

Figure 4. The redox cycle of phenainze-1-carboxylic acid. Left: oxidized PCA. Right: reduced PCA. Notably, oxidized PCA is colorless and reduced PCA is bright green and fluorescent.

So, the reaction will not cease until the ratio of products to reactants is almost incomprehensibly high. In other words, the reaction should go to completion. We can perform the same analysis for other terminal electron acceptors that bacteria can use for anaerobic respiration. Some common ones (read: ones that become relevant in the ensuing chapters) are fumarate ($E^{o'}_{1/2}$ = +33 mV), DMSO ($E^{o'}_{1/2}$ = +160 mV), TMAO ($E^{o'}_{1/2}$ = + 130 mV), and nitrite ($E^{o'}_{1/2}$ = +350 mV) (Thauer et al., 1977; Unden and Bongaerts, 1997). Thus:

- PCA oxidation coupled to fumarate respiration, $\Delta G^{o'}$ = -29 kJ mol^{-1}, and the reaction stops being favorable when the ratio of products to reactants is over 1.2×10^5;
- PCA oxidation coupled to DMSO respiration, $\Delta G^{o'}$ = -53 kJ mol^{-1}, and the reaction stops being favorable when the ratio of products to reactants is over 2×10^9;
- PCA oxidation coupled to TMAO respiration, $\Delta G^{o'}$ = -47 kJ mol^{-1}, and the reaction stops being favorable when the ratio of products to reactants is over 1.7×10^8;
- And PCA oxidation coupled to nitrite respiration, $\Delta G^{o'}$ = -90 kJ mol^{-1}, and the reaction stops being favorable when the ratio of products to reactants is over 6×10^{15}

Altogether, the logic is as follows:

- The biosynthesis of phenazines is such that PCA is going to be produced anywhere there are phenazines;

- The global distribution of phenazine producers indicates that PCA will be produced in root-associated soils;
- The half-life of PCA in soil is short enough that it must be actively synthesized to explain the concentrations that are detected;
- PCA is bioactive in these environments;
- And it is thermodynamically feasible for bacteria to couple the oxidation of PCA to the reduction of terminal electron acceptors (specifically in the form of anaerobic respiration) under realistic conditions, and the reactions should go to completion;
- Thus, by the Principle of Microbial Infallibility, if we create the appropriate enrichment conditions in the lab, we should be able to discover biological PCA oxidation.

In the following chapters, I describe my work to isolate a PCA-oxidizing bacterium and to characterize the underlying genetic mechanisms for the process. In Chapter 2, I provide an expanded description of the enrichment, isolation, and identification of the bacterium that my colleagues and I published several years ago (Tsypin et al., 2020b). In Chapter 3, I recount our publication describing the phenomenon of PCA oxidation by the isolate and some other species (Tsypin and Newman, 2021). In Chapter 4, I describe my (as yet) unpublished work in which I tease apart the mechanisms of how PCA is oxidized by the isolate. In Chapter 5, I think about the conclusions and implications of this work. In Appendix I, I provide detailed protocols for the experiments I describe in Chapters 2–4. Finally, in Appendix II, I discuss a side project I did a little bit of work for, which has legs, and which I do not want to lose to the ether.

CHAPTER 2: ENRICHMENT FOR AND ISOLATION OF A PHENAZINE OXIDIZER

Chance favors the prepared mind.
—Louis Pasteur (attributed)

ABSTRACT

We grew a soil enrichment culture to identify organisms that anaerobically oxidize phenazine-1-carboxylic acid. A strain of *Citrobacter portucalensis* proved to be the fastest PCA-oxidizing isolate from this enrichment. I isolated and sequenced it by both Illumina and PacBio technologies. It has a genome with a length of 5.3 Mb, a G+C content of 51.8%, and at least one plasmid.

NARRATIVE

During the 2017 Microbial Diversity course at the Marine Biological Laboratory (MBL) in Woods Hole, MA, we aimed to isolate organisms that anaerobically oxidize reduced phenazine-1-carboxylic acid (PCAred) (Figure 4, right), a process that had never been described. In order to prevent the abiotic oxidation of PCAred, Yinon Bar-On and Scott Saunders developed cultivation conditions free of oxygen and with a very low concentration of metals such as iron. Yinon sampled topsoil from several locations around Falmouth, MA (41°36'58.9"N, 70°34'31.2"W; 41°32'42.8"N, 70°37'52.4"W; and 41°31'34.3"N, 70°39'05.3"W). Yinon and Scott incubated the samples in Balch tubes with a minimal growth medium containing acetate as a nonfermentable carbon source so that the cultivated bacteria could employ only a respiratory metabolism; the medium included PCAred as an electron donor and nitrate as the terminal electron acceptor (TEA) (Tsypin et al., 2020a). Because PCAred is green and oxidized PCA (PCAox) is colorless, PCA oxidation activity was determined by loss of green color in the enrichment cultures. After Scott and Yinon established enrichment cultures that robustly oxidized PCA, I began isolating the phenazine oxidizer(s) from the mixed cultures. I identified three strains in the enrichment: two strains of *Pseudomonas nitroreducens* and one strain of *Citrobacter portucalensis*, which I named strain MBL after its point of origin.

Stock solutions and media for enrichment and isolation

The enrichment media were developed by Scott Saunders and Yinon Bar-On, and the stock solution compositions (Tables 1–3) were developed by Jared Leadbetter and Dianne Newman. The enrichment and isolation media were prepared modularly from stock solutions that were sterilized separately. The 100x freshwater stock solution (Table 1) was kept non-sterilized at room temperature. The 1000x trace elements stock solution (Table 2) was autoclaved. The 1000x 13-vitamin stock solution (Table 3) was filter-sterilized, wrapped in foil, and kept in the dark at 4 ºC. The 2mM PCAred stock solution was prepared in ultrapure water in a sealed serum vial or Balch tube by adding a trace amount of a $PdCl_2$ catalyst and vigorously sparging the solution with 80:20 (vol/vol) H_2/CO_2 gas until it turned yellow-green. The solution was agitated with a magnetic stir bar during sparging and overnight afterwards. The anoxic enrichment medium comprised 45 mM sodium bicarbonate as a buffer, 10 mM ammonium chloride as a nitrogen source, 1 mM potassium phosphate as a phosphorus source, 1 mM PCAred as a potential electron donor, 100 μM sodium acetate as a carbon source and electron donor, 10 mM sodium nitrate as an electron acceptor and nitrogen source, 50 μM sodium sulfide as a sulfur source, 1x freshwater salts, 1x trace elements, and 1x vitamins. The isolation medium was 1 mM sodium phosphate buffer (pH 7), 10 mM ammonium chloride, 100 μM sodium acetate[5], 100 μM sodium sulfate, 10 mM sodium nitrate, 1x freshwater salts, 1x trace elements, 1x vitamins, and 1.5% agar. For the isolation medium, the agar was autoclaved in water at a 2x concentration and the appropriate sterile stock solutions were added to the desired final concentration once the molten agar was below 60 ºC. The various nutrient stock solutions were prepared at 100 or 1000x concentrations and either filter sterilized or autoclaved according to their stability. To ensure anoxia, the concentrated stock solutions were added to freshly

[5] Some of my old notes say 100 μM sodium acetate, and some say 1 mM sodium acetate. If anyone follows up on this work and this detail is important, please keep this in mind.

autoclaved (hot) aqueous medium under nitrogen sparging. The gas line was kept anoxic by passage over hot copper tubing.[6]

Table 1. Recipe for the 100x freshwater salts stock solution.

Compound	100x Stock Concentration	1x Medium Concentration
NaCl	1.71 M	17.1 mM
MgCl	197 mM	1.97 mM
CaCl	68 mM	680 μM
KCl	671 mM	6.71 mM

Table 2. Recipe for the 1000x trace elements stock solution.

Compound	1000x Stock Concentration	1x Medium Concentration
HCl	20 mM	20 μM
$FeCl_3$ $6H_2O$	7.5 mM	7.5 μM
H_3BO_3	480 μM	480 nM
$MnCl_2$ $4H_2O$	500 μM	500 nM
$CoCl_2$ $6H_2O$	6.8 mM	6.8 μM
$NiCl_2$ $6H_2O$	1 mM	1 μM
$CuCl_2$ $2H_2O$	12 μM	12 nM
$ZnCl_2$	500 μM	500 nM
Na_2SeO_3	23 μM	23 nM
Na_2MoO_4	150 μM	150 nM

Table 3. Recipe for the 1000x 13-vitamin stock solution.

Compound	1000x Stock Concentration	1x Medium Concentration
MOPS pH 7.2	1 mM	1 μM
Riboflavin	100 μg/mL	100 ng/mL
Biotin	30 μg/mL	30 ng/mL
Thiamine HCl	100 μg/mL	100 ng/mL
L-ascorbic acid	100 μg/mL	100 ng/mL
d-Ca-pantothenate	100 μg/mL	100 ng/mL
Folic acid	100 μg/mL	100 ng/mL
Nicotinic acid	100 μg/mL	100 ng/mL
4-aminobenzoic acid	100 μg/mL	100 ng/mL
Pyridoxine HCl	100 μg/mL	100 ng/mL
Lipoic acid	100 μg/mL	100 ng/mL

[6] Oxygen reacts with heated copper to produce copper oxide, thus scrubbing the trace oxygen out of the nitrogen gas line. This method can be used to determine the concentration of oxygen in the atmosphere by passing air over heated copper pellets in a closed system and measuring the loss of gaseous volume once the system equilibrates.

Nicotinamide adenine dinucleotide	100 µg/mL	100 ng/mL
Thiamine pyrophosphate	100 µg/mL	100 ng/mL
Cyanocobalamin	10 µg/mL	10 ng/mL

Sampling and Inoculation

The sampling and inoculation of initial enrichment cultures was done by Yinon Bar-On. Topsoil was scooped directly into sterile 50 mL conical tubes. Once in the lab, the samples were ground with a mortar and pestle and passed through a 2 mm sieve to remove large debris and organic matter. The fine soil was brought into an anoxic Coy-brand chamber in plastic weigh boats and allowed to rest between several hours and days to equilibrate with the headspace. Once equilibrated, the fine soil was subsampled and inoculated into the enrichment medium in either 96-well plates (20 mg of fine soil into 190 µL volume of the anoxic enrichment medium) or Balch tubes (1 g of fine soil into 9 mL of the anoxic enrichment medium). In both cases, the wells and tubes were observed over several days for PCA oxidation via the proxy of loss of green coloration. Candidate enrichment cultures with apparent PCAred activity were then passaged into fresh enrichment media by 10x dilution while maintaining anoxic conditions (Figure 5).

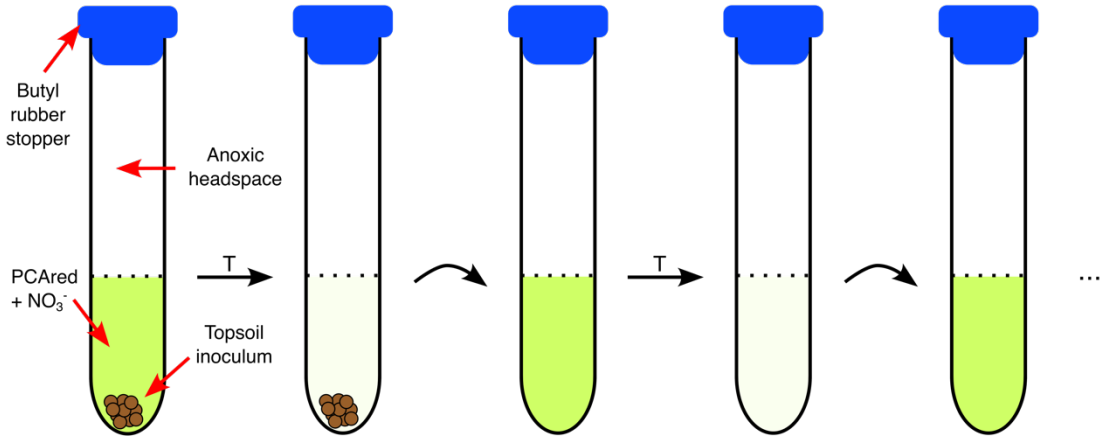

Figure 5. Enrichment strategy. Topsoil inocula were added to stoppered anoxic tubes with a reduced PCA medium and nitrate. Once the medium lost its green color, indicating PCA oxidation, the enrichment was passaged to a fresh tube, and the process was repeated.

Electrochemical PCA oxidation assays

The initial electrochemical oxidation assays were performed by Scott Saunders, which I then followed up on. Candidate enrichment cultures were grown up in 5 mL LB overnight (~18

hours) at 30 ºC in slanted glass culture tubes that were shaken at 250 rpm. After the incubation, the cultures reached an optical density at 600 nm light (OD_{600}) > 8 and 100 μL were inoculated into anoxic 100 mL electrode chambers with a modified PCAred oxidizer enrichment medium: 1x freshwater salts, 1x trace elements, 1x 13-vitamin solution, 20 mM sodium phosphate buffer (pH 7), 10 mM ammonium chloride, 100 μM sodium sulfate, 100 μM sodium acetate, 10 mM sodium nitrate, and 100 μM PCAred. The three-electrode chambers were set up connected to a Gamry potentiostat inside an mBraun-brand anoxic glove box as described in previous lab publications (Glasser et al., 2014; Wang et al., 2010). The electrode chamber setup was modified in the following ways (Figure 6): 1) The reference electrode was plugged into a gel-loading pipette tip filled with molten 1% ultrapure agarose in 3 M sodium chloride, which was allowed to solidify around the reference electrode, thus creating a salt bridge. Once solidified, the very end of the pipette tip was cut off with a fresh razor blade to exclude any air bubbles that might have formed. The tip was then secured against the reference electrode by applying strips of Parafilm, only ever applying force to keep the electrode inserted into the gel-loading tip.[7] 2) The working electrode was poised to constantly reduce PCA, rather than oxidize it, at -500 mV using a Gamry potentiostat. The main chamber of the electrode setup was filled to a final volume of 100 mL and the sidearm was filled to a final volume of 7 mL. The cultures were maintained in these electrode chambers for days at a time in an mBraun anoxic glovebox, tracking the current generated due to biological PCA oxidation. The cultures were periodically sampled to assess the number of viable cells, as colony-forming units (CFUs), on lysogeny broth (LB) agar or the isolation medium.

Plate reader PCA oxidation assays

To measure the PCA oxidation activity of different cultures in a high-throughput manner, I developed a plate reader assay using a BioTek Synergy 5 instrument. I set up black-walled, clear-bottom 96-well plates (BRAND PureGrade™ S, Cat. No. 781671) with a similar medium to the one used in the electrode chamber assays, with the exceptions that there was 1 mM sodium acetate, that the final PCA concentration was 200 μM (PCA was pre-reduced by sparging with

[7] More on these electrodes in Scott's thesis (Saunders, 2020).

5% H_2 over a palladium catalyst), and different wells contained different terminal electron acceptors (TEAs) at a 10 mM concentration. I pre-grew the cultures in an overnight culture in rich medium (LB for all strains except *Pseudogulbenkiania* MAI-1, which was grown in a tryptone yeast extract medium (TYEM)). Prior to inoculating adding the TEA, I washed the overnight cultures three times into the anoxic assay medium (spun 1 mL culture three times for 2 minutes at 8,000 × g three times and resuspended into a 1 mL final volume). I then diluted the washed cells to an OD_{600} = 0.125, as calculated from the OD_{600} measurement prior to washes.[8] After the washes, I let the cultures stand for at least an hour and a half to quench any carried over oxygen. I determined this timing from initial experiments incubating washed cultures with resazurin until it turned pink or colorless. Once the cultures became anoxic, I added the appropriate TEA and aliquoted 200 μL per well in the 96-well plate. I measured PCA fluorescence over time using 360/40 excitation and 528/20 emission bandpass filters (Sullivan et al., 2011). I quantified the oxidation using a LOWESS fit of the data (fitting the means of three technical replicates for each experiment with a sliding window of six data points, corresponding to three hours of experimental time). After the fitting, I computed a derivative of the curves to find the maximum oxidation rate. I also determined the time it took the cultures to reach 50% of the maximum PCAred signal. Here all the rates and PCAred concentrations are in arbitrary units because I did not include a calibration curve for these initial experiments.

Isolation

I plated enrichment cultures and electrode chamber oxidation assay cultures on LB agar or isolation medium as 10 μL serial dilution droplets. Once I placed the droplets onto the agar in a single row at one edge of the Petri dish using a multichannel pipette, I tilted the plate to allow the droplets to spread vertically as separated lanes. I then incubated the plates at room temperature or 30 ºC, and inspected the colonies for their size, shape, and number under a dissecting

[8] Because I did these washes in the anoxic Coy chamber, I did not have ready access to a spectrophotometer. I wanted a final density of OD_{600} = 0.1 in the experiment and decided to aim for OD_{600} = 0.125 after washes to account for losing cells during the washes.

microscope. I then struck unique colonies onto fresh agar plates, re-incubated, and assessed the streaks for homogeneity.

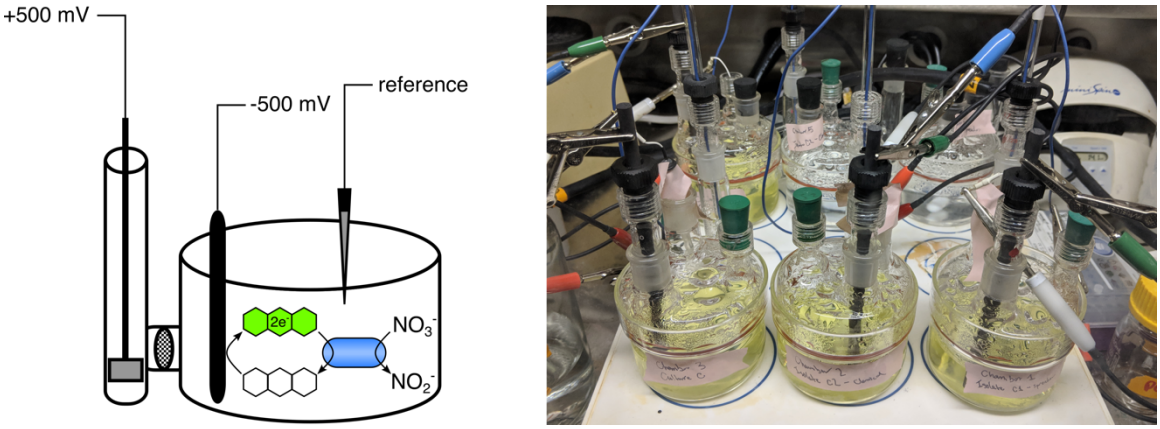

Figure 6. Electrochemical assay setup. Left: Diagram of electrode chamber. The sidearm is separated from the main chamber by a fine glass frit that allows the passage of small molecules but not cells. The potentiostat maintains the voltage at the working (-500 mV) and counter (+500 mV) electrodes using the Ag/AgCl reference electrode, which is immersed in a 3 M NaCl (1% ultrapure agarose) salt bridge inside a conical gel loading tip. Right: The electrochemical setup inside the mBraun glovebox. This picture was taken at the beginning of the experiment, so all the PCA is still reduced and green.

DNA extraction and sequencing

I identified PCAred oxidizing isolates via either 16S rRNA or whole-genome sequencing. For 16S rRNA sequencing, I amplified DNA by PCR (Forward primer 357F: 5'- CTCCTACGG-GAGGCAGCAG-3'; reverse primer 895R: 5'- CCGTACTCCCCAGGCG-3') directly from representative colonies of the strain and then submitted the samples for Sanger sequencing through Laragen. For whole-genome sequencing, I used a combination of Illumina short-read and PacBio long-read sequencing. In the case of the Illumina samples, I extracted DNA using the Qiagen DNeasy Blood & Tissue kit (product number 69504). I then submitted the samples to the Caltech Millard and Muriel Jacobs Genetics and Genomics Laboratory, where they were processed and sequenced by Igor Antoshechkin. The Illumina library was prepared using a NEBNext kit (New England Biolabs, product number E7335) and sequenced to 100x coverage (5 million 100-bp single-end reads) on a HiSeq 2500 instrument. In the case of the PacBio samples, I extracted high molecular weight DNA using a phenol/chloroform, CTAB approach (Wilson, 2001). I then submitted the high molecular weight DNA to the Genomics High-

Throughput Facility at the University of California, Irvine, where it was prepared using the SMRTbell Express template preparation kit v2.0 with barcoded overhang adapters and sequenced in a multiplexed PacBio Sequel II single-molecule real-time (SMRT) cell.

Genomic sequence processing, assembly, and annotation

The only strain that had its whole genome sequenced was the *Citrobacter* isolate. Illumina sequencing base calls were performed with RTA v1.13.48.0, followed by conversion to fastq files with bcl2fastq v1.8.4 by Igor Antoshechkin. I concatenated the reads into a single file, trimmed them with Trimmomatic v0.39 (with the following parameters: leading, 27; trailing, 27; slidingwindow, 4:20; minlen, 80) (Bolger et al., 2014), and analyzed them for quality using FastQC v0.11.8 (http://www.bioinformatics.babraham.ac.uk/projects/fastqc) (Brown et al., 2017). I processed the PacBio sequencing output using Canu v2.0 (set genomesize, 5.3m; mininputcoverage, 7; stoponlowcoverage, 7) (Koren et al., 2017). The PacBio fastq and trimmed Illumina reads were co-assembled using SPAdes v1.13.1 (Bankevich et al., 2012). The resulting scaffolds were further improved by comparison to reference Citrobacter genomes using MeDuSa v1.6 (Bosi et al., 2015). Contaminant sequences from eukaryotes were identified using NCBI BLAST (Johnson et al., 2008) and removed from the genome, along with scaffolds shorter than 200 nt, and the remaining scaffolds were analyzed with QUAST v5.0.2 (Gurevich et al., 2013). Default parameters were used for all software unless otherwise specified.

I identified the *Citrobacter* isolate species by average nucleotide identity (ANI) and tetranucleotide usage correlations using JspeciesWS (Richter et al., 2016), and I validated this finding using multilocus sequence analysis (MLSA) (7). MLSA was performed using anvi'o v6.1 to generate hidden Markov model (HMM) profiles for 32 nonribosomal single-copy housekeeping genes common to all reference strains compared (Eren et al., 2015). These HMM profiles were aligned using MUSCLE, and a phylogeny was constructed with MrBayes v3.2.7a on the CIPRES Science Gateway, with the reference *Escherichia coli* strain as the outgroup (Edgar, 2004; Miller et al., 2010; Ronquist and Huelsenbeck, 2003). I annotated the genome using the Prokaryotic Genome Annotation Pipeline (PGAP) (Haft et al., 2018; Tatusova et al., 2016). The genome is available on the NCBI under the BioProject accession number PRJNA638116.

Plasmid sequencing

I submitted the native *C. portucalensis* MBL plasmid for sequencing through Primordium labs, which uses Oxford NanoPore long reads for attaining the sequences.

Data analysis

The data and code for the graphs generated in this chapter can be found at https://github.com/ltsypin/PhD_Thesis.

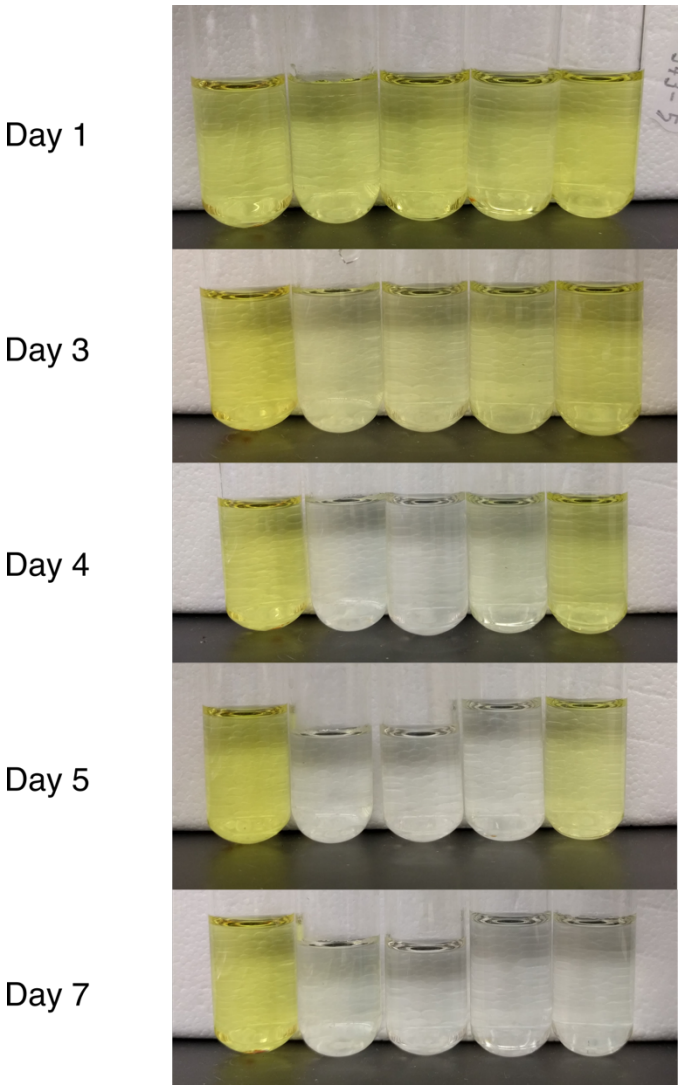

Figure 7. Photos of enrichment cultures over the course of a week. Leftmost tube: an uninoculated control with reduced PCA. The second and third tubes oxidized PCA the fastest (the loss of volume between days four and five is due to sampling for the next inoculation.

RESULTS

The enrichments that Scott and Yinon developed yielded cultures that oxidized 1 mM PCAred over the course of several days. In my hands, after the enrichment cultures had been passaged multiple times and transported from the MBL to Caltech, some of the enrichments were faster than others (Figure 7). Once it was clear that the activity was robust, I inoculated the fastest enrichments into LB, grew them overnight, and prepared freezer stocks for further experiments. I grew the cultures both at 30 and 37 ºC, which did not seem to have any effect on the colony morphology composition once plated, but I eventually settled on using 30 ºC as my default cultivation and experimentation temperature.

The enrichments that I selected for their speed of activity (tubes two and three in Figure 7) reproduced the activity when assayed in anoxic electrode chambers, showing a strong current over many hours (Figure 8). Scott initially compared my enrichment cultures to *Pseudomonas aeruginosa* (strain UCBPP-PA14) (Figure 8, top), but he did not normalize the density of the inocula into the electrode chambers. Nonetheless, it was apparent that, while *P. aeruginosa* did oxidize PCA during nitrate respiration, which was a discovery in its own right, its capacity to do so was lower than that of the two enrichments. Meanwhile, I began separating some of the strains of bacteria within the enrichments by sampling Scott's electrode chambers for colony forming units (CFUs) (Figure 8, bottom).

Upon plating the enrichment and electrode chamber cultures for CFUs, I first noticed two different colony morphologies. On LB plates, the colonies were almost indistinguishable, but on the isolation agar medium, the difference was obvious (Figure 9, left and middle): one colony type was punctate and domed; the other was thin, spread out, and had elegant spiral waves. Once I noticed these differences, I began plating single-colony isolates of the punctate and spreading bacteria on LB, and noticed that the punctate isolates gave two different morphologies on the rich medium: one strain formed smooth colonies, and another that I had not appreciated previously that grew faster and formed curls like solar flares around the colony perimeter (Figure 9, right). Imaging the colony in Figure 9 (middle) under phase contrast (with John Ciemniecki), I saw that the spirals were appreciably moving on the scale of 10 seconds a frame (Figure 10). It was difficult to manually hold focus over the requisite time, but it was clear that different areas

of the colony had different dynamics: near the center, there were spiral eddies (Figures 9, middle, and 10); at the very periphery, there were few or no waves; somewhere close to the half-radius mark, the waves propagated linearly.

By 16S rRNA sequencing, I identified that the three isolates corresponded to two strains of *Pseudomonas nitroreducens* and one strain of *Citrobacter*, the former corresponding the smooth punctate and spreading colonies and the latter to the curly colonies on LB. I initially misidentified the *Citrobacter* as a strain of *C. freundii* based on its 16S rRNA. This is because members of this Complex all share nearly identical 16S rRNA sequences (Borenshtein and Schauer, 2006). I later identified it using whole-genome analyses, which I describe farther below. The two *P. nitroreducens* isolates gave relatively low, though present PCA oxidizing activity in the electrode chambers (Figure 8, middle), which implied that the *Citrobacter* isolate may be the dominant PCA oxidizer in the enrichment. To confirm the relative PCA oxidation activities, I developed a new assay based on reduced PCA fluorescence in a plate reader, rather than the current generated at an electrode.

The *Citrobacter* isolate gave the fastest PCA oxidation activity (Figures 11 and 12) among the isolates, and as compared to the laboratory strains of *P. aeruginosa*, and appeared to explain the majority of the oxidation rate with nitrate in the mixed enrichment cultures. The pseudomonads were more active with nitrite than the *Citrobacter*, and *Pseuodogulbenkiania* MAI-1 showed significant PCA oxidation with both nitrate and nitrite, showing overall very similar dynamics to the *Citrobacter*'s. Fumarate induced the least PCA oxidation for all cultures.

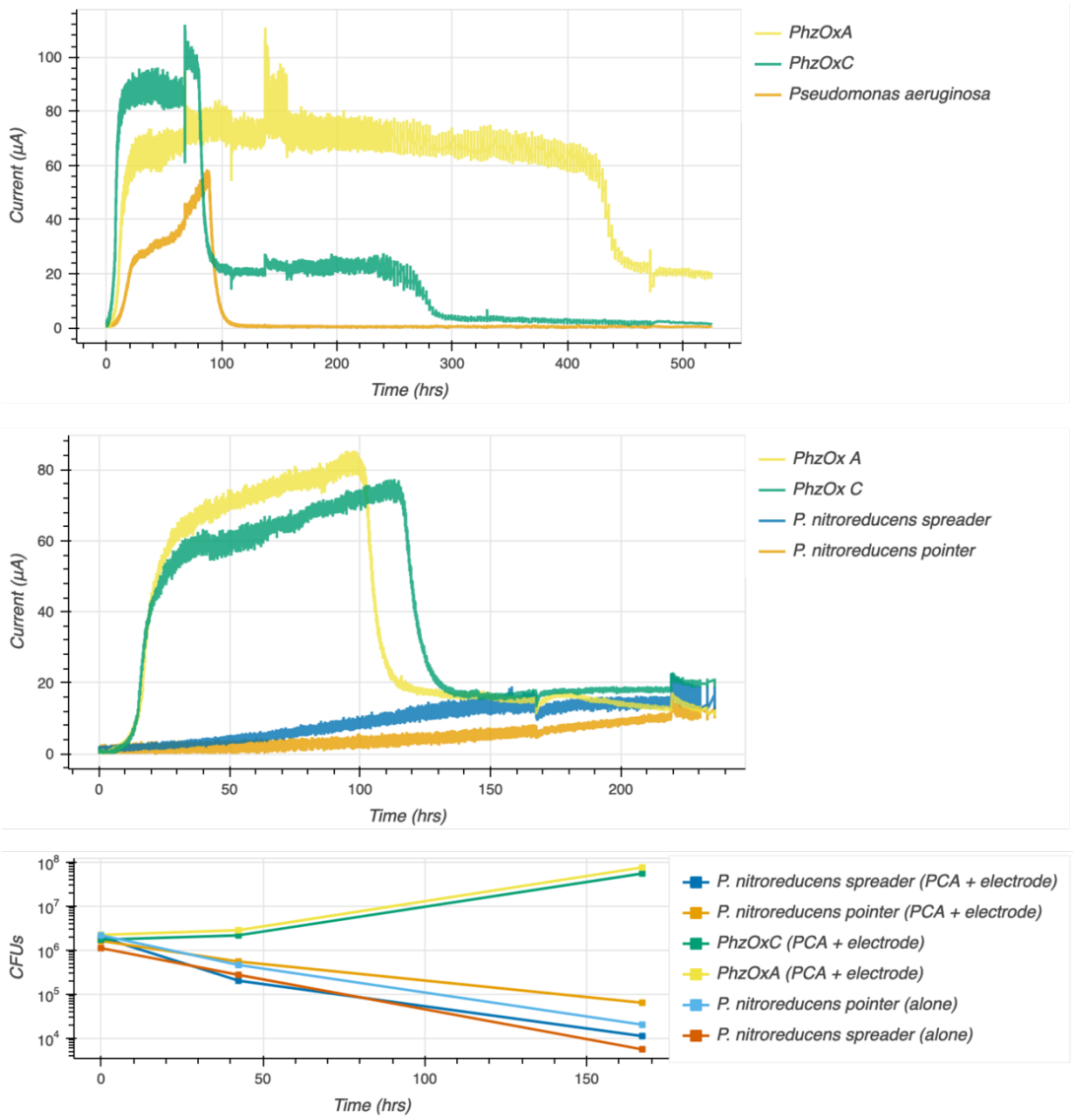

Figure 8. Initial electrochemical assays of PCA oxidation. The x-axes are showing time in hours (note that the scale is different in the top and bottom graphs), and the y-axes are showing current in μA. Top: Results of the experiment performed by Scott Saunders. The two enrichment cultures and the *P. aeruginosa* culture all show current, with enrichment culture PhzOxA showing the highest activity for the longest time. Middle: A repetition of the experiment by me, with the starting densities of cells in each electrode chamber equalized and clonal isolates of the two *Pseudomonas nitroreducens* strains compared to the enrichment cultures. Bottom: CFU counts from the experiment in the middle panel. The legend indicates whether the cultures were given the PCA and an electrode to continuously cycle.

Figure 9. Colony morphologies of isolates from a PCA oxidizing enrichment. All images were taken through the eyepiece of a dissecting microscope, which is why there are no scale bars. Left: Mixture of punctate and spreading colonies on isolation agar. This is an image of one of the CFU counting lanes. Middle: An image of a single spreading colony on isolation agar. Right: The curly morphotype on LB of a bacterium that formed punctate colonies on isolation agar.

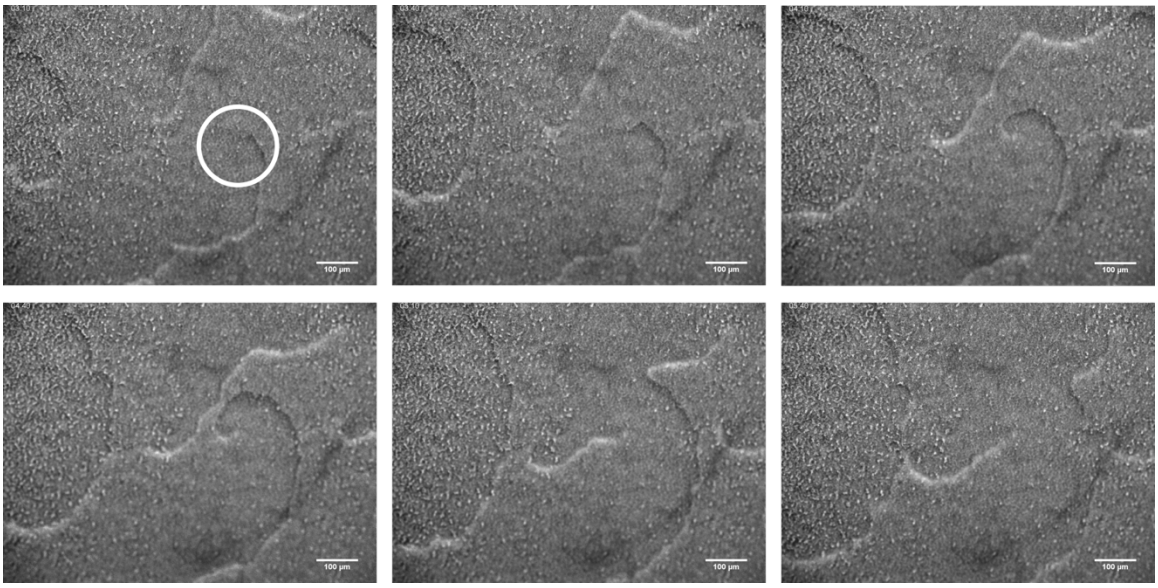

Figure 10. Spiral colony waves. These are still frames from a video, depicting 30-second intervals over the same field of view. The scale bar corresponds to 100 μm. Read left-to-right, these images show a wave of cells that cyclically runs around a set point (circled in the top left panel).

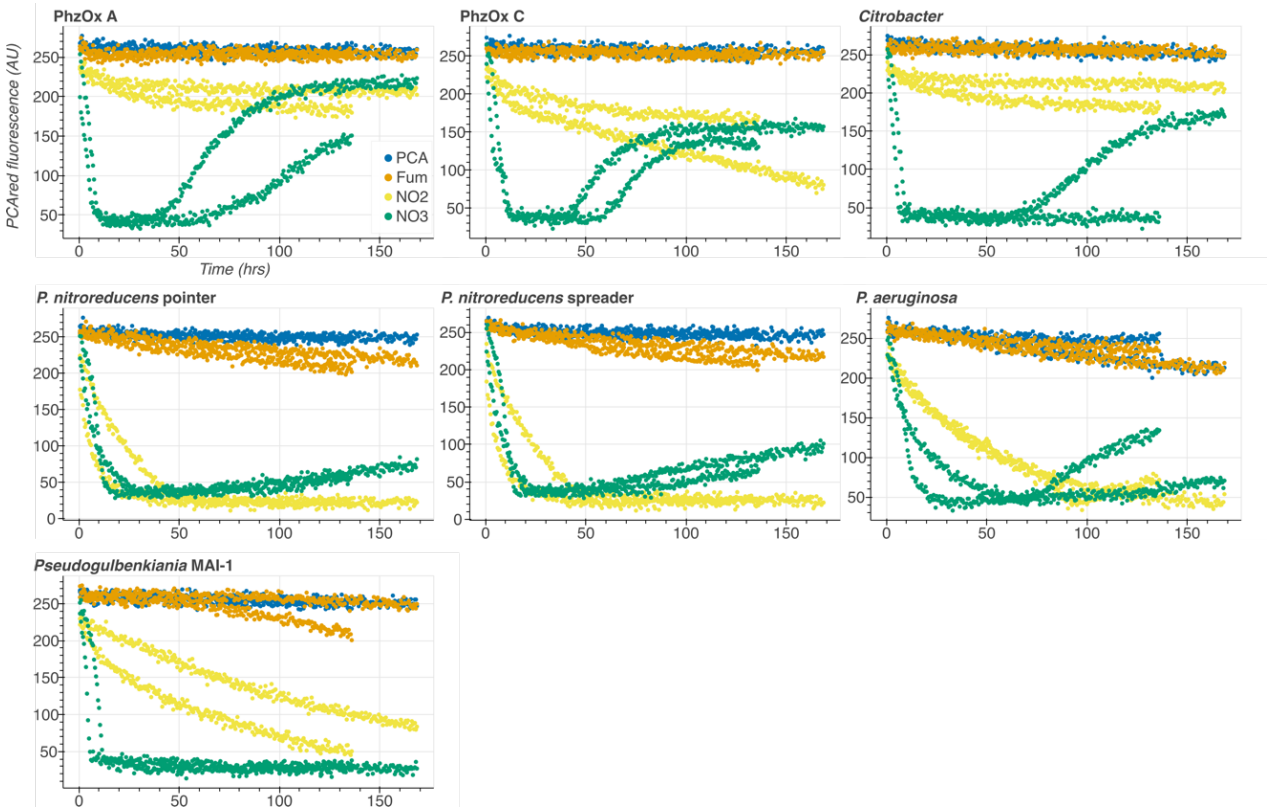

Figure 11. PCA oxidation by enrichments, isolates, and lab strains. The two enrichments are PhzOx A and C. The legend and colors correspond to the TEA added to the assay ("PCA" is PCAred without any TEA). The data comprise two experiments from separate days with technical triplicates.

I selected the *Citrobacter* as my isolate for studying the nature and mechanisms of PCA oxidation. The initial enrichment used nitrate as the TEA, so I wanted to focus on the organism that was the most efficient at oxidizing PCA with nitrate. I also wanted to use the *Citrobacter* over *Pseudogulbenkiania* MAI-1 because it was less fastidious about growth media. Finally, I simply wanted to work with something out of the enrichment, rather than from our strain collection.

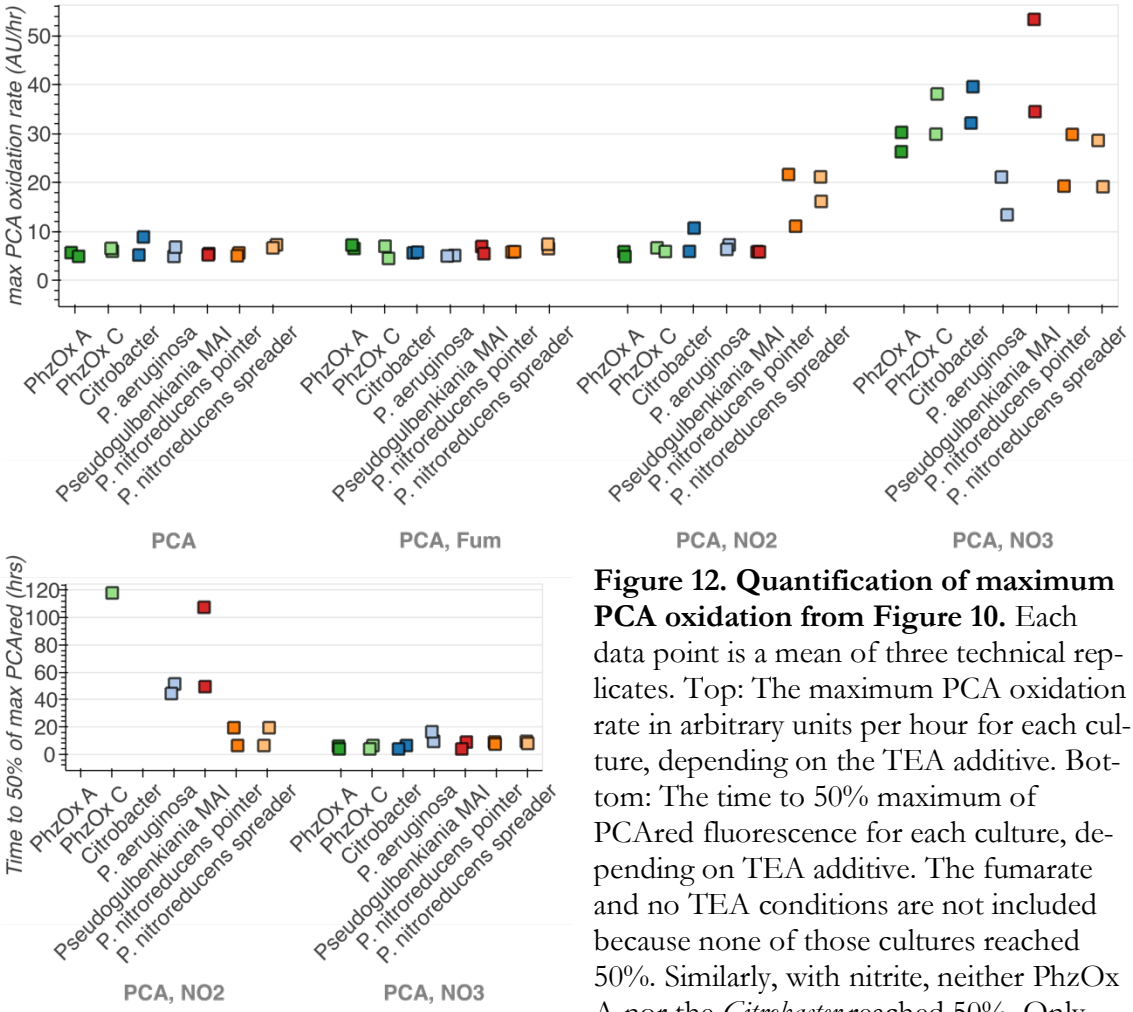

Figure 12. Quantification of maximum PCA oxidation from Figure 10. Each data point is a mean of three technical replicates. Top: The maximum PCA oxidation rate in arbitrary units per hour for each culture, depending on the TEA additive. Bottom: The time to 50% maximum of PCAred fluorescence for each culture, depending on TEA additive. The fumarate and no TEA conditions are not included because none of those cultures reached 50%. Similarly, with nitrite, neither PhzOx A nor the *Citrobacter* reached 50%. Only one set of triplicate for PhzOx C reached 50%.

Identifying the *Citrobacter* required a whole-genome analysis. After assembling a high-quality genome by combining highly accurate Illumina short reads with longer, more error-prone PacBio reads, I used multilocus sequence alignment (MLSA) phylogeny (Figure 13) and whole-genome

comparisons (Table 4) to discover that the *Citrobacter* isolate is a strain of *C. portucalensis*, which was first described in 2017 (Ribeiro et al., 2017). I named the isolate *C. portucalensis* MBL.

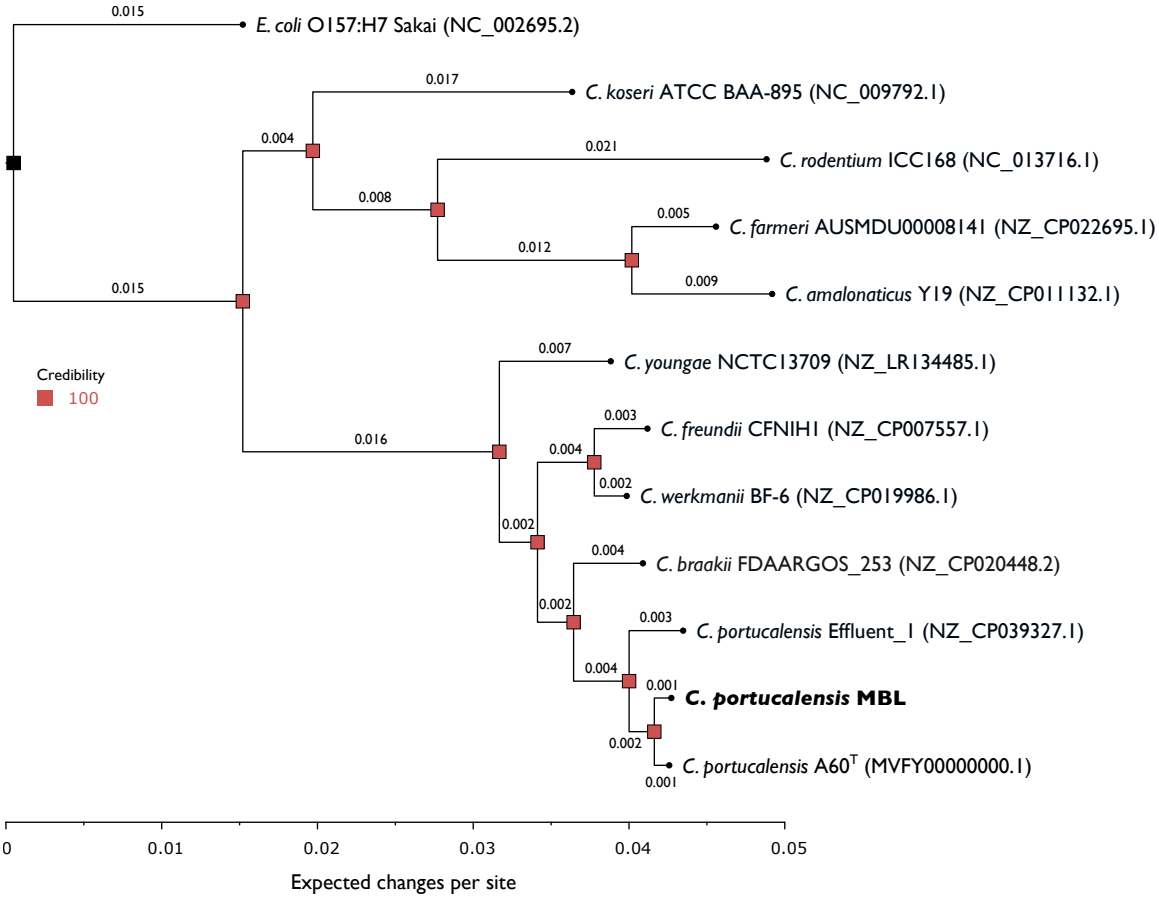

Figure 13. MLSA phylogeny identifying the *Citrobacter* isolate. The strains in this phylogeny are the same as listed in Table 4. *C. portucalensis* MBL is shown in bold at the bottom of the tree. The *E. coli* strain is the outgroup and roots the tree. This phylogeny was calculated based on the alignment of concatenated hidden Markov model profiles of 32 single-copy non-ribosomal housekeeping genes that are shared across all 12 genomes (PFAM accession numbers PF00709.21, PF00406.22, PF01808.18, PF00231.19, PF00119.20, PF01264.21, PF00889.19, PF01176.19, PF02601.15, PF01025.19, PF01725.16, PF01715.17, PF00213.18, PF01195.19, PF00162.19, PF02033.18, PF02565.15, PF00825.18, PF01193.24, PF01192.22, PF01765.19, PF02410.15, PF03652.15, PF00584.20, PF03840.14, PF00344.20, PF01668.18, PF00750.19, PF01746.21, PF02367.17, PF02130.17, and PF02699.15). This is a Bayesian phylogeny, and each node represents 100% credibility based on the model. Branch lengths are the number of expected changes per site (amino acid in the proteins). Figure reused from Tsypin et. al (Tsypin et al., 2020b).

Both the MLSA phylogeny (Figure 13) and whole-genome comparisons (Table 4) returned the type strain *C. portucalensis* A60T as the closest relative to *C. portucalensis* MBL. In the whole-genome comparisons, only *C. portucalensis* Effluent_1 and A60T gave values above the thresholds for species identity (Goris et al., 2007; Kurtz et al., 2004; Ribeiro et al., 2017; Richter et al., 2016; Richter and Rosselló-Móra, 2009; Teeling et al., 2004). The *C. portucalensis* MBL genome has a total length of 5,311,497 nt with seven total scaffolds, none of which are circularized. The N50 value is 5,245,291 nt and corresponds to the single chromosome scaffold. There are two putative plasmid scaffolds, which we named pCpMBL1 and pCpMBL2 (50,894 bp and 5,198 bp, respectively) and which we identified by homology; pCpMBL1 is likely an F plasmid and contains homologs to all components of the conjugation apparatus, and I was able to circularize it via Primordium sequencing. I annotated the genome using the Prokaryotic Genome Annotation Pipeline (PGAP) (Haft et al., 2018; Tatusova et al., 2016). Current research on *C. portucalensis* MBL is directed toward understanding its redox physiology.

Table 4. Whole genome comparisons used to identify *C. portucalensis* MBL.

Reference genome (GenBank accession no.)	BLAST ANI (%)	Proportion BLAST aligned (%)	MUMmer ANI (%)	Proportion MUMmer aligned (%)	Pearson's correlation coefficient for tetranucleotide usage
C. portucalensis A60^{T} (MVFY00000000.1)	98.42[a]	84.79	98.78[a]	85.43	0.99923[a]
C. portucalensis Effluent_1 (NZ_CP039327.1)	97.81[a]	82.92	98.31[a]	83.43	0.99908[a]
Citrobacter braakii FDAARGOS_253 (NZ_CP020448.2)	92.5	79.75	93.15	80.66	0.99707[b]
Citrobacter werkmanii BF-6 (NZ_CP019986.1)	90.32	78.4	91.15	78.6	0.9963[b]
Citrobacter freundii CFNIH1 (NZ_CP007557.1)	90.32	77.25	91.1	77.87	0.99596[b]
Citrobacter youngae NCTC13709 (NZ_LR134485.1)	89.27	75.07	90.33	74.52	0.99759[b]

Citrobacter koseri ATCC BAA-895 (NC_009792.1)	83.05	65.21	85.43	54.95	0.97119
Citrobacter amalonaticus Y19 (NZ_CP011132.1)	81.74	66.53	85.23	49.16	0.98547
Citrobacter farmeri AUSMDU00008141 (NZ_CP022695.1)	81.47	66.96	85.01	49.17	0.98683
Citrobacter rodentium ICC168 (NC_013716.1)	81.28	62.37	84.98	43.83	0.94412
E. coli O157:H7 Sakai (NC_002695.2)	80.28	62.16	84.67	38.66	0.97933

[a] Values above the threshold for species identity (Richter et al., 2016). [b] Values within the range for species identity (Richter et al., 2016). Table reused from Tsypin et al. (Tsypin et al., 2020b).

DISCUSSION

The primary result of this chapter that is that we were able to discover PCA oxidation where we expected it: in topsoil under anoxic conditions when cells were provided a respirable terminal electron acceptor. The secondary result is that it appears that we need not have looked very far because all the isolates from the enrichment and two quasi-random laboratory strains all performed the activity. This was intriguing to me because I expected that the ability to oxidize PCA, should it exist, would have evolved under selection in a specific niche, meaning that evolutionary distant organisms would not necessarily share the trait. Yet, in Figures 11 and 12, we see that it is present in both γ- and β-proteobacteria, the former including *C. portucalensis* MBL (a member of the Enterics) and the sundry pseudomonads and the latter including *Pseudogulbenkiania* MAI-1. Furthermore, these organisms were all isolated from different environments: *C. portucalensis* MBL and the *P. nitroreducens* strains came from our topsoil enrichment; *P. aeruginosa* UCBPP-PA14 came from a human burn wound (Mathee, 2018); *Pseudogulbenkiania* MAI-1 was isolated from Lake Matano in Indonesia, which is rich in iron oxides. The mechanism for PCA oxidation must then be shared or similar among these disparate organisms.

All of the experiments in this chapter are exploratory and preliminary. For example, I did not have the wherewithal to develop calibration curves for the PCA fluorescence data, and the

electrochemical assays were not replicated. In part, this is because my attention was pulled in many directions. The *P. nitroreducens* colony waves, for example, were very enticing, but the difficulty of doing the electrochemical experiment setup just to see them was too much of a task to follow up on curiosity. My notes from that time do say that *P. aeruginosa* UCBPP-PA14 had a very similar colony morphology under the same conditions, but I never followed up to see if I could find any propagating waves. It is certainly possible that one could drive the spreading strain of *P. nitroreducens* or *P. aeruginosa* to form the waves after a more simple procedure, maybe just starving them or pre-growing them in the PCA oxidation medium, but I cannot be sure. It also is not obvious what these waves actually are: the phase contrast (Figure 10) images imply that there is a change in either cell density or focal plane as the wave propagates. Maybe it is some kind of water evaporation phenomenon. Maybe it is collective motion. Who knows?

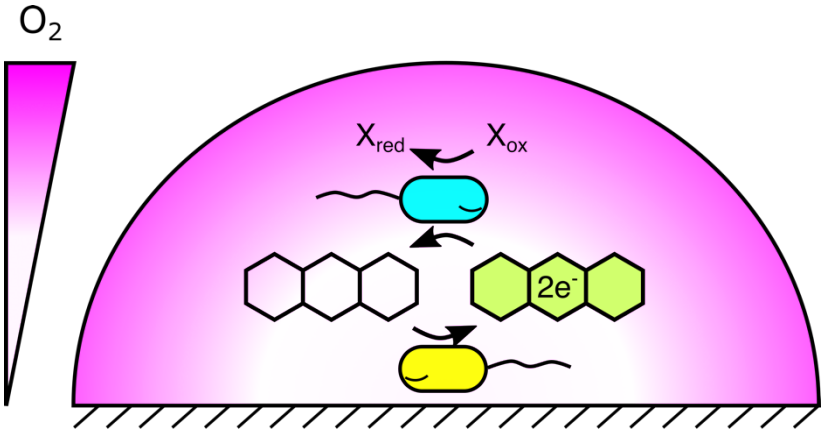

Figure 14. A model for phenazine redox cycling in a biofilm. A modification of the phenazine redox cycling depicted in Figure 2. A cell lacking a TEA may reduce a phenazine in its stead, which may then be re-oxidized by a different cell that does have access to a TEA such as oxygen (symbolized by X). This schema would provide a way for the cells to compensate for each other's metabolic lacks without generating toxic intermediates like superoxide, which benefits the biofilm as a whole.

It was interesting to see from the *C. Portucalensis* MBL genome that it cannot synthesize phenazines. This was also apparent from the supernatants of *C. portucalensis* MBL and *P. nitroreducens* cultures, which never developed any color. While I did not attain whole genome sequences for the *P. nitroreducens* strains, their relatives in available databases do not have phenazine biosynthesis genes either. So, these phenazine-oxidizing organisms rely on their neighbors to get access to the molecules. This invites an electron-shuttle cross-feeding model, in which one

bacterium that is starved for a terminal electron acceptor reduces phenazines (as has been observed for *P. aeruginosa* (Glasser et al., 2014)) and another that is starved for an electron donor oxidizes phenazines, thus completing a local redox cycle (Figure 14). Intriguingly, some of the cultures in Figure 11 showed PCA reduction *following* PCA oxidation, specifically when provided nitrate. A testable hypothesis, which I will discuss in the following chapter, is that the point at which the cells start to reduce PCA is the point at which they run out of the provided TEA. If this is the case, then the two cells in Figure 14 do not have to be of different species, but simply members of the same species with different compounds available to them. Thus, an organism like *P. aeruginosa*, which synthesizes its own phenazines, could be self-sufficient in its phenazine redox cycle.

Looking at the PCA oxidation dynamics of *C. portucalensis* MBL and the two *P. nitroreducens* strains that were co-enriched with it, I see another potential cross-feeding mechanic. When cells respire nitrate, they convert it to nitrite (Sparacino-Watkins et al., 2014). *C. portucalensis* is more efficient than the *P. nitroreducens* strains at oxidizing PCA with nitrate, but the reverse is true for nitrite. Thus, a co-culture of *C. portucalensis* MBL with either *P. nitroreducens* strain is likely to drive PCA oxidation further than either would on its own. Recalling the results in Equations 6–10 in Chapter 1, any of these cultures should drive PCA oxidation to completion if it can couple this oxidation to anaerobic respiration. In the case when multiple strains may be competing for a TEA, such as nitrate, but only some strains can use nitrite, they can split their TEA usage. The more limiting factor becomes the reduced PCA, as its oxidation can be driven to completion by two parallel reactions. This will occur even if the culture was initially provided only nitrate because it will be converted to nitrite during respiration. While I did not try to isolate any bacteria from the slower enrichment cultures, it would stand to reason that, perhaps, those cultures did not have bacteria that could couple PCA oxidation to nitrite respiration.

Altogether, this chapter leaves us with a phenomenon (PCA oxidation) that appears widespread and robust. The following two chapters aim to rigorously show that the observed PCA oxidation is not due to some abiotic artifact and go on to describe the underlying biological mechanism.

CHAPTER 3: THE PHENOMENOLOGY OF PCA OXIDATION

> *Her answer is simple. Over and over again, she tells us one must have the time to look, the patience to "hear what the material has to say to you," the openness to "let it come to you." Above all, one must have "a feeling for the organism."*
> —Evelyn Fox Keller on Barbara McClintock in *A Feeling for the Organism* (p. 198)

ABSTRACT

I found that PCA oxidation by various γ-proteobacterial strains proceeds in a nitrate-dependent manner and is decoupled from growth. However, the dynamics of PCA oxidation are dependent on the assayed strain. I infer that bacterial PCA oxidation is widespread and genetically determined. Notably, oxidizing PCA enhances the rate of nitrate reduction to nitrite by *C. portucalensis* MBL beyond the stoichiometric exchange of electrons from PCA to nitrate, which I attribute to *C. portucalensis* MBL's ability to also reduce oxidized PCA, thereby catalyzing a complete PCA redox cycle. This bidirectionality highlights the versatility of PCA as a biological redox agent. Because nitrate is a prevalent terminal electron acceptor in diverse anoxic environments, including soils, and phenazine producers are widespread, this observation of linked phenazine and nitrogen redox cycling suggests an underappreciated role for redox-active secreted metabolites in the environment. This chapter is a reanalysis and expansion of our 2021 publication (Tsypin and Newman, 2021).

NARRATIVE

After identifying *C. portucalensis* MBL as the dominant PCA-oxidizing organism (when provided nitrate as a TEA) in the most active enrichment cultures, I set out to describe the phenomenology of PCA oxidation more rigorously. Specifically, I wanted to show that (1) PCA oxidation is biologically driven process and not an artifact of some abiotic reaction(s) (Figure 15); (2) PCA oxidation is directly coupled to anaerobic respiration; (3) PCA oxidation is phylogenetically widespread. I saw these as three prerequisites to beginning to understand the underlying mechanisms of PCA oxidation. My basic approach was to elaborate upon the experiments I described in Chapter 2 with more robust protocols, calibration curves, etc.

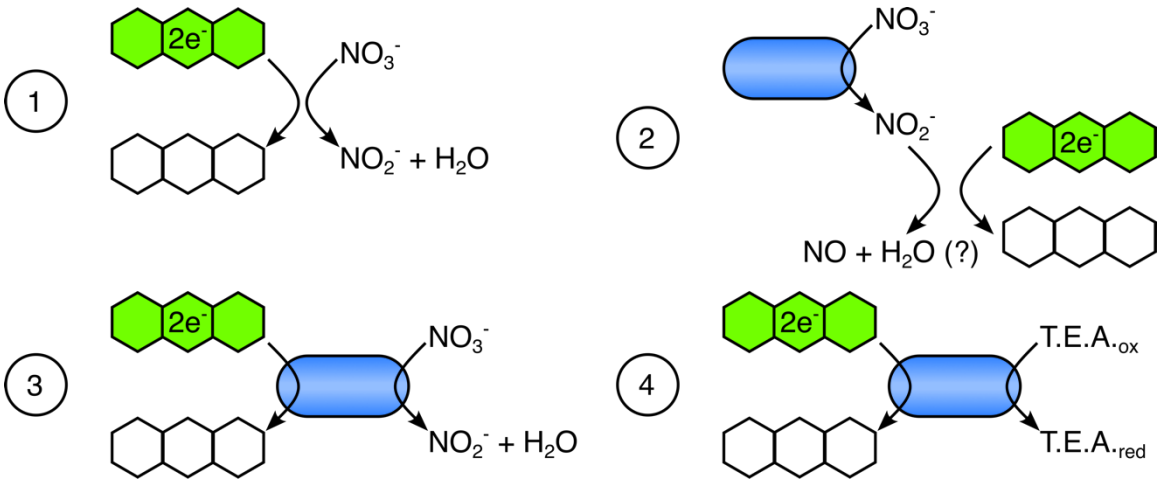

Figure 15. Possible models of PCA oxidation. There are four formal models of PCA oxidation that need to be explored: 1) a abiotic oxidation by nitrate; 2) an abiotic oxidation by nitrite, which is produced by cells during PCA oxidation; 3) biological coupling of PCA oxidation to nitrate respiration; 4) biological coupling of PCA oxidation to any appropriate anaerobic respiration of a given terminal electron acceptor (TEA).

Materials and Methods

Strains and media

Citrobacter portucalensis MBL was isolated in Chapter 1 (Tsypin et al., 2020b, 2020a). In the comparative PCA oxidation and reduction experiments, I used strains of γ-proteobacteria that cannot synthesize phenazines, either natively or due to mutations. I used *E. coli* MG1655, *P. aeruginosa* UCBPP-PA14 Δphz* (Meirelles et al., 2021), *Pseudomonas chlororaphis* phzB::TnLuxAB (strain PCL1119 obtained from G. Bloemberg, Leiden University (Hernandez et al., 2004)), and *Pseudomonas aureofaciens* phzB::lacZ (strain 30-84Z obtained from L. Pierson, University of Arizona (Morello et al., 2004)). The wild-type pseudomonads can synthesize PCA, but the mutants I employed cannot. All strains were grown and incubated under the same conditions. The basal medium for the experiments contained 20 mM potassium phosphate buffer (final pH 7), 1 mM sodium sulfate, 10 mM ammonium chloride, 1× SL-10 trace elements (MediaDive solution ID S4178), 1× freshwater salt solution (17.1 mM sodium chloride, 1.97 mM magnesium chloride, 0.68 mM calcium chloride, and 6.71 mM potassium chloride), and 1× 13-vitamin solution (10 µM morpholinepropanesulfonic acid [MOPS] [pH 7.2], 0.1 µg/ml riboflavin, 0.03 µg/ml biotin, 0.1 µg/ml thiamine HCl, 0.1 µg/ml l-ascorbic acid, 0.1 µg/ml d-Ca-pantothenate,

0.1 μg/ml folic acid, 0.1 μg/ml nicotinic acid, 0.1 μg/ml 4-aminobenzoic acid, 0.1 μg/ml pyridoxine HCl, 0.1 μg/ml lipoic acid, 0.1 μg/ml NAD, 0.1 μg/ml thiamine pyrophosphate, and 0.01 μg/ml cyanocobalamin). Depending on the experimental condition, as indicated in the figure legends, a terminal electron acceptor would be added or omitted. For oxidized PCA, a 10 mM stock in 20 mM NaOH was prepared. For reduced PCA, an 800 μM stock in the basal medium was reduced by electrolysis using the same electrode chamber set up as in Chapter 1. Both oxidized and reduced stocks were diluted into wells in 96-well plates (BRAND Cat./No 781671) to a final target concentration of 200 μM.

Cell preparation for plate reader experiments

All cell incubations and experiments were performed at 30°C. Cell stocks were preserved in 35% glycerol at −80°C. Two days prior to the experiments, frozen cells for each strain assayed were struck out on lysogeny broth (LB) agar plates and incubated overnight. The evening prior to the experiment, a patch from the streaks was inoculated into liquid LB in a respective culture tube and incubated slanted, shaking at 250 rpm, overnight. The morning of the experiment, 1 ml of each cell culture was washed three times into the basal medium by spinning for 2 min at 6,000 × g, aspirating the supernatant, and gently resuspending with a pipette. The optical density at 600 nm (OD_{600}) of each washed culture was measured. The cultures were brought into a Coy glove box, where they were washed three times into the same basal medium that had been made anoxic, following the same procedure as described above. After being left to stand for 1 to 2 h, the cells were inoculated into the different experimental conditions at a target starting OD_{600} of 0.1.

PCA redox plate reader measurements and nitrogen oxide concentration measurements

All PCA redox measurements were performed in a Coy chamber (5% hydrogen/95% nitrogen headspace) using a BioTek Synergy 5 plate reader. Reduced PCA concentration was measured by fluorescence (excitation 360/40 nm and emission 528/20 nm) (Sullivan et al., 2011) and calibrated against a curve included with every experiment. Plates were incubated shaking on the "medium" setting. For nitrogen oxide concentration measurements, *C. portucalensis* MBL cells were prepared as described above but incubated in culture tubes in the Coy chamber to allow for sampling. In these cultures, either 0 mM, 10 mM, or 50 mM acetate was provided. The tubes

were kept at 30°C, but not shaking. Samples were filtered through a 0.2-μm cellulose-acetate spin filter and stored at -80°C prior to analysis. Nitrate and nitrite concentrations were measured by ion chromatography using a Dionex ICS-2000 instrument or colorimetry using the Greiss reaction (Miranda et al., 2001).

Electrochemistry survival experiments

Electrode chambers were set up as in Chapter 2, using the medium described in the *Strain and media* section above. Cells were pre-grown in LB overnight at 30 ºC in slanted tubes shaking at 250 rpm to stationary phase. The cells were then washed three times into the basal medium and resuspended at an OD_{600} of 70, after which they were transferred to the mBraun anoxic glove-box. There, 1 mL of the cell suspension was added to a 100 mL final volume in the electrode chamber. When PCA was provided, it was at a concentration of 100 μM and pre-reduced by electrolysis the previous day. The cultures were sampled for CFUs, bulk ATP content, and nitrite concentrations over time. For the ATP content measurement, 20 μL of a given electrode chamber culture was mixed into 180 μL DMSO, which was then diluted into 800 μL 0.1 M HEPES buffer (pH 7.5) and stored at -80 ºC for up to a week (Glasser et al., 2014). The ATP samples were then assayed with a Promega BacTiter-Glo kit according to manufacturer instructions. As discussed in a previous lab paper, the high DMSO concentration had no effect on the assay (Glasser et al., 2014). Samples for nitrite concentration were filtered through a 0.2 μm cellulose-acetate filter and stored at -80 ºC before being measured colorimetrically (Miranda et al., 2001). Samples for CFU counts were serially diluted in ten-fold increments and plated on LB agar.

Data analysis

The data and code for the graphs generated in this chapter can be found at https://github.com/ltsypin/PhD_Thesis.

RESULTS

In Chapter 1, we saw that the enrichments and clonal strains that I tested could all oxidize PCA with nitrate. In certain conditions (Figure 11, nitrate added (green points)), the cultures began to reduce PCA after a certain period of time, implying a direct relationship between the availability of nitrate and PCA oxidation. Still, there remained a possibility that the PCA oxidation was due to some abiotic process: for example, the PCA could be oxidized by nitrate abiotically (Figure

15-1), or the PCA could be oxidized by nitrite abiotically, even if that nitrite comes from cellular activity (Figure 15-2). In order to determine whether there truly is a biologically mechanism underlying PCA oxidation in my experiments, I set out to test more rigorously how different species oxidize PCA and whether the oxidation activity can be directly attributed to anaerobic respiration.

First, I repeated an analogous experiment to that in Figures 11 and 12, with the adjustments that no acetate was added (to keep PCAred as the only provided electron donor) and with a calibration curve to compute PCAred concentrations from the fluorescence data (Figure 16). Here, I compared my *C. portucalensis* MBL isolate (labeled MBL in the figure) against *E. coli* MG1655, *P. aeruginosa* UCBPP-PA14 Δ*phz**, *P. aureofaciens* PhzB::lacZ, and *P. chlororaphis* PhzB::TnLuxAB. These pseudomonad strains cannot synthesize phenazines.

The only abiotic condition that stimulated PCA oxidation was the one with nitrite (Figure 16, dark blue squares, top and middle panels), which rules out the scenario in Figure 15-1, but allows for the one in Figure 15-2. However, *C. portucalensis* MBL, when provided nitrate, oxidizes PCA much faster than the abiotic nitrite condition, which indicates that this activity cannot be explained by the model in Figure 15-2. Moreover, *C. portucalensis* MBL is the only organism that appreciably oxidizes PCA with fumarate under these conditions, and fumarate has no abiotic activity with PCA. Both *E. coli* and *P. aeruginosa* Δ*phz** oxidize PCA with nitrate at a rate that cannot be explained by an abiotic reaction with nitrite. *P. chlororaphis* PhzB::TnLuxAB and *P. aureofaciens* PhzB::lacZ oxidize PCA with nitrite faster than the abiotic rate.

Looking at the time it takes the different strains to reach a threshold of 75% of the maximum PCAred concentration, we see a complementary picture: when no TEA is provided, the PCA is not appreciably oxidized by any strain. With fumarate, only *C. portucalensis* MBL can reach the threshold within 24 hours. Given nitrite, the abiotic condition and the pseudomonads reach the threshold, with *P. chlororaphis* PhzB::TnLuxAB and *P. aureofaciens* PhzB::lacZ being the fastest, and *P. aeruginosa* Δ*phz** roughly equivalent to the abiotic control. Provided nitrate, *C. portucalensis* MBL reached the threshold the fastest, followed by *P. aeruginosa* Δ*phz** and then *E. coli*.

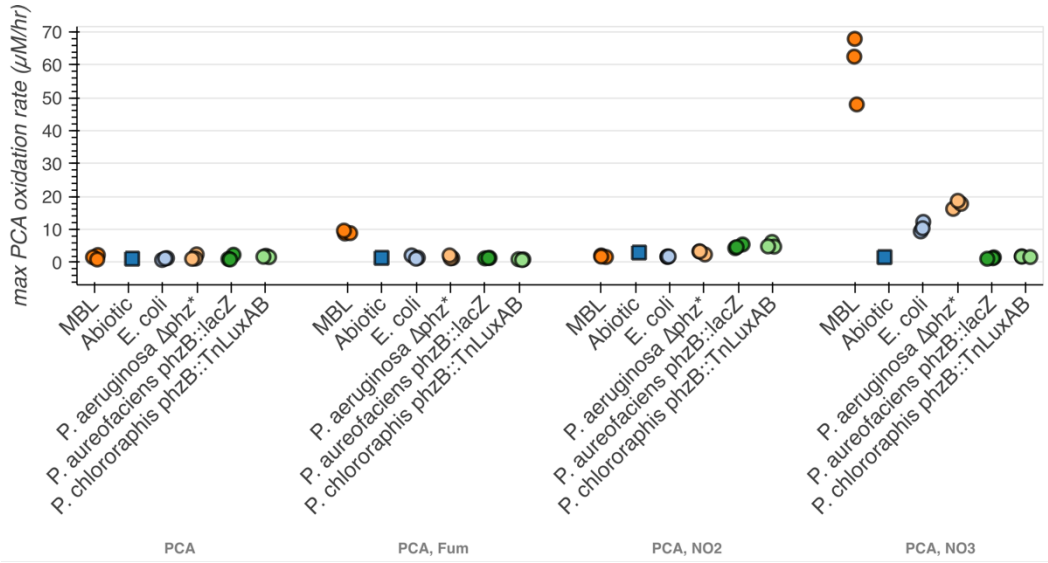
max PCA oxidation rate (μM/hr)
70
60
50
40
30
20
10
0
MBL
Abiotic
E. coli
P. aeruginosa Δphz*
P. aureofaciens phzB::lacZ
P. chlororaphis phzB::TnLuxAB
PCA
PCA, Fum
PCA, NO2
PCA, NO3

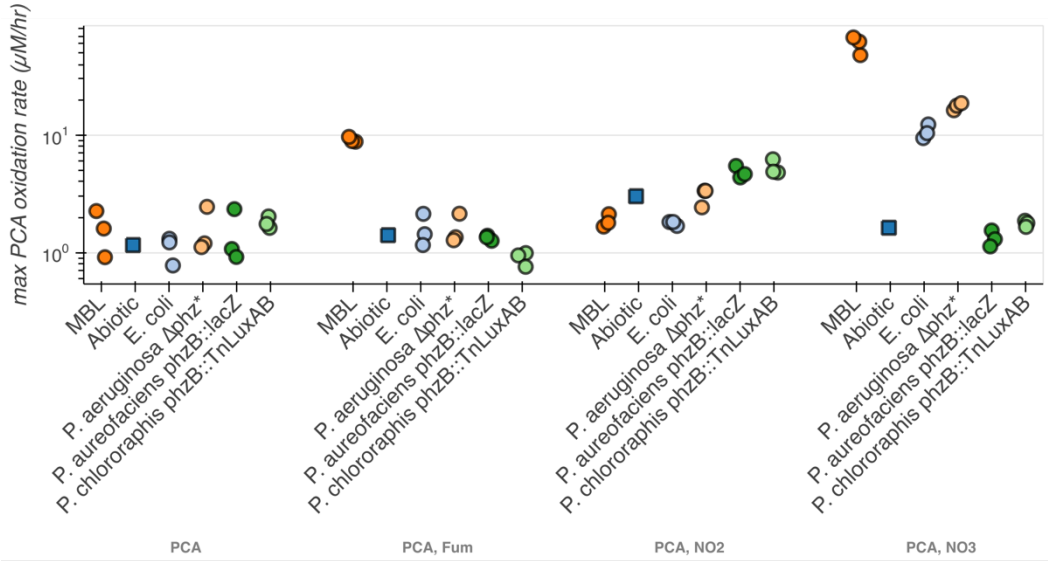
max PCA oxidation rate (μM/hr)
10^1
10^0
MBL
Abiotic
E. coli
P. aeruginosa Δphz*
P. aureofaciens phzB::lacZ
P. chlororaphis phzB::TnLuxAB
PCA
PCA, Fum
PCA, NO2
PCA, NO3

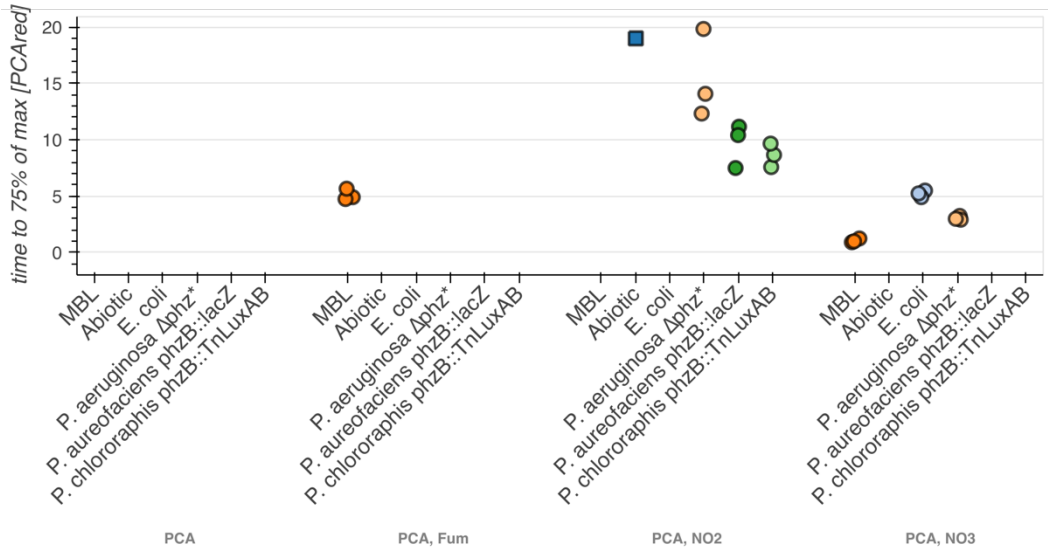
time to 75% of max [PCAred]
20
15
10
5
0
MBL
Abiotic
E. coli
P. aeruginosa Δphz*
P. aureofaciens phzB::lacZ
P. chlororaphis phzB::TnLuxAB
PCA
PCA, Fum
PCA, NO2
PCA, NO3

Figure 16. A more rigorous comparison of PCA oxidation activities. Assay performed and analyzed as in Figures 11 and 12, with the exceptions that no acetate was provided and the PCAred concentration were computed from a calibration curve. Circles represent biological replicates, and squares represent technical replicates. The labels on the x-axis represent the different strains, grouped by condition, where "PCA" indicates assays with no TEA provided, "PCA, Fum" indicates assays with PCAred and 10 mM fumarate, etc. Top: The maximum PCA oxidation rate in μM/hr for each strain and condition. Middle: Same data, but with the y-axis on a logarithmic scale. Bottom: The time (in hours) it took for each strain under each condition to reach 75% of the maximum PCAred concentration. The assay was run over the course of 24 hours, so any conditions that did not reach the threshold by that point are not charted.

Altogether, these data indicate that for some organisms, such as *E. coli*, the model in Figure 15-3 is correct, at least under the tested conditions: it only oxidizes PCA with nitrate, and the oxidation rate cannot be explained by abiotic reactions with either nitrate or nitrite. For other organisms, though, it is clear that the scenario in Figure 15-4 is correct. *C. portucalensis* can drive PCA oxidation with either nitrate or fumarate. The pseudomonads can do so with either nitrate or nitrite (with the exception of *P. aeruginosa* Δ*phz**, for which it is not clear whether it does anything in addition to the abiotic reaction).

To test more directly whether the presence of nitrate is causative for *C. portucalensis*' oxidation of PCA, I monitored the current in electrode chambers inoculated with *C. portucalensis* MBL, which started with either 0 or 5 mM nitrate, to which I spiked more nitrate at different intervals (Figure 17). Without any nitrate provided, there was no current in the system (Figure 17, top left). When given 5 mM nitrate, the cells immediately produced a current by oxidizing PCA, but that current mostly dissipated after 12–16 hours (Figure 17, top right). Spiking in 5 mM nitrate every 24 hours was sufficient to stimulate a second cycle of PCA oxidation (Figure 17, bottom left), and spiking it in every 12 hours led to a constant current. In all conditions with nitrate, the maximum current was roughly equivalent.

These results correspond to the observation that *C. portucalensis* MBL does not effectively couple PCA oxidation to nitrite respiration (Figures 11, 12, and 16). However, there remains the possibility that the cells still reduce nitrite to nitric oxide (the next step in denitrification) without coupling it to PCA oxidation. I tracked the consumption of nitrate and production of nitrite using ion chromatography, comparing conditions with and without 200 μM reduced or oxidized PCA and with 0, 10, or 50 mM acetate in anaerobic incubations (without an electrode to cycle the PCA) (Figure 18). Regardless of the PCA or acetate content, the conversion of nitrate to nitrite was stoichiometric, and nitrite concentrations never dropped, indicating that *C. portucalensis* MBL does not further reduce nitrite once it is produced during nitrate respiration, as is the case for *E. coli* (Abou-Jaoudé et al., 1979; Lin and Iuchi, 1991).

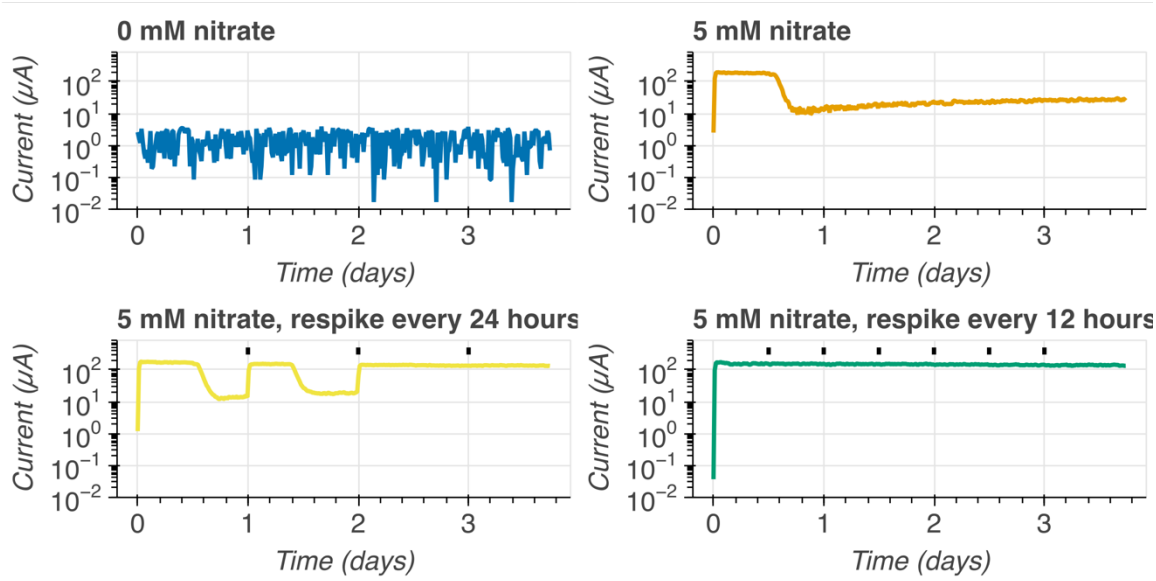

Figure 17. PCA oxidation in direct response to nitrate addition. Current traces of cultures in electrode chambers, all containing 100 μM PCA in the basal medium and a working electrode poised at -500 mV to continuously reduce the PCA. A current indicates that the cells (*C. portucalensis* MBL) are oxidizing PCA. Vertical black bars indicate when more nitrate was spiked into the electrode chamber. These data comprise a single replicate.

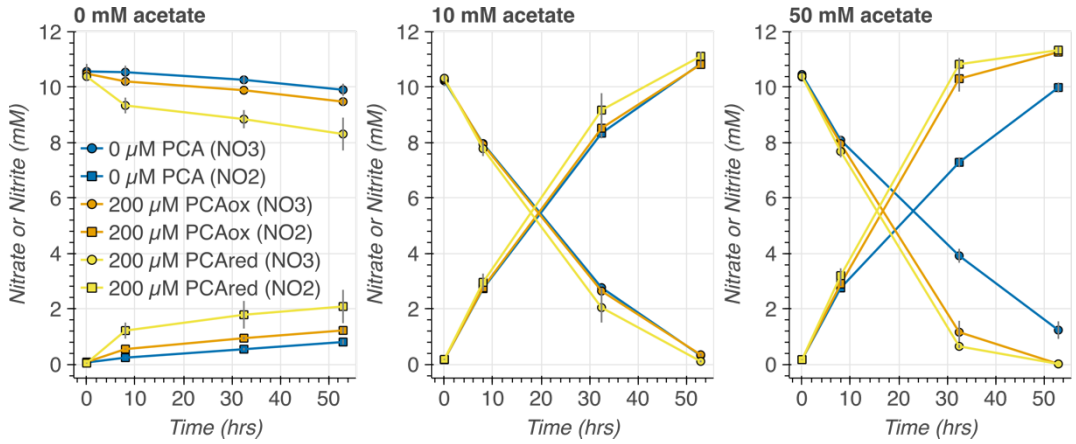

Figure 18. *C. portucalensis* MBL stops at nitrite. Ion chromatography results for nitrate and nitrite concentrations over time (hours). Circles, starting from ~10 mM, correspond to nitrate concentrations, and squares, starting from 0 mM correspond to nitrite concentrations. Error bars represent 95% confidence intervals around the mean of three biological replicates. Blue traces represent cultures with no PCA, orange traces to ones starting with 200 μM oxidized PCA (PCAox), and yellow traces to ones starting with 200 μM reduced PCA (PCAred). The left panel is reused from our published work, distributed under a CC-BY 4.0 license © Tsypin and Newman (2021).

In the case with no acetate (Figure 18, left), providing reduced PCA (yellow traces), as opposed to the oxidized PCA or no PCA conditions, induces a disproportionally greater rate of nitrate respiration. In fact, over the first eight hours, the rate of nitrite production was 22 ± 3 μM/hr with no PCA, 58 ± 2 μM/hr with initially oxidized PCA, and 147 ± 4 μM/hr with initially reduced PCA. Under these conditions, 200 μM PCA is oxidized within 10 hours (Tsypin and Newman, 2021), so the expected average rate of PCA oxidation is only 20 μM/hr. Thus, the presence of reduced PCA stimulates an approximately seven-fold greater increase in nitrate respiration than would be expected by the stoichiometry of a single course of PCA oxidation.

In the 10 mM acetate condition (Figure 18, middle), there is no difference between the different PCA additives. In the 50 mM acetate condition (Figure 18, right), the difference emerges after the second time point. Here, it does not matter whether the cultures started with reduced or oxidized PCA, just that the PCA is available. This indicates that, after the first period of the incubation, the PCA helps *C. portucalensis* MBL convey electrons from acetate to nitrate. Given that PCA oxidation helps stimulate nitrate respiration under either 0 or 50 mM acetate conditions, I wanted to assess whether this has an effect on cell viability or ATP content.

I assayed a matrix of conditions in the electrode chamber setup to compare the effects of sustained PCA oxidation with an initial concentration of 10 mM nitrate on CFUs, bulk ATP content, and nitrite concentrations (Table 5; the pluses indicate inclusion, and the minuses indicate omission). For the CFU, ATP, and nitrite measurements, the cultures were sampled at the start of the assay, 4 hours, 8 hours, 16 hours, 40 hours, 64 hours, and 88 hours). First, comparing the currents generated, the addition of acetate greatly reduces the duration of PCA oxidation (Figure 19). Drawing upon the results in Figures 17 and 18, this indicates that the cultures with acetate quickly deplete nitrate, which is reflected by the nitrite concentrations I measured (Figure 20). Without acetate in the electrode chambers, the PCA oxidizing cultures (Figure 20, top left) typically take between one and two days to deplete the nitrate, corresponding to the loss of current (Figure 19, top left). Meanwhile the cultures that have neither acetate nor PCA take between two and three days to deplete their nitrate. Once again, PCA oxidation increases the rate of nitrate respiration by the cells. When acetate is provided, its contribution to nitrate reduction overwhelms most effects from PCA or its oxidation (Figure 20, bottom two rows). The only potential

difference is in the nitrite concentrations at the second time point (~4 hours), where it appears that the presence of PCA may slightly slow down the production of nitrite.

Table 5. Condition matrix for assessing physiological effects of PCA oxidation.

Chamber	*100 μM PCA*	*50 mM Acetate*	*-500 mV electrode*
0	+	-	+
1	-	-	+
2	+	+	+
3	-	+	+
4	+	+	-
5	-	+	-

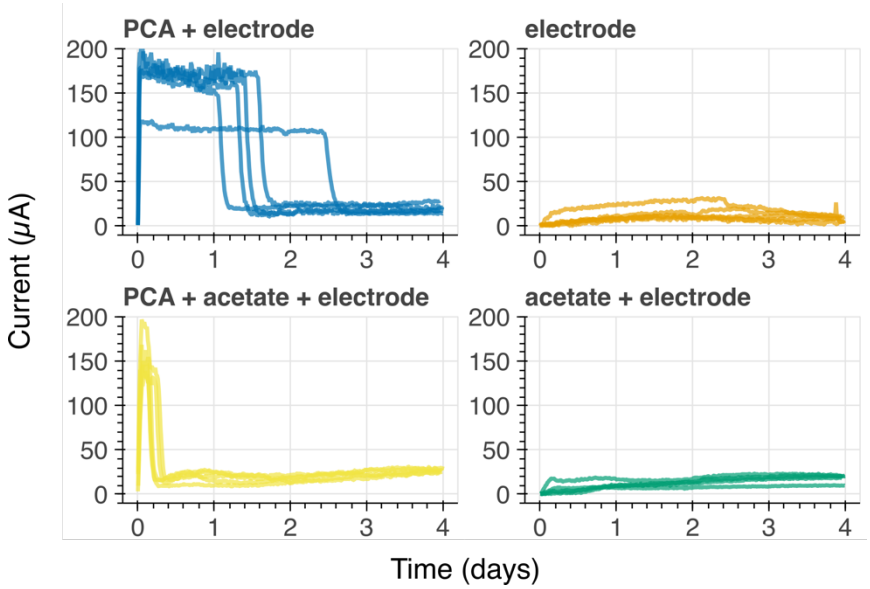

Figure 19. Duration of PCA oxidation in electrode chambers. The cells (*C. portucalensis* MBL) generate a current only when both PCA and a reducing electrode are available (left column). When acetate is provided, the duration of PCA oxidation is greatly reduced from a minimum of one day to a maximum of ~10 hours. Each trace is a biological replicate.

These differences between the PCA oxidizing and no-PCA conditions suggest that there may be a reflection in bulk ATP content (Figure 21) and CFU counts (Figure 22). In the case of bulk ATP content, there are two differences: first, comparing PCA oxidizing vs. no-PCA conditions without acetate (Figure 21, top row), it appears that the PCA oxidizing cultures have greater variance in their ATP levels at the Day 2 mark than the cultures without PCA. Second, comparing PCA oxidizing vs. no-PCA conditions with 50 mM acetate (Figure 21, middle row), the PCA-

oxidizing cultures have a higher ATP content at 16 hours than the non-oxidizing cultures. A similar, though smaller effect may be present in the +/- PCA comparison with acetate and no electrode (Figure 21, bottom row).

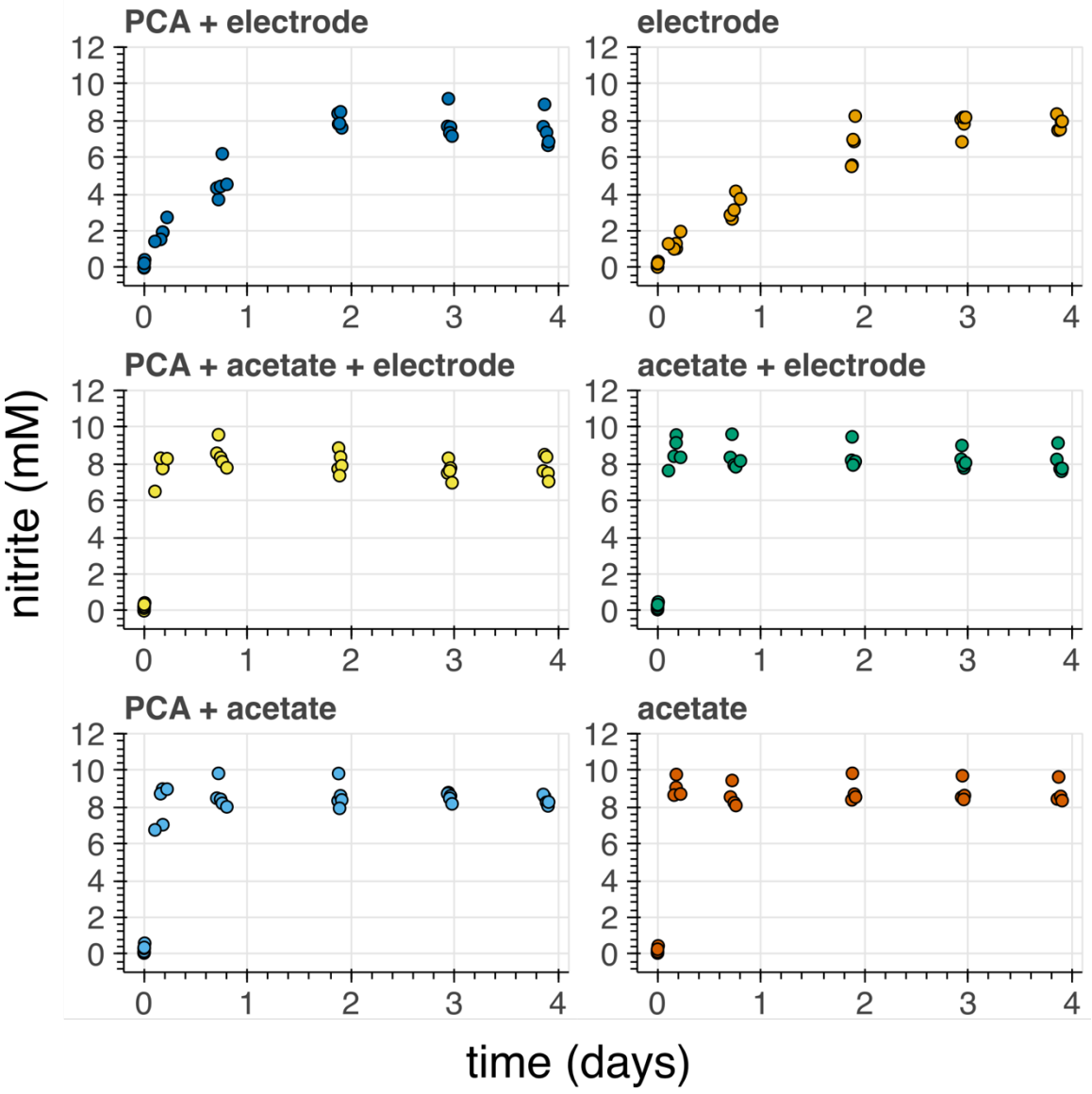

Figure 20. Nitrite concentrations during PCA oxidation in electrode chambers. All the conditions showed nitrate reduction to nitrite, and the strongest effect on the rate came from the addition of acetate. However, when comparing the two conditions without acetate, which differ in whether there is sustained PCA oxidation, it is clear that PCA oxidation increases the rate of nitrate respiration. Every point is a biological replicate.

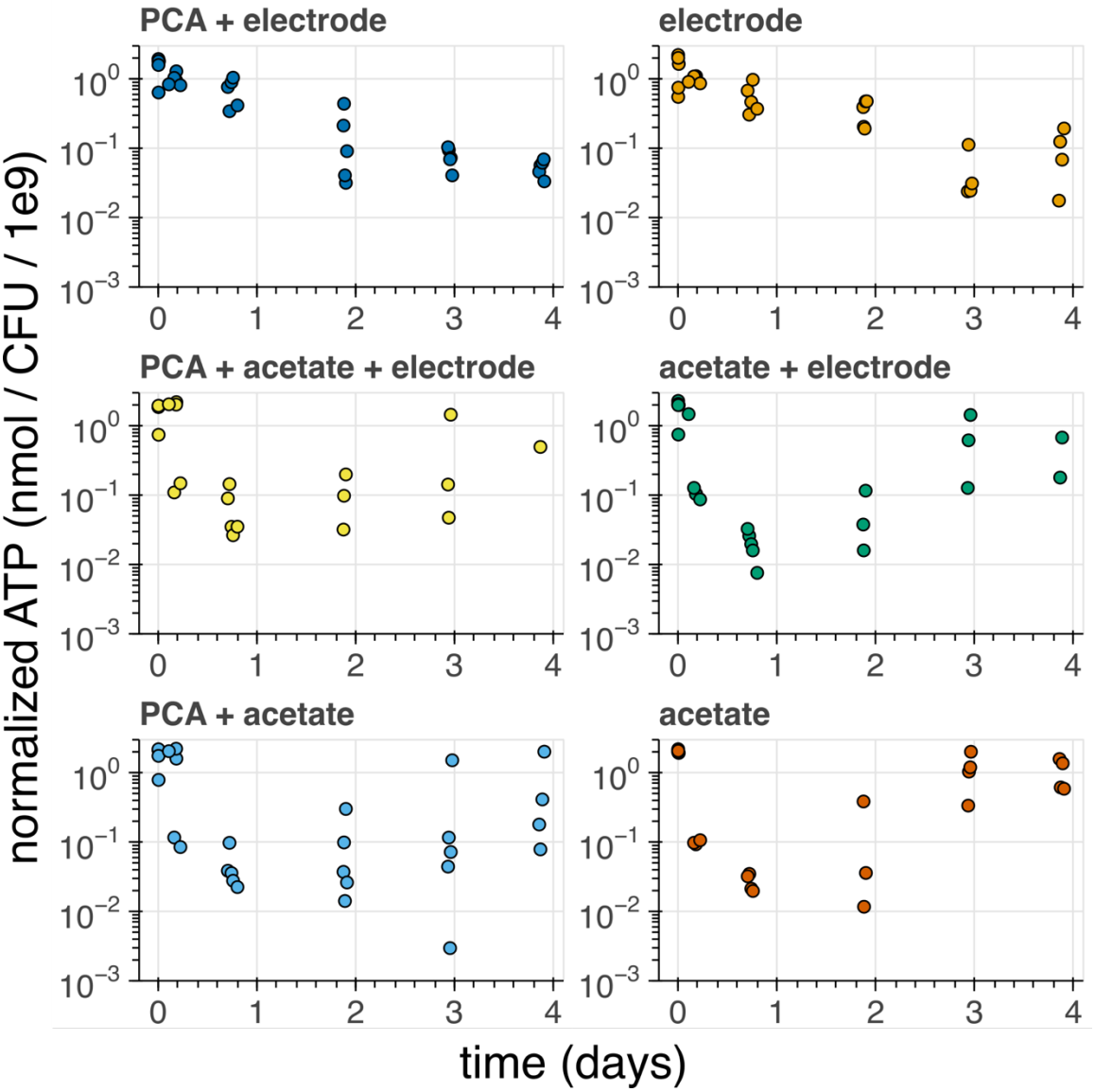

Figure 21. Bulk ATP content during PCA oxidation in electrode chambers. Comparing the same conditions as in Figure 20, these data present the bulk ATP content in electrode chambers over time. The ATP content is calculated as nmol ATP per CFU and scaled by a factor of 10^9 to be more easily comprehensible. The y-axes are on a logarithmic scale.

The cell viability/survival data, as indicated by CFUs, indicated that the addition of acetate was the most harmful intervention for the cells (Figure 22). Without acetate, the PCA-oxidizing cultures maintained a steady viability through the duration of the experiment (Figure 22, top left), but the cultures without PCA began to die off around the fourth day (Figure 22, top right). With acetate but no electrode, the cultures with PCA (Figure 22, bottom left) fared better on average than the cultures without PCA (Figure 22, bottom right). Provided

the electrode and acetate, the cultures had equivalent viabilities regardless of PCA oxidation until the fourth day, when cultures that oxidized PCA (Figure 22, middle left) had a lower average CFU Count that the cultures that did not have PCA (Figure 22, middle right).

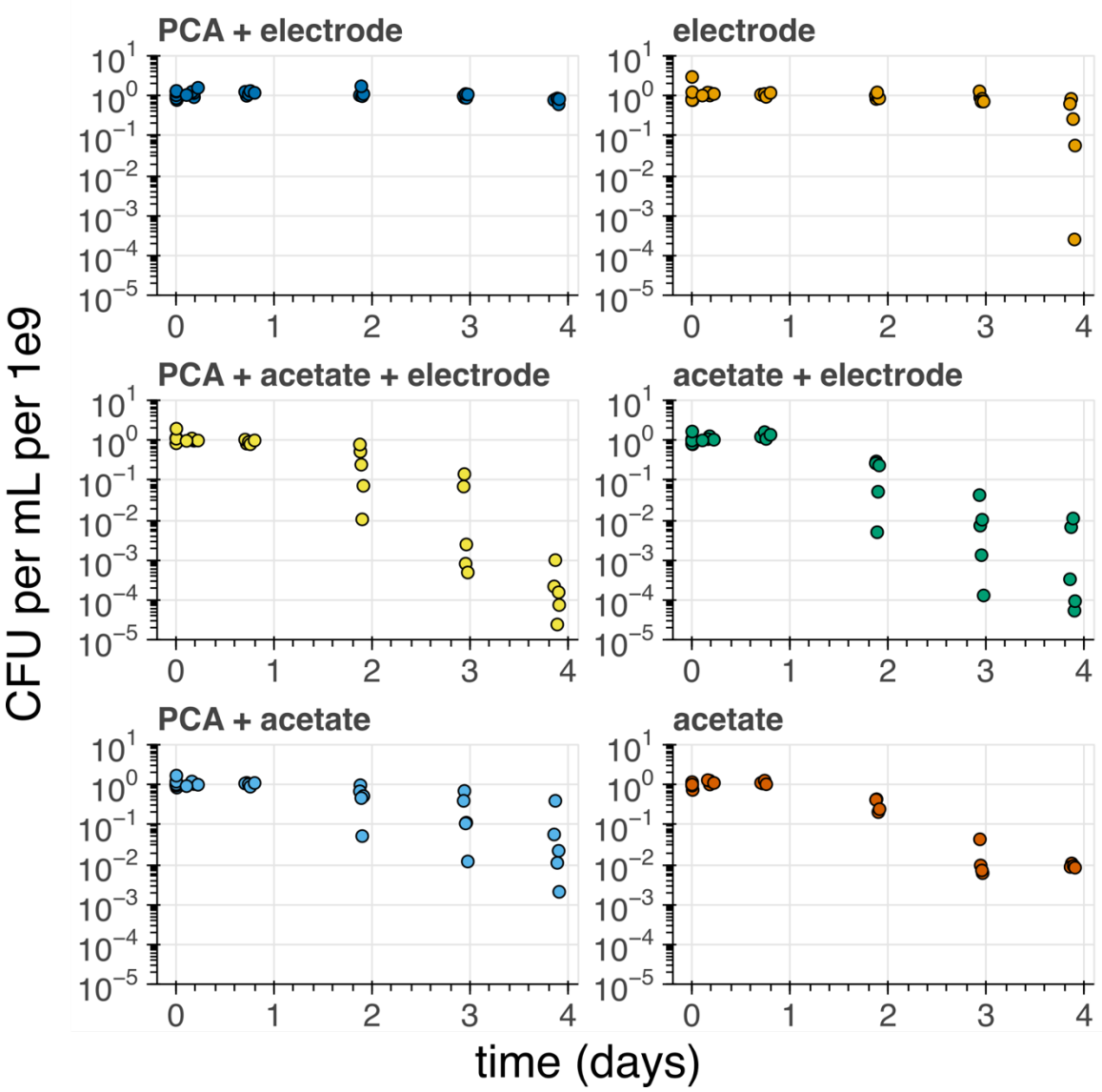

Figure 22. CFU counts during PCA oxidation in electrode chambers. Comparing the same conditions as in Figures 20 and 21, these data show the viable colony counts (CFUs) over the course of the electrode chamber experiments. At each sampling, the culture aliquots were serially diluted 10-fold and plated on LB agar. The colonies were allowed to grow over several days to allow for long lag-phases of slow but viable cells. To avoid overgrowth obscuring new colonies, the plates were incubated at room temperature after the first night and examined every day for new colonies.

DISCUSSION

This chapter aims to outline what happens during PCA oxidation. Without invoking any particular mechanism, I wanted to use the above experiments to understand all the knobs I could turn to induce or halt PCA oxidation. I also wanted to be able to make a statement on whether oxidizing PCA has any consequence for the cells. The primary observation is that rapid, sustained PCA oxidation requires both bacteria and an appropriate terminal electron acceptor (TEA) to be present. Which TEA is appropriate depends on the species or strain of bacteria and the medium. With *C. Portucalensis* MBL, the initial observation in Figures 11 and 12 showed that only nitrate was an appropriate TEA, but the follow up experiment in Figure 16 showed that fumarate also works. The main difference between these two experiments is that the latter does not include acetate. This means that when the cells have access to acetate, they do not use fumarate as a TEA, but they do in the absence of acetate. Similarly, the other assayed species couple PCA oxidation to different combinations of TEAs. This begins to suggest two things: 1) the underlying mechanism of PCA oxidation during anaerobic respiration is shared regardless of which compound is being respired; 2) whether a bacterium can oxidize PCA under a given condition will be determined by which anaerobic respiratory machinery is expressed. I follow up on both these ideas in the next chapter.

In trying to assess what happens when *C. portucalensis* MBL oxidizes PCA, I came upon a very tangled set of interactions between the PCA being oxidized, the carbon source, and the terminal electron acceptor. I limited my study here to only acetate and nitrate as the carbon source and TEA, but I am not sure that I have fully wrapped my head around that combination, much less explored what would happen with other compounds. It was relatively easy to show that, as I predicted from the result in Figure 11, *C. portucalensis* MBL begins to reduce PCA when it runs out of an appropriate terminal electron acceptor. The fact that it stops oxidizing PCA when nitrate runs out (and resumes oxidizing it) is clear from the current data in Figure 19. An indirect bit of evidence that it begins *reducing* PCA when nitrate is unavailable is that *C. portucalensis* MBL quells the abiotic oxidation activity of nitrite (Figure 16). Finally, in our published work (Figure S1), I was able to show that *C. portucalensis* MBL (and other assayed bacteria) reduces PCA when given only oxidized PCA to start with an no appropriate TEA for its oxidation (Tsypin and Newman, 2021).

Leaving aside the addition of acetate for now, I found that there is a positive feedback loop: nitrate stimulates *C. portucalensis* MBL to oxidize PCA, and oxidizing PCA increases the rate of nitrate respiration. Furthermore, it is not the case that the PCA simply donates its electrons to nitrate once because the increase in nitrate reduction is not stoichiometric to the 200 μM PCAred that was provided in the assay (Figure 18, left). In these assays, the cells are pre-grown to stationary phase in LB, which presumably leaves them with copious intracellular carbon stores (e.g., glycogen and polyhydroxyalkanoates), meaning that they have the capacity to reduce terminal electron acceptors without any additional electron donors. This is evident in the blue and orange traces in Figure 18, left. Thus, the cells may be catalyzing a complete PCA redox cycle: during nitrate respiration, the cells (1) oxidize PCA and deliver those electrons to nitrate, (2) oxidize intracellular carbon stores and reduce nitrate and PCA, (3) oxidize the PCA again to reduce more nitrate (Figure 23).

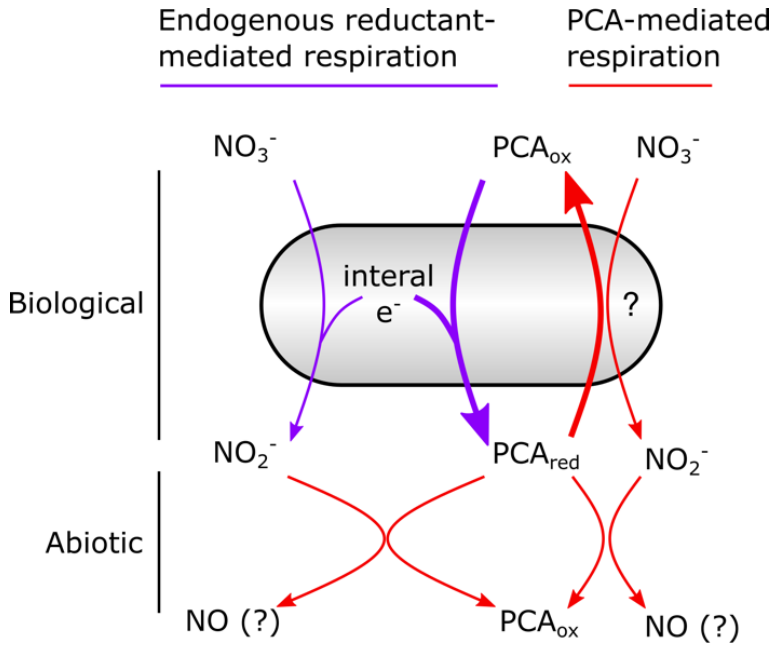

Figure 23. A model of a PCA redox cycle driven by a single cell. Red arrows correspond to reactions that drive PCA oxidation, and purple arrows correspond to ones that drive PCA reduction. During nitrate respiration after being grown to stationary phase in LB, *C. portucalensis* MBL may drive all the depicted reactions, depending on the balance of compound concentrations. The different effects of these reactions are seen in the experiments above, but these experiments do not speak to the actual mechanism that connects PCA oxidation to nitrate respirate (represented by a question mark). This figure is adapted from our published work, distributed under a CC-BY 4.0 license © Tsypin and Newman, 2021.

When provided 10 mM nitrate in an electrode chamber, thanks to an electrode that re-reduces the PCA, *C. portucalensis* MBL continuously oxidizes PCA for at least a day until the nitrate is consumed (Figure 19). When compared to a condition that has no PCA but retains the electrode, the cells that oxidized PCA for a day maintain a higher average viability on day four of the experiment (Figure 22), despite consuming nitrate faster (Figure 20). I am not sure that I have a cogent explanation for this, especially given the fact that running out of nitrate fast when given acetate corresponded to a faster loss of viability regardless of condition (Figure 22). It appears that acetate dysregulated the cells' metabolism: whenever I tried to culture *C. portucalensis* MBL on acetate in the minimal medium I used for all my assays, they never grew regardless of whether I tried 10 or 50 mM acetate concentrations (Wolfe, 2005). Notably, they grew in the same medium with citrate. Combined with the nitrate depletion and loss of viability, the fact that the cells do not seem to be able to use acetate to grow may mean that my experiments inadvertently put them under reductive stress (an excess of electrons and reducing equivalents). This is not ideal for experiments meant to test the possible contributions of PCA oxidation to cell fitness (it would be better for the cells to be under oxidative stress), but it may help explain why PCA oxidation compounded appears to compound the loss of viability due to acetate (Figure 22, left bottom and middle). That said, simply the addition of a reducing electrode with no PCA had a similar effect (Figure 22, right bottom and middle), so it may be that the electrode itself is sufficient to compound the reductive stress.

While there are subtle difference in bulk ATP content under the different conditions in Figure 21, there only clear effect is that the ATP levels drop when nitrate is depleted, which makes sense because the cells lose their ability to respire. At this point, the cells would like to reduce PCA, but the electrode may outcompete them, leaving them under the aforementioned reductive stress. It may be the case that I inadvertently used a poor medium for assessing ATP content: it has a high concentration of inorganic phosphate as a buffer, which may have destabilized the ATP before I could measure it (Nate Glasser, personal communication). Perhaps, were these experiments done with a different buffer, such as MOPS, more subtle effects on the ATP levels would have been evident.

When looking at an analogous experiment, but with no electrode to continuously re-reduce PCA (or cause reductive stress), the interactions between PCA and acetate insofar as the effect nitrate respiration rates are a bit easier to explain. In Figure 18, the left panel showed that PCA oxidation stimulates nitrate reduction, as I discussed above. In the middle panel, with 10 mM added, whether PCA is present (or whether is starts as oxidized or reduced) no longer has an effect. However, the right panel shows that, without PCA, nitrate reduction is slower with 50 mM acetate than with 10 mM acetate, but, with PCA, nitrate reduction is *faster* than with 10 mM acetate. Again, it does not matter here whether the PCA was initially reduced or oxidized. This result indicates that, somehow, PCA is more effective at conveying electrons to nitrate than is acetate: when cells reduce PCA with acetate, more nitrate is ultimately reduced over time.

Having done the experiments described in this chapter, I felt confident that I could reproducibly control PCA oxidation by *C. portucalensis* MBL and develop the appropriate experimental conditions to determine the underlying mechanisms. Based on the species comparisons in Figures 11, 12, and 16, I had a suspicion that the key was the presence and regulation of elements of the electron transport chain. My target became the question mark in Figure 23.

CHAPTER 4: THE GENETIC MECHANISMS OF PCA OXIDATION

The obstacle is the path.
—Zen proverb

ABSTRACT

PCA oxidation by *C. portucalensis* MBL is directly coupled to anaerobic respiration. It can respire nitrate, fumarate, DMSO, and TMAO, each of which stimulates PCA oxidation in the presence of cells. For compounds that have multiple redundant terminal reductases, such as nitrate, for which *C. portucalensis* encodes NarG, NarZ, and NapA, any reductase is sufficient to drive oxidation. However, whether that reductase is expressed appears to depend on the pre-growth conditions, according to the regulatory modes of the genes. Consequently, knocking out all available terminal reductases for a given TEA (e.g., a *narGnarZnapA* mutant provided nitrate) abolishes PCA oxidation activity. Thus, an *frdA* mutant loses PCA oxidation activity with fumarate, and a *dmsA* mutant loses PCA oxidation activity with DMSO. The DMSO reductase complex is promiscuous, also reducing TMAO, and the *dmsA* mutant loses some of its PCA oxidation activity with TMAO. I was not able to fully abolish PCA oxidation activity with TMAO even in a *dmsAtorA* double mutant, implying that there is another TMAO reductase in *C. portucalensis* MBL that I did not identify. Knocking out all three quinones—ubiqinone (UQ), menaquinone (MQ), and demethylmenaquinone (DMQ)—in *C. portucalensis* MBL stopped the majority of PCA oxidation activity, but in certain cases, such as with nitrate, some activity remained. For example, the *menAubiCnapAnarZ* quadruple mutant retained PCA oxidation activity with nitrate via NarG. This indicates that, while any anaerobic respiration ETC can drive PCA oxidation via electron flux through the quinone-quinol pool, some terminal reductases can accept electrons from reduced PCA instead of a quinol.

NARRATIVE

In the preceding chapters I found three key facts: 1) every strain I tested could oxidize PCA with an appropriate TEA; 2) the appropriate TEA was not necessarily the same for each strain; 3) a single strain could use multiple distinct TEAs to oxidize PCA. This implies that the different strains may have different means for accomplishing PCA oxidation, but within a strain the PCA oxidizing the underlying mechanisms may be shared between multiple pathways, which would

be a more parsimonious explanation than every terminal reductase having evolved a unique means of taking electrons from PCA. This prompts two questions: Do the different strains that have different appropriate TEAs have different terminal reductases? Do all anaerobic respiration pathways have a common underlying mechanism?

The first question is complicated by the fact that a given organism may have gene(s) for a terminal reductase that are not expressed under the assayed condition, rendering it equivalent to a total absence. However, this can only be determined by direct measurement of gene expression (and preferably protein detection). Consequently, a presence of a gene in a strain's genome does not necessarily mean that that gene is active; only the absence of a gene from a genome is definitive. This is evident in comparing Figure 12 to Figure 16, in the case of *C. portucalensis* MBL and fumarate. In Figure 12, fumarate does not induce PCA oxidation, but it does in Figure 16, the difference between the two experiments being the presence or absence of acetate, respectively. Thus, acetate appears to "turn off" the causative gene(s) that couple PCA oxidation to fumarate respiration.

In *E. coli* MG1655 and *C. portucalensis* MBL, there are two protein complexes that can participate in terminal fumarate reduction: the succinate dehydrogenase (SDH) and the fumarate reductase (FRD). Normally, the SDH functions to oxidize succinate to fumarate as part of the tricarboxylic acid cycle, but it can function in reverse if necessary. The pseudomonads I tested possess the SDH complex but lack the FRD complex.[9] The FRD complex which appears to be rare within the whole Pseudomonad phylogenetic group unless recently acquired by horizontal gene transfer (Unden and Cole, 1983). Thus, one possible interpretation of the fact that, in Figure 16, only *C. portucalensis* MBL oxidizes PCA when given fumarate is that the pseudomonads simply cannot do so because they lack the FRD, and the *E. coli* does not because it does not express the FRD under these conditions, much as *C. portucalensis* MBL did not express it in Figure 12.

---

[9] Assessed by searching the pseudomonas.com database and by running a protein BLAST of the *E. coli* MG1655 FrdA sequence against *P. aeruginosa* UCBPP-PA14, *P. aureofaciens*, and *P. aureofaciens* subspecies *chlororaphis* 30-84.

Given that the situation of multiple redundant protein complexes that may be differentially expressed is poorly constrained, it is more intelligible to think about the second question: whether there is a shared mechanism for PCA oxidation when a strain can use several different TEAs to drive the process. Every respiratory electron transport chain (ETC) depends on the quinone/quinol pool, quinones being similar to phenazines in that they act as electron shuttles that may be reduced or oxidized depending on the conditions. The different quinones all have midpoint potentials that are more positive than that of PCA:

7) $UQ + 2e^- + 2H^+ \rightarrow UQH_2$ $E^{o'}_{1/2} = +113$ mV (Thauer et al., 1977);

8) $DMQ + 2e^- + 2H^+ \rightarrow DMQH_2$ $E^{o'}_{1/2} = +40$ mV (Unden and Bongaerts, 1997);

9) $MQ + 2e^- + 2H^+ \rightarrow MQH_2$ $E^{o'}_{1/2} = -74$ mV (Thauer et al., 1977).

Consequently, as I calculated for the various TEAs in Chapter 1, the oxidation of PCA by any of the quinones will be thermodynamically favorable under standard conditions. Applying the same calculation as in equations 3–6 in Chapter 1, we get that

10) $PCAred + UQ \rightarrow PCAox + UQH_2$ $E^{o'} = +229$ mV; $\Delta G^{o'} = -44$ kJ
Reaction stops when the ratio of products to reactants is 5×10^7 to 1;

11) $PCAred + DMQ \rightarrow PCAox + DMQH_2$ $E^{o'} = +156$ mV; $\Delta G^{o'} = -30$ kJ
Reaction stops when the ratio of products to reactants is 2×10^5 to 1;

12) $PCAred + MQ \rightarrow PCAox + MQH_2$ $E^{o'} = +42$ mV; $\Delta G^{o'} = -8$ kJ
Reaction stops when the ratio of products to reactants is 25 to 1.

Reaction 12 is the only one we have seen that could be said to not proceed to completion. However, since the purpose of a quinol (e.g., MQH_2) is to deliver its electrons to the TEA (e.g., fumarate), the quinone (e.g., MQ) is regenerated if the TEA is being respired. In other words, one of the products of reaction 12 will be converted back into a reactant by the cell under the relevant metabolic context. Consequently, so long as there is electron flux through the quinone-quinol pool, PCA can be fully oxidized via any of the quinones.

You may have noticed that some of the quinones are incompatible with some of the TEAs, based on their midpoint potentials. For example, the reaction between ubiquinol and fumarate would give

13) UQH_2 + fumarate → UQ + succinate $E^{o'} = -80$ mV; $\Delta G^{o'} = +15$ kJ
Reaction stops when the ratio of products to reactants is 2×10^{-3} to 1.

In other words, the reaction would proceed only when there is at least 2000 times more reactants than products, which is possible but not at all necessary in a cell during the course of its regular metabolism. Consequently, the heuristic hierarchy is that all quinols can participate in nitrate respiration; menaquinols (and, to a lesser extent, demethylmenaquinols) can participate in fumarate respiration; menaquinols and demethylmenaquinols (and, to a lesser extent, ubiquinols) can participate in DMSO and TMAO respiration. Thus, the prediction is that if menaquinone is of principal importance for PCA oxidation, its role should be evident in every form of anaerobic respiration. If it is demethylmenaquinone, its role will manifest mostly in DMSO and TMAO respiration, and perhaps subtly in fumarate respiration. If it is ubiquinone, it will have the most obvious effect on nitrate respiration. However, if PCA can circumvent the quinone-quinol pool and be oxidized by the terminal reductase more directly, the various quinones will appear to have no role.

Figure 24 shows a visual representation for the two different models of PCA oxidation: (1) terminal reductase interaction and (2) quinol regeneration. Here, the PCA is depicted in the periplasm because its carboxylic acid group is deprotonated at circumneutral pH, making the molecule charged (Figure 3). Small, charged molecules cannot easily cross the polarized inner membrane of metabolically active cells, and so PCA will not passively diffuse into the cytosol. Formally, it is possible that there are transporters that may bring it into the cytosol, but I do not consider this case in my analysis.[10] This picture holds for every terminal reductase in *C. portucalensis* MBL except for the periplasmic nitrate reductase Nap, which, appropriate to its name, is in the periplasm, which would grant PCA direct access to the active site of nitrate reduction

[10] Unlike the inner membrane, the outer membrane is permeable to charge molecules due to porin complexes.

(Sparacino-Watkins et al., 2014). Nonetheless, the basic quinone-quinol architecture holds as well for Nap as for the other complexes.

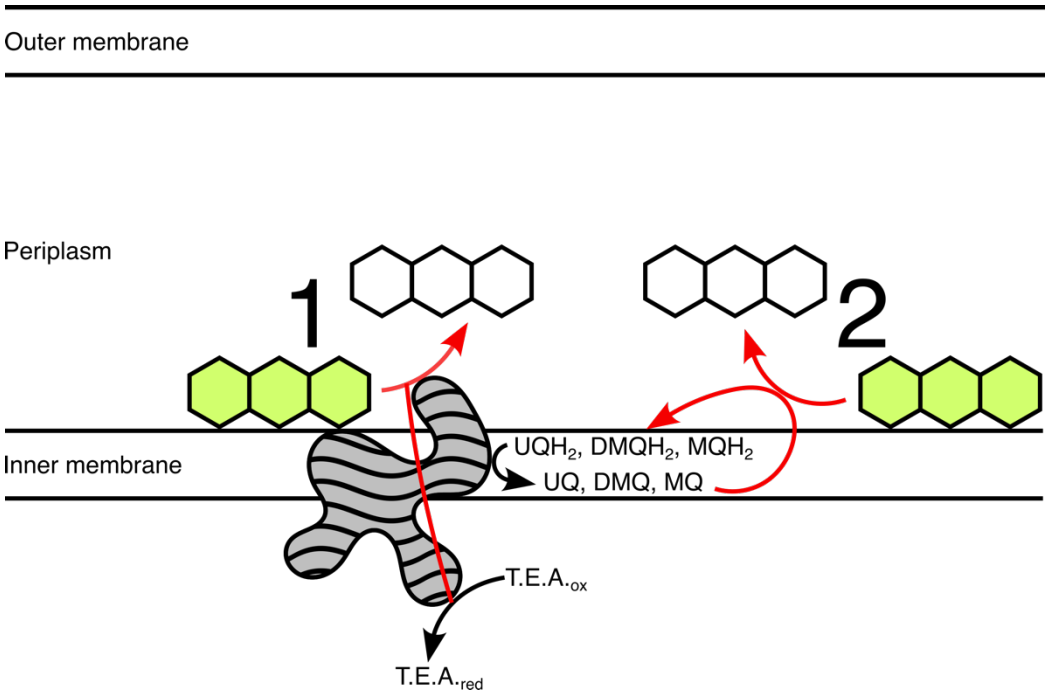

Figure 24. How PCA oxidation may be coupled to anaerobic respiration. This figure is an abstracted diagram of the very end of anaerobic respiration, where quinols donate electrons to the terminal reductase (grey, wavy object). The reduced phenazine (green) may donate electrons by either (1) delivering them to the terminal reductase or (2) regenerating the quinol pool. This diagram does not consider whether there are any intermediary steps in either process.

This schema in Figure 24 provides a guide to systematically dissecting what might be the underlying mechanism of PCA oxidation. In the preceding chapters, I began to establish that nitrate and fumarate are sufficient for *C. portucalensis* MBL. Below, I establish this for DMSO and TMAO as well. To address Model 1 in Figure 24, I knock out the terminal reductases for a given TEA, combinatorically if there are redundant reductases. To address Model 2, I knockout the ubi- and –(demethyl)menaquinones, separately and in combination. To address the possibility of both models being relevant, I knock out quinones and terminal reductases in various combinations. But first, I needed to do some experiments to decide which approach to knocking out genes I wanted to pursue—classical deletions or translational knockouts—and I needed to establish the conditions when all the terminal reductases are present and play a role.

Strains, media, and plate reader assays

The strains used in this chapter are all different genotypes of the original *C. portucalensis* MBL isolate (Table 6). The medium used for plate reader experiments, which were conducted as in Chapter 3, was the same as in Chapter 3, except that the trace elements and vitamins were omitted. Thus, the basal medium comprised: 20 mM potassium phosphate buffer (pH 7-7.1); 1 mM sodium sulfate; 10 mM ammonium chloride; and 1× freshwater salt solution (17.1 mM sodium chloride, 1.97 mM magnesium chloride, 0.68 mM calcium chloride, and 6.71 mM potassium chloride). For the experiments in this chapter, I prepared a new stock of reduced PCA in this basal medium at a concentration of 1.2 mM by electrolysis. In every experiment, cultures were pre-grown in 5 mL LB for 17 hours ± 10 minutes at 30 ºC. As indicated in the experiment descriptions, the pre-growths were done in either slanted tubes shaken at 250 rpm, vertical tubes sealed with Parafilm around the caps without shaking, or vertical tubes sealed with Parafilm around the caps without shaking amended with an additional 40 mM nitrate. After the pre-growth incubation, the bacteria were washed three times into the basal medium (6000 × g for 2 minutes in microcentrifuge tubes). After the washes, the OD_{600} was measured for each culture. Depending on the genotype of the strain, they grew faster or slower, so I adjusted the final resuspension volume accordingly to be able to normalize the final concentration to OD_{600} between 0.2 and 1 for each culture. By the end of my PhD, I was able to consistently normalize each culture to an $OD_{600} = 0.5$. These washed cultures were brought into the Coy anoxic glovebox, transferred to anoxic microcentrifuge tubes, and allowed to deplete any dissolved oxygen for 1-2 hours. Following this incubation, I set up 96-well plate assays with the same clear-bottom black-walled plates as before (BRAND PureGrade™ S, Cat. No. 781671). In every experimental well, there would be 200 μM PCAred, 0 or 10 mM TEA, and cells at a starting $OD_{600} = 0.1$ (or an abiotic control), all suspended in the anoxic basal medium. The experiments were performed in either a BioTek Synergy 4 or Synergy HTX plate reader, and each run lasted at 24–48 hours. The exact protocol can be found in Appendix I. Data analysis pipeline for generating the graphs in this chapter can be found at https://github.com/ltsypin/PhD_Thesis.

Table 6. Genotypes of *C. portucalensis* MBL mutants used.

Genotype	Purpose
WT, wt, or MBL	The original "wildtype" isolate *C. portucalensis* MBL
menA	Translational knock out of menaquinones and demethylmenaquinones. This is a ubiquinone-only strain
ubiC	Translational knock out of ubiquinones. This is a menaquinone and demethylmenaquinone strain
menAubiC	Translational knock out of all quinones. Abolish the respiratory ETC
napA	Translational knock out of the periplasmic nitrate reductase catalytic subunit
narG	Translational knock out of the dominant respiratory nitrate reductase catalytic subunit
narZ	Translational knock out of the auxiliary respiratory nitrate reductase catalytic subunit
napAnarZ	A NarG-only strain for assessing its individual activity
narGnapA	A NarZ-only strain for assessing its individual activity
narGnarZ	A NapA-only strain for assessing its individual activity
napAnarZnarG	Translational knock out of all the nitrate reductases to assess their total necessity for PCA oxidation
frdA	Translational knock out of the fumarate reductase catalytic subunit
dmsA	Translational knock out of the DMSO reductase catalytic subunit
torA	Translational knock out of the TMAO reductase catalytic subunit
dmsAtorA	Double translational knock out of the DMSO and TMAO reductase catalytic subunits
menAubiCnapAnarZ	Quadruple translational knockout to assess the activity of NarG in the absence of quinones
menAubiC-narGnapA	Quadruple translational knockout to assess the activity of NarZ in the absence of quinones
menAubiCnarGnarZ	Quadruple translational knockout to assess the activity of NapA in the absence of quinones
WT/pHelper	The wildtype strain carrying the oligo-mediated recombineering helper plasmid
menA/pHelper	The *menA* translational knockout strain carrying the oligo-mediated recombineering helper plasmid
menAubiC/pHelper	The *menAubiC* double translational knockout strain carrying the oligo-mediated recombineering helper plasmid
menAubiC-napA/pHelper	The *menAubiCnapA* triple translational knockout strain carrying the oligo-mediated recombineering helper plasmid
menAubiC-narG/pHelper	The *menAubiCnarG* triple translational knockout strain carrying the oligo-mediated recombineering helper plasmid
napA/pHelper	The *napA* translational knockout strain carrying the oligo-mediated recombineering helper plasmid
napAnarZ/pHelper	The *napAnarZ* double translational knockout strain carrying the oligo-mediated recombineering helper plasmid

narG/pHelper	The *narG* translational knockout strain carrying the oligo-mediated recombineering helper plasmid
dmsA/pHelper	The *dmsA* translational knockout strain carrying the oligo-mediated recombineering helper plasmid
menAubiC/pFE21-MenA	Inducible expression of MenA in the full quinone knockout background to assess complementation
menAubiC/pFE21-UbiC	Inducible expression of UbiC in the full quinone knockout background to assess complementation
napA-narZnarG/pFE21-NapA	Inducible expression of NapA in the full nitrate reductase knockout background to assess complementation
napA-narZnarG/pFE21-NarZ	Inducible expression of NarZ in the full nitrate reductase knockout background to assess complementation
napA-narZnarG/pFE21-NarG	Inducible expression of NarG in the full nitrate reductase knockout background to assess complementation
frdA/pFE21-FrdA	Inducible expression of FrdA in the fumarate reductase knockout background
dmsA/pFE21-DmsA	Inducible expression of DmsA in the DMSO reductase knockout background
MBL/pKD46	WT strain carrying the helper plasmid for deletion by homologous recombination
Δ*napFDAGHBC*	Deletion of the entire Nap operon
Δ*narGHJI*	Deletion of the entire NarG operon
Δ*narUZYWV*	Deletion of the entire NarZ operon
Δ*narZYWV*	Deletion of the entire NarZ operon except for the nitrate-nitrite antiporter NarU
PA14	The wildtype *P. aeruginosa* UCBPP-PA14 strain
PA14 Δ*nar*	Δ*narG* deletion in the PA14 strain. Constructed by Steven Wilbert.
PA14 Δ*nap*	Δ*napAB* deletion in the PA14 strain. Constructed by Steven Wilbert.

Designing and engineering mutant strains

Nearly all the mutations I introduced were translational knockouts by way of oligo-mediated recombineering (Wannier et al., 2020), using a helper plasmid adapted by Scott Saunders. My exact protocol for oligo-mediated recombineering in *C. portucalensis* MBL is found in Appendix I. Allen Chen assisted me in making the *frdA* strain. When making combinations of knockouts in one background, I named the strains according the order in which genes were knocked out.

Table 7. Oligos used for oligo-mediated recombineering.

Name	5'-3' sequence
ubiC_MAGE_28-30	t*t*tggtcatggaatcttccaatTacTaTcagtcgagcagttgggcgtccagcgccgg-gatcgcatcaaaataacgcagcgcacgcagttg
ubiC_MASC_28-30_Rmut1	gacgcccaactgctcgactgAtAgtA
ubiC_MASC_28-30_Rwt1	gcccaactgctcgactggttgtt
ubiC_MASC_28-30_F330	gccaatctcaataaaatctcgggtcaatgtcg
ubiC_28-30_SeqR	gcgatacaatgccttcaggttataaatcgg
menA_MAGE_37-39	g*t*acggcattagcatAgtgATaaggatacttcgatccgctggttgctctgctggcattgat-tacggcaggactgctgcaaattctgtcca
menA_MASC_37-39_Fmut2	catcgtcggtacggcattagcatAgtgAT
menA_MASC_37-39_Fwt2	cggtacggcattagcatggtggc
menA_MASC_37-39_R250	cagcccggacagacagatcagca
menA_37-39_SeqF	atgactgaacaacaacaaattagccgctcac
napA_MAGE_92-94	c*t*gcgttaaacggtcttAtcACtacatgattttcggcaggaagtaacctttgatgcagttaa-gcccacggttaaccggcgcatccggatc
napA_MASC_92-94_Fmut2	caaaggttacttcctgccgaaaatcatgtaGTgaT
napA_MASC_92-94_Fwt2	ggttacttcctgccgaaaatcatgtacggaa
napA_MASC_92-94_R200	agagccgaacataccgatagactccgg
napA_92-94_seqF	cggaacgcagcagggg
napA_92-94_seqR	ggtcccagctaatcgggg
narZ_MAGE_109-111	c*a*cgcggcgccagctactcgtggtatctctatagcgctaaccgcTAgTaatGA cctctggtgcgtaaacgcttaatcgaattgtggcgcg
narZ_MASC_109-111_Fmut2	cgattaagcgtttacgcaccagaggTCattAcTA
narZ_MASC_109-111_Fwt2	cgattaagcgtttacgcaccagaggatatttcag
narZ_MASC_109-111_R300	gggcacgggcaagtgatgca
narZ_109_111_seqF	tttttgcgggtcgttcataatggatt
narZ_109_111_seqR	agatctacgttaaaaacgggctgg
natG_MAGE_163-165	t*g*atggtgtaaacgttagatgcagcaatcagttcattcacttActATcaggaagaac-gaacaaatccaccacgaccacgcgcttgtttga
narG_MASC_163-165_Fmut2	cgtggtggatttgttcgttcttcctgATagT
narG_MASC_163-165_Fwt2	gtggatttgttcgttcttcctggcagg
narG_MASC_163-165_R200	agtaccagtcgtagaagctcaggcagg
narG_163-165_SeqF	ggtagacgcatgggcatccatcatc
frdA_MAGE_121-123	a*g*cgtcaacgtacgtcgcttcggcggcatgTaaTGATagcgtacctggtttgccgcg-gataagaccggcttccacatgctgcatacgctg
frdA_MASC_121-123_Fmut	cgcttcggcggcatgTaaTGAT
frdA_MASC_121-123_Fwt	cgcttcggcggcatgaaaatcg
frdA_MASC_121-123_R343	cgaattccatatcacgcagcggaacg
frdA_121-123_SeqF	tcgcgcaggatcatgacagc
dmsA_MAGE_17-19	c*c*accgccagtccgcctatcgccgtcgttttcaccTaTcAtTAgcgactaac-ctcagctgccagcatggcatcggggatcttagttttca
dmsA_MASC_17-19_Fmut	cctatcgccgtcgttttcaccTaTcAtTA
dmsA_MASC_17-19_Fwt	cctatcgccgtcgttttcaccaaacctcg

dmsA_MASC_17-19_R244	gcctacctccataggagtaatactgcc
dmsA_17-19_SeqF	tgttgtcggtttcaacatactttatttcaccg
torA_MAGE_63-65	t*a*agcatatcgcaggggtatttgtcatgtttgaacggacgggtttcTTATcactAac-cgttgaccactttggcttcaaaagcgccatagt
torA_MASC_63-65_Fmut	agccaaagtggtcaacggtTagtgATAA
torA_MASC_63-65_Fwt	agccaaagtggtcaacggtgagtggacc
torA_MASC_63-65_R200	gcgcctgatcccaactgaccc
torA_63-65_SeqF	gcgatgtgtctgaaaccaacaaaaagtaagg

Asterisks indicate phosphorothioate bonds between nucleotides. Uppercase nucleotides indicate mutations from the wildtype sequence. MAGE oligos were used to introduce translational knockout mutations. MASC oligos were used to verify mutations by PCR. Seq oligos were used to amplify mutated regions for verification by sequencing.

To verify the translational knockout approach, I also engineered a couple of deletion strains using homologous recombination via the λRed recombinase (Datsenko and Wanner, 2000). The overall approach is similar to the one for translational knockouts described above, except instead of an oligo that converts three sequential codons to stops, you electroporate in an antibiotic resistance cassette (in my case, one with a gene for kanamycin resistance with flanking FRT sites) that replaces an entire genetic region by recombination. The protocol I used is in Appendix I.

Table 8. Oligos used for knocking out genes by homologous recombination.

Name	5'-3' sequence
Δnap_F	cgagggagggcgtcattatggaaggacaatgtcatgGTGTAGGCTG-GAGCTGCTTC
Δnap_R	acagtattctgtcatctcgctcgcaaagtaatttaCATATGAA-TATCCTCCTTAG
Δnap_check_F	ataaatagtgcagttttttatgtcgttcaacccg
Δnap_check_R	acgcgaaatgacagattgctgaacag
ΔnarGHJI_F	agagagccgtcaggctcctacaggagaaaaccgatgGTGTAGGCTG-GAGCTGCTTC
ΔnarGHJI_R	cgaagcagggttttgtcattctcaaatatacgattaCATATGAA-TATCCTCCTTAG
ΔnarGHJI_check_F	ttcgctctcaatcaagcaatgtcgatttatc
ΔnarGHJI_check_R	aaacaggcataaaaaaaccccgccg
ΔnarZYWV_F	cgtcggcaatattatcgaagcaggagttatgtcatgGTGTAGGCTG-GAGCTGCTTC
ΔnarZYWV_R	taagcacaagcgctaccgggcatcagagttcaattaCATATGAA-TATCCTCCTTAG
ΔnarUZYWV_F	tatctattctttcagtcaatattcctaaaactttcGTGTAGGCTG-GAGCTGCTTC
ΔnarUZYWV_R	aattatcggcgggaacgcactatctgatagcggcgaCATATGAA-TATCCTCCTTAG

ΔnarUZYWV_check_F	ttaagcaacgtgtaattctcccatcacg
ΔnarUZYWV_check_R	atcataacgtacaaaaagcgggatcgc
KanR_arbF	attcgcagcgcatcgccttctatc
λRed_F	tccacattgattatttgcacggcgtcac
λRed_R	ccggtgtcatgctgccaccttc

Lowercase letters in Δ primers indicate homology to the *C. portucalensis* MBL genome. Uppercase letters indicate homology to the pKD4 plasmid (Table 10).

I used the Gibson reaction to clone my complementation vectors, and my protocol is in Appendix I.

Table 9. Oligos used for cloning complementation vectors.

Name	5'-3' sequence
pZ/FE_backbone_F	caaataaaacgaaaggctcagtcgaaagac
pZ/FE_backbone_R	CTAGTAtttctcctctttaatgaattcggtcagtgc
pZ/FE_screen_F2	gacattaacctataaaaataggcgtatcacgagg
pZ/FE_screen_R2	ggcggatttgtcctactcaggagag
MenA_pZ/FE_F	accgaattcattaaagaggagaaaTACTAGtttttattggcgctaaa-tatgactgaacaacaac
MenA_pZ/FE_R	gtctttcgactgagcctttcgttttatttgttaaagagaccactgacttaa-gaaaattccaaagacaaac
UbiC_pZ/FE_F	accgaattcattaaagaggagaaaTACTAGatgccacaccctgcgttaac
UbiC_pZ/FE_R	gtctttcgactgagcctttcgttttatttgtttatcttcctctcagtacaacggcg
NapA_pZ/FE_F	accgaattcattaaagaggagaaaTACTAGtgagcaaggtgaggaaacaccatgaaac
NapA_pZ/FE_R2	gtctttcgactgagcctttcgttttatttgcagaaagcggcggcgg
NarZ_pZ/FE_F	accgaattcattaaagaggagaaaTACTAGatgagtaaactgttagaccgctttcgc
NarZ_pZ/FE_R	gtctttcgactgagcctttcgttttatttgtcatttttcgcctcctgtacctgatc
NarG_pZ/FE_F	accgaattcattaaagaggagaaaTACTAGaggagaaaaccgatgagtaaattcctg-gac
NarG_pZ/FE_R	gtctttcgactgagcctttcgttttatttgtcattttacgctctcctgtacctggtc
FrdA_pZ/FE_F	accgaattcattaaagaggagaaaTACTAGatgaagcatctgatttcaggcaggg
FrdA_pZ/FE_R	gtctttcgactgagcctttcgttttatttgttatagcgcaccacctcaactttcagg
dmsA_pZ/FE_F	accgaattcattaaagaggagaaaTACTAGatgaaaactaagatccccgatgccatgc
dmsA_pZ/FE_R	gtctttcgactgagcctttcgttttatttgttacacctttttcaacctgaacaaggttcg

Uppercase nucleotides indicate a modified spacer sequence between the ribosomal binding site and start codon. The first 30 nucleotides at the 5' end of each oligo starting with a gene name are homologous to the pFE21 plasmid (Table 10) to place the gene between the tetracycline-inducible promoter and the terminator in the correct orientation.

I electroporated plasmids (Table 10) into the desired strains according to the protocol in Appendix I. When assessing complementations, I performed the plate reader assays as described above, with the adjustment that 54 nM anhydrotetracyline was included in the overnight pre-

growth to induce gene expression in the plasmid. I determined this concentration with a pilot experiment measuring GFP fluorescence when titrating anhydrotetracycline added to MBL/pFE21-sfGFP cultures (data not shown).

Table 10. Plasmids used for knockouts and complementations.

Name	Purpose	Reference
pKD46	λRed helper, temperature-sensitive origin of replication, confers ampicillin resistance	(Datsenko and Wanner, 2000)
pKD4	Kanamycin vector with FRT sites	(Datsenko and Wanner, 2000)
pCP20	FLPase vector, temperature-sensitive origin of replication, confers ampicillin resistance	(Datsenko and Wanner, 2000)
pHelper	Oligo recombineering helper vector, cloned into backbone with SacB, confers gentamicin resistance	Scott Saunders, adapted from (Wannier et al., 2020)
pFE21-sfGFP	Tetracycline-inducible promoter driving gene expression, confers kanamycin resistance	(Flamholz et al., 2020)
pFE21-MenA	pFE21 for inducible MenA expression	This work
pFE21-UbiC	pFE21 for inducible UbiC expression	This work
pFE21-NapA	pFE21 for inducible NapA expression	This work
pFE21-NarZ	pFE21 for inducible NarZ expression	This work
pFE21-NarG	pFE21 for inducible NarG expression	This work
pFE21-FrdA	pFE21 for inducible NarG expression	This work
pFE21-DmsA	pFE21 for inducible DmsA expression	This work

RESULTS

To validate my translational knockout approach against the more classical gene deletion approach, I grew Δ*napFDAGHBC*, Δ*narGHJI*, Δ*narZYWV*, and Δ*narUZYWV* strains in parallel with *napA*, *narG,* and *narZ* strains and assessed their phenotypes during PCA oxidation with nitrate (Figure 25).[11] In this experiment, the cultures were all pre-grown in shaking tubes. Δ*narZYWV* and *narZ* had the same phenotype (Figure 25, left), a more severe delay than for *narG* and Δ*narGHJI* (Figure 25, middle). However, Δ*narUZYWV* had an even more severe delay

[11] A difference between the NarG and NarZ operons is that NarK, the nitrate-nitrite antiporter associated with NarG is in a separate operon from NarG, but NarU is in the same operon as NarZ.

in PCA oxidation (Figure 25, left, green). The Δ*narGHJI* and *narG* strains had overlapping PCA oxidation curves (Figure 25, middle), both showing a slight delay in oxidation compared to the wildtype. In the case of the periplasmic nitrate reductase, Δ*napFDAGHBC* did not have a significantly different phenotype from the wildtype until the three-hour mark (Figure 25, right blue and green traces), and *napA* had a slight delay in PCA oxidation (Figure 25, right, orange), though it might be explained by those cultures starting with a higher initial PCAred concentration. These data indicate that knocking out translation of the catalytic subunit is equivalent to knocking out the entire nitrate reductase complex, so long as nitrate-nitrite antiporting is not disrupted, which is likely important only because NarG can utilize NarU in addition to NarK.

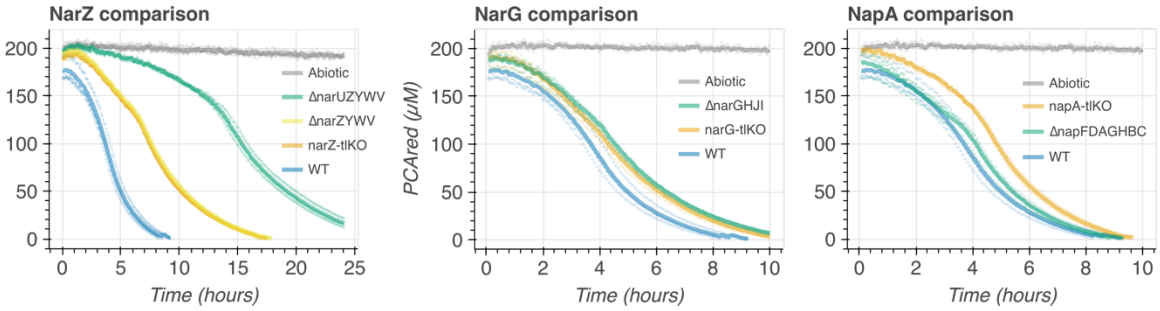

Figure 25. Comparison of nitrate reductase deletions and translational knockouts. This figure shows PCAred concentration over time in a plate reader assay. Each trace depicts three technical replicates as dots, with their mean as a bold line. In all three panels, WT is in blue, and the abiotic control is in grey. Left: comparison of *narZ* deletion (green and yellow) and translational knockout (orange) strains. Middle: comparison of *narG* deletion (green) and translational knockout (orange) strains. Right: comparison of *napA* deletion (green) and translational knockout (orange) strains. In the *narZ* panel, the orange *narZ*-tlKO and yellow Δ*narZYWV* data points are practically overlying each other. Similarly, in the *narG* panel, the orange *narG*-tlKO and Δ*narGHJI* data points are overlying each other. In the *napA* panel, Δ*napFDAGHBC* is nearly identical to the WT, deviating slightly after three hours. The *napA*-tlKO curve begins at a higher PCAred oxidaiton than the other strains did, and retains a higher PCAred concentration throughout, following a parallel trajectory to the Δ*napFDAGHBC* trace. Note: the time scale for the *narZ* data is longer than for the other two data sets. The suffix -tlKO stands for "translational knockout."

Having identified that the translational knockout approach is no worse than the classical deletion one, I proceeded to make all combinations of knockouts of the three nitrate reductases. In order to determine whether each of them could drive PCA oxidation, I tested their phenotypes after pre-growth in standing tubes (Figure 26), standing tubes with 40 mM nitrate (Figure 27), and shaking tubes (Figure 38), expecting that these different regimes would like to differential gene

regulation through RpoS and Fnr systems. I found that under standing conditions (Figure 26), all three nitrate reductases could drive PCA oxidation. The wildtype, *narZ,* and, *napA* cultures had similar distributions of maximum PCA oxidation rates across replicates. *narG* had a maximum PCA oxidation rate that was approximately twice slower than the wildtype. However, only the triple knockout *napAnarZnarG* fully lost oxidation activity; each of the double knockouts still oxidized PCA. The time it took cultures to reach 50% of the maximum PCAred concentration inversely correlated with the maximum oxidation rates: the abiotic control and triple knockout never reached the threshold, but all the other cultures did in accordance with the maximum oxidation rates. In the case of *napA* the time to 50% maximum PCAred concentration makes it more apparent that it has a subtle phenotype.

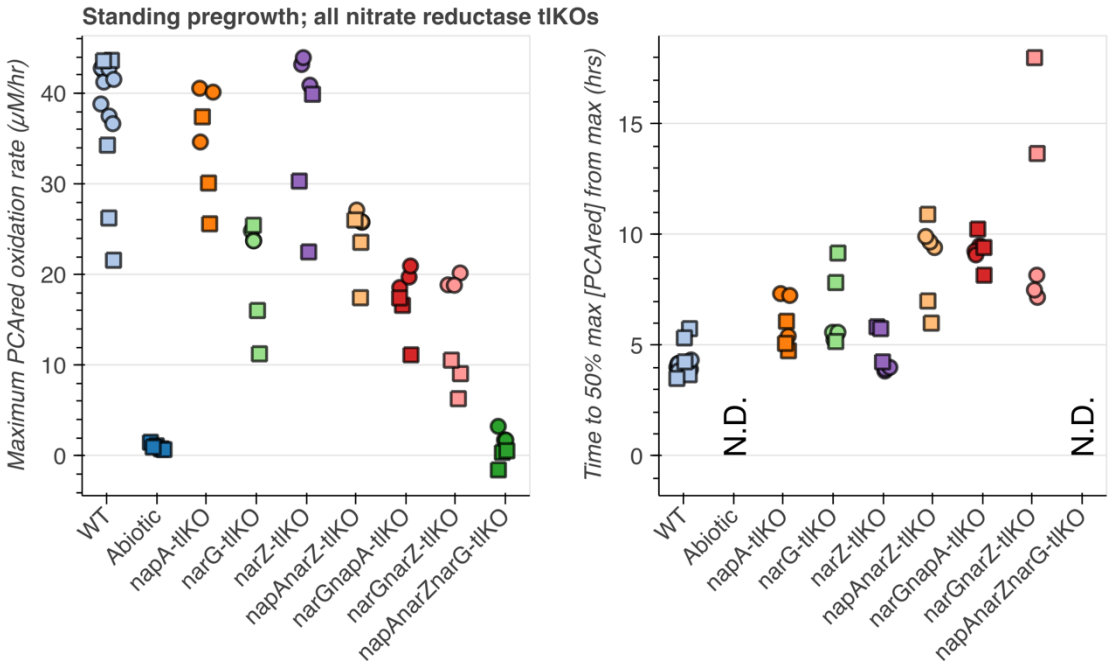

Figure 26. Nitrate reductase knockout phenotypes after standing pre-growth. Left: Maximum PCA oxidation rates in μM/hr. Right: Time to 50% of maximum PCAred concentration in hours. N.D. stands for "not determined" in the cases when the cultures did not reach the threshold during the course of the experiment. Circles represent biological replicates and squares represent means of technical triplicates. The suffix "-tlKO" stands for "translational knockout."

When I performed the same experiment but added 40 mM nitrate to the standing overnight cultures, I saw that NapA seemed to lose its, albeit subtle, activity (Figure 27). There was no longer an increase in the time to 50% maximum PCA concentration in the *napA* background

relative to the wildtype, and the *narGnarZ* phenotype became more severe than in Figure 26, indicating that NapA was not compensating for the loss of the other two nitrate reductases as well as after the simple standing pre-growth. Overall, cells with the *narG* knockout (in single or double mutants) were slower to oxidize PCA after the simple standing pre-growth.

After the shaking pre-growth, which corresponds to the experiments done in the preceding chapters, the picture is different still (Figure 28). The *narGnarZ* cells fully lost PCA oxidation activity, rendering them no different than the *napAnarZnarG* triple knockout. This implies that, after a shaking pre-growth, NapA plays no role in PCA oxidation. *narZ* had the biggest loss of PCA oxidation activity among the single knockouts, in contrast to the other two pre-growth conditions, in which it was *narG*. Because the simple standing pre-growth produced cells in which each nitrate reductase contributed to PCA oxidation (Figure 26), I decided to use this approach for all the experiments going forward.

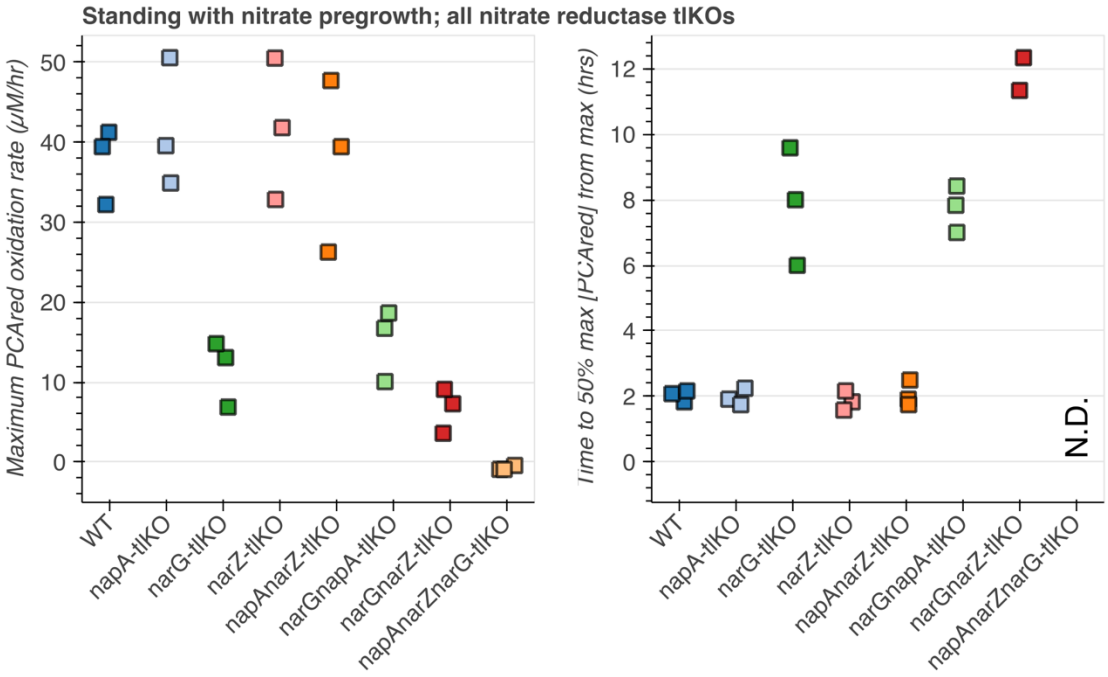

Figure 27. Nitrate reductase knockout phenotypes after standing with nitrate. Left: Maximum PCA oxidation rates in μM/hr. Right: Time to 50% of maximum PCAred concentration in hours. N.D. stands for "not determined" in the cases when the cultures did not reach the threshold during the course of the experiment. Circles represent biological replicates and squares represent means of technical triplicates. The suffix "-tlKO" stands for "translational knockout."

Having established that each of the nitrate reductases can drive PCA oxidation, and that a triple knockout is sufficient to abolish the activity, I tested the analogous situation with fumarate, DMSO, and TMAO (Figure 29). The *frdA* and *dmsA* knockouts are sufficient to abolish oxidation with fumarate and DMSO, respectively. However, the *torA* knockout increases the rate of PCA oxidation with TMAO, while the *dmsA* mutation partially reduces it. Likewise, the *dmsAtorA* double knockout is a bit faster at oxidizing PCA with TMAO than the *dmsA* knockout alone.

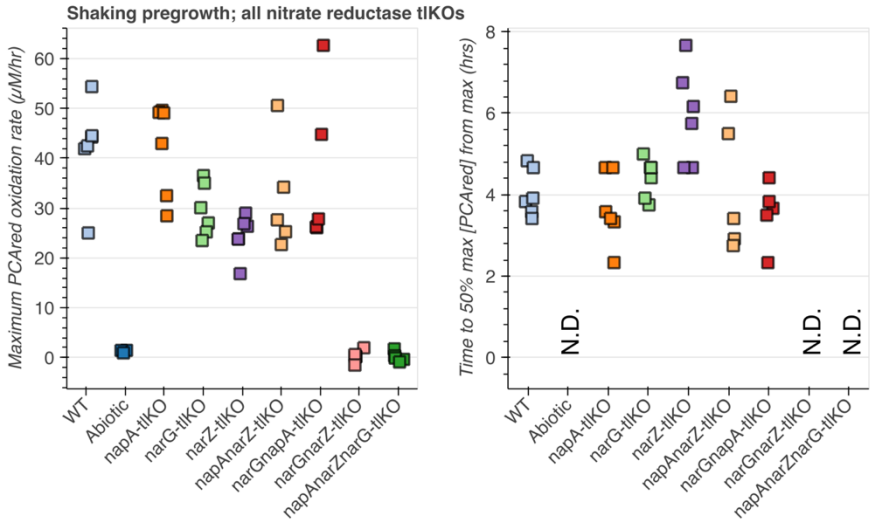

Figure 28. Nitrate reductase knockout phenotypes after shaking pre-growth. Left: Maximum PCA oxidation rates in μM/hr. Right: Time to 50% of maximum PCAred concentration in hours. N.D. stands for "not determined" in the cases when the cultures did not reach the threshold during the course of the experiment. Circles represent biological replicates and squares represent means of technical triplicates. The suffix "-tIKO" stands for "translational knockout."

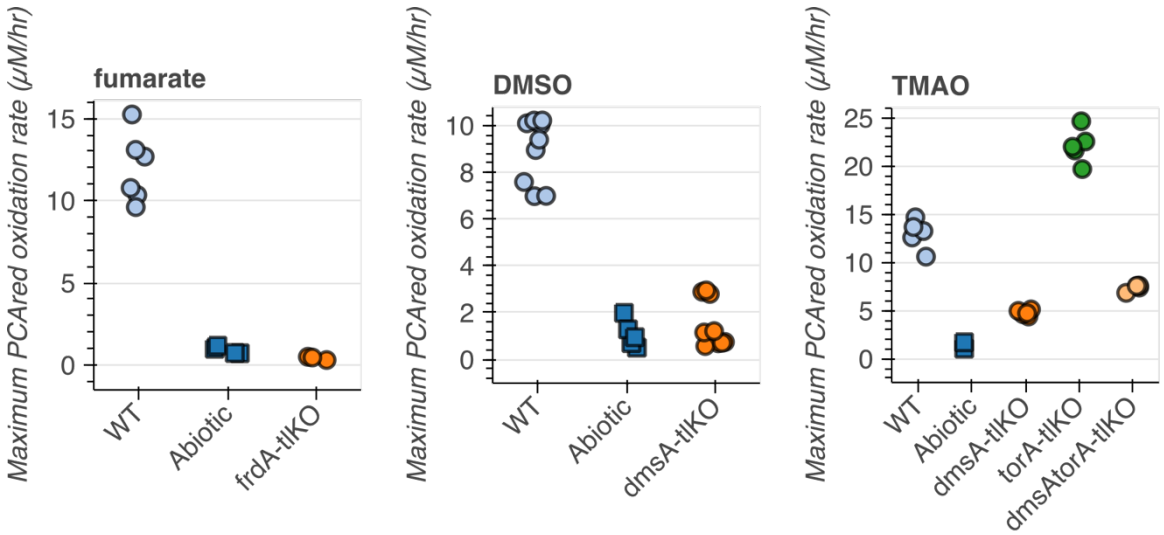

Figure 29. Fumarate, DMSO, and TMAO knockout phenotypes. Left: PCA oxidation phenotypes with fumarate. Middle: PCA oxidation phenotypes with DMSO. Right: PCA oxidaiton phenotypes with TMAO. Circles represent biological replicates and squares represent means of technical triplicates. The suffix "-tlKO" stands for "translational knockout."

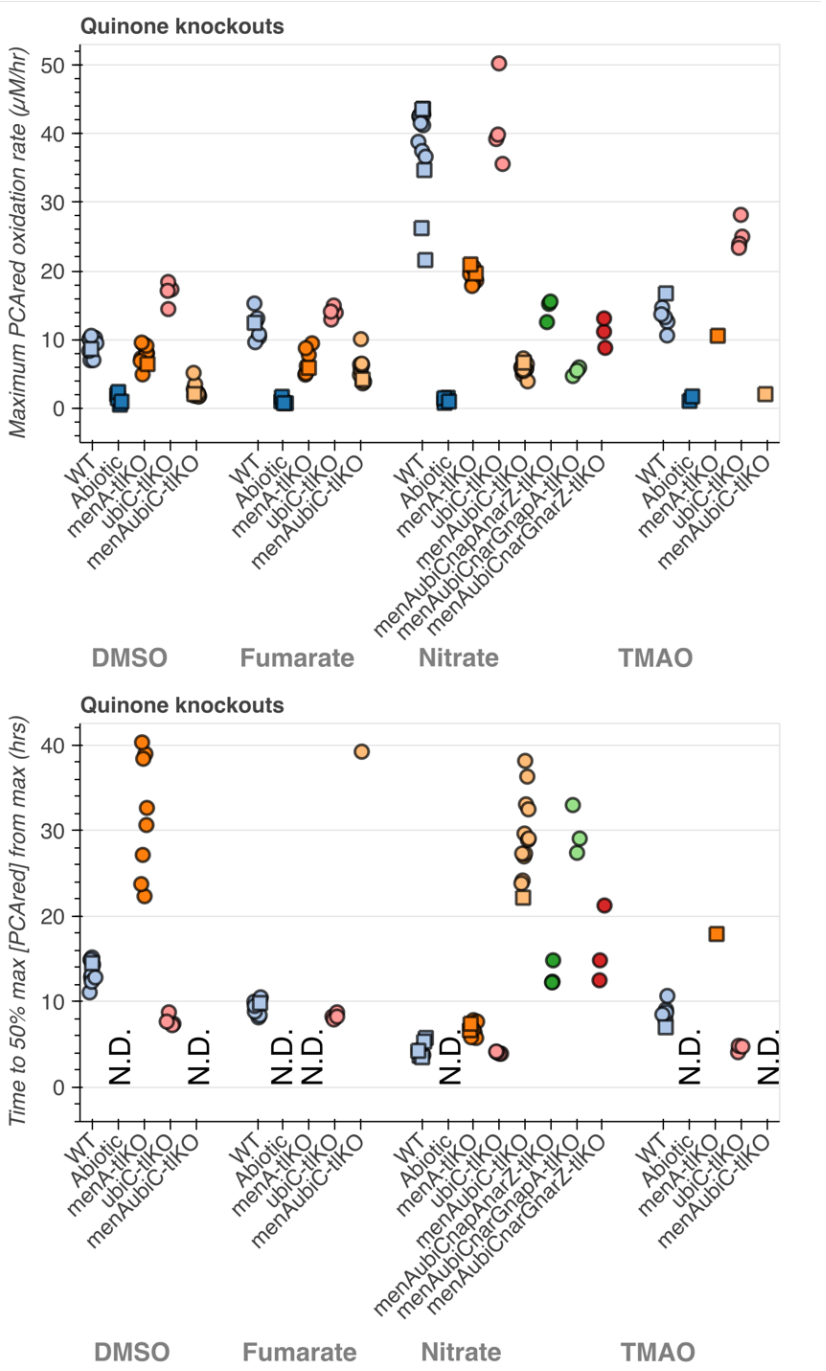

Figure 30. PCA oxidation phenotypes of quinone knockouts. Top: maximum PCA oxidation rates. Bottom: Times to 50% of maximum PCAred concentration. N.D. means that the cultures did not reach the threshold in the allotted time. Data is grouped by provided TEA.

Knocking out terminal reductases after standing pre-growth was sufficient to "turn off" PCA oxidation. The case of TMAO is exceptional, where there is apparent cross-talk between the TMAO reductase TorA, the DMSO reductase DmsA, and some other reductase(s) that are active in a *dmsAtorA* double knockout. Next, I tested whether knocking out the quinones affects PCA oxidation rates (Figure 30). In every case, knocking out ubiquinones along (*ubiC* strains) either did not affect or *increased* the PCA oxidation rate relative to the wildtype control. On the contrary, knocking out the (demethyl-)menaquinones (*menA* strains) caused a partial loss of PCA oxidation with all TEAs.

Knocking out all quinones (*menAubiC* strains) caused PCA oxidation to completely cease when provided TMAO. In the case of DMSO, there was a lingering PCA oxidation rate above the abiotic control, but the cultures did not reach a 50% threshold of PCAred concentration in the allotted time. When given fumarate and nitrate, however, the *menAubiC* strains had an appreciable remaining PCA oxidation rate. For fumarate, this indicates that either the succinate dehydrogenase (SDH) or fumarate reductase (FRD) complexes may have PCA oxidizing activity without quinones. Likewise, for nitrate, this indicates that NapA, NarG, or NarZ may drive PCA oxidation without quinones.

Given that I could isolate each nitrate reductase in the full quinone knockout background, I tested the quadruple knockouts *menAubiCnapAnarZ*, *menAubiCnarGnapA*, and *menAubiCnarGnarZ*. As shown in Figure 30, *menAubiCnapAnarZ* and *menAubiCnarGnapZ* both had PCA oxidation activity that was faster than the parental quinone knockout *menAubiC*. However, *menAubiCnarGnapA* did not have a distinct phenotype from the parental quinone knockout. Thus, these data indicate that, under these conditions, NarG, NarZ, and NapA are all sufficient to drive PCA oxidation in the absence of quinones, and NarG and NapA induction can even increase the rate. To validate these results, I tested inducible complementation vectors in the *menAubiC*, *napAnarZnarG*, *dmsA*, and *frdA* backgrounds (Figure 31–34).

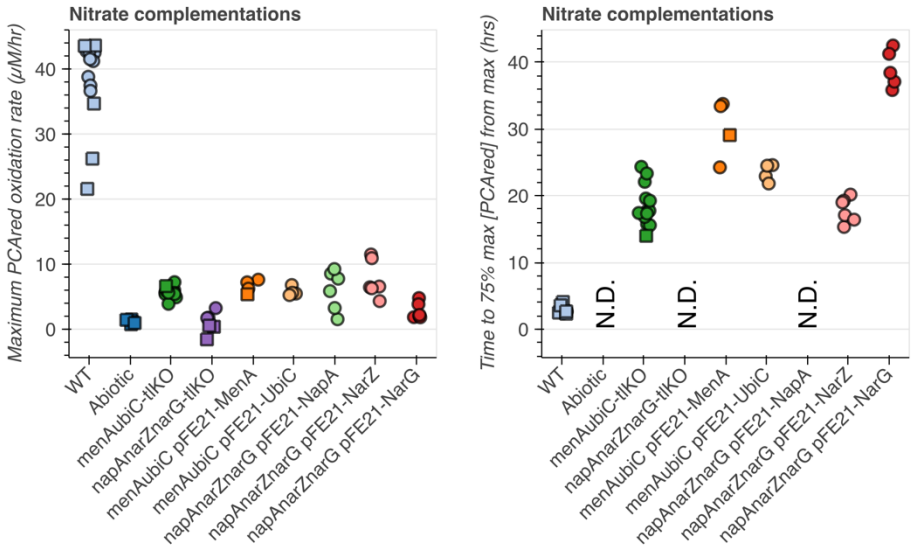

Figure 31. Complementation of nitrate-driven PCA oxidation phenotypes. Left: maximum PCA oxidation rates. Right: Time to reach 75% of the maximum PCAred concentration. The WT, Abiotic, and -tlKO strain data is reproduced from Figures 28 and 30. N.D. stands for conditions under which the 75% threshold was not reached in the allotted time. Circles: biological replicates. Squares: means of technical triplicates.

Comparing the *menAubiC*/pFE21-MenA and /pFE21-UbiC strains against the parental knockout strain, when given nitrate (Figure 31), there is no apparent difference in the maximum PCA oxidation rate, and the time it takes these strains to reach the 75% PCAred concentration threshold is slower than for the parental strain. Each of the individual nitrate reductase complementations—*napAnarZnarG*/pFE21-NapA, -NarZ, and -NarG—gives a slightly faster maximum PCA oxidation rate than the parental knockout strain. The NarZ and NarG complementation strains are able to reach the 75% PCAred concentration threshold, while neither the NapA complementation strain nor the parental knockout do.

In the context of fumarate-driven PCA oxidation, the complementation strains had more pronounced recovery of PCA oxidation (Figure 34). The FrdA complementation strain recovered the majority of the PCA maximum PCA oxidation rate that was lost in the *frdA* knockout. The MenA complementation recovered PCA oxidation activity to the wildtype level from the *menAubiC* parental knockout strain. As with nitrate-driven PCA oxidation, the UbiC complementation appeared to have no effect relative to the *menAubiC* parental knockout.

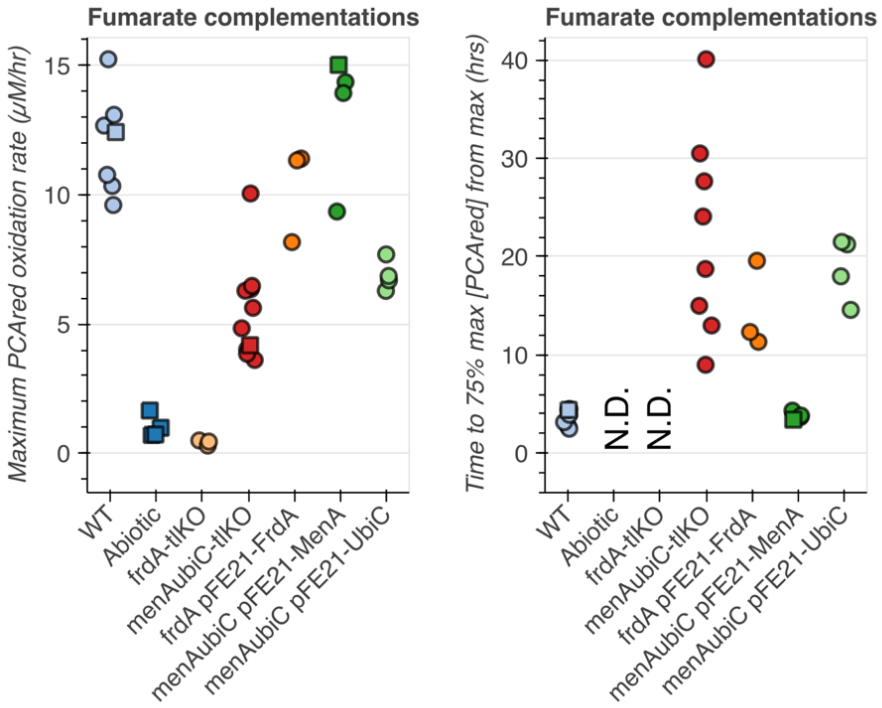

Figure 32. Complementation of fumarate-driven PCA oxidation phenotypes. Left: maximum PCA oxidation rates. Right: Time to reach 75% of the maximum PCAred concentration. The WT, Abiotic, and -tlKO strain data is reproduced from Figures 29 and 30, N.D. stands for conditions under which the 75% threshold was not reached in the allotted time. Circles: biological replicates. Squares: means of technical triplicates.

In the case of DMSO-driven PCA oxidation complementation strains, the DmsA complementation achieved a faster maximum PCA oxidation rate than the wildtype, but this rate was not sustained, resulting in a slower time to reach the 75% of maximum PCAred concentration threshold than for the wildtype. The MenA and UbiC complementation strains recovered the maximum PCA oxidation rate slightly, compared to the *menAubiC* parental strain, but they did not reach 75% of the maximum PCAred concentration.

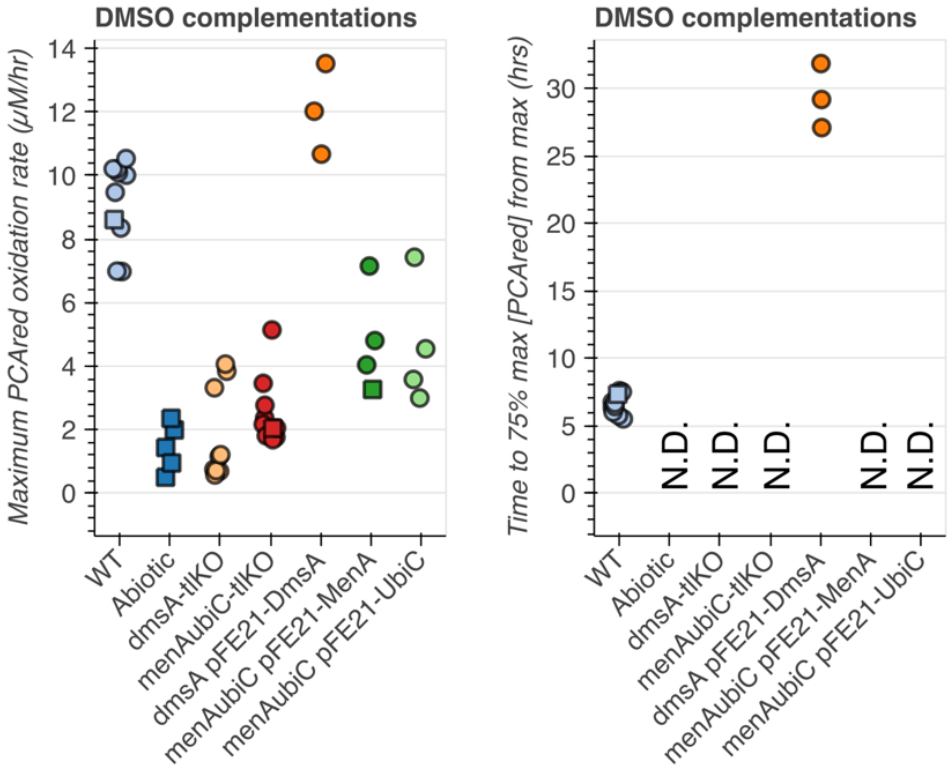

Figure 33. Complementation of DMSO-driven PCA oxidation phenotypes. Left: maximum PCA oxidation rates. Right: Time to reach 75% of the maximum PCAred concentration. The WT, Abiotic, and -tlKO strain data is reproduced from Figures 29 and 30, N.D. stands for conditions under which the 75% threshold was not reached in the allotted time. Circles: biological replicates. Squares: means of technical triplicates.

During TMAO-driven PCA oxidation, the complementation strains provided a similar picture. The DmsA complementation strain recovered some of the maximum PCA oxidation rate that was lost in the parental *dmsA* knockout strain. The DmsA complementation also shortened the time to reach 75% of the maximum PCAred concentration, relative to the parental strain. While the MenA and UbiC complementation strains appear to increase the maximum PCA oxidation

rate relative to the *menAubiC* parental knockout, neither reached the 75% PCAred concentration threshold in the allotted time.

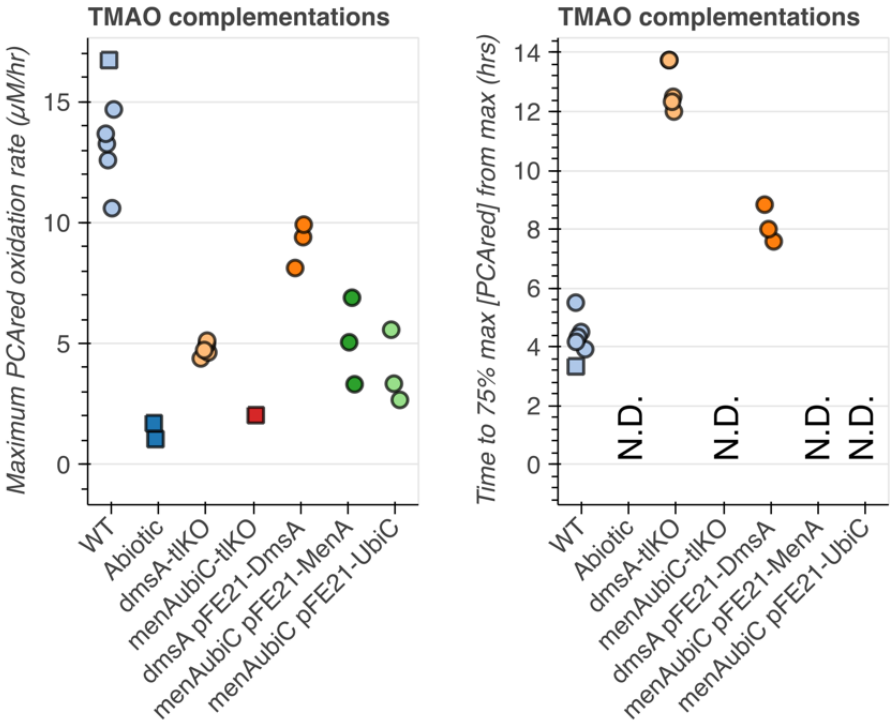

Figure 34. Complementation of TMAO-driven PCA oxidation phenotypes. Analogous to Figure 33.

As a test of whether the insights from *C. portucalensis* MBL translate to other organisms, I performed a couple analogous experiments with nitrate reductase deletion strains of *P. aeruginosa* UCBPP-PA14, which had been previously constructed by Steven Wilbert. In first experiment (Figure 35), I grew the wildtype PA14 strain, along with *nap* and *nar* deletion strains, and the same *P. aureofaciens* PhzB::*lacZ* strain from Figure 16. Here, the cultures were grown overnight, shaking for 12 hours before the assay. As in Figure 16, the *P. aureofaciens* strain does not show PCA oxidation activity with nitrate. The PA14 wildtype oxidizes PCA over the course of the assay, but the PA14 Δ*nap* strain does not. The PA14 Δ*nar* strain is at first faster at oxidizing PCA than the wildtype but does not oxidize as much total PCA over the course of the assay.

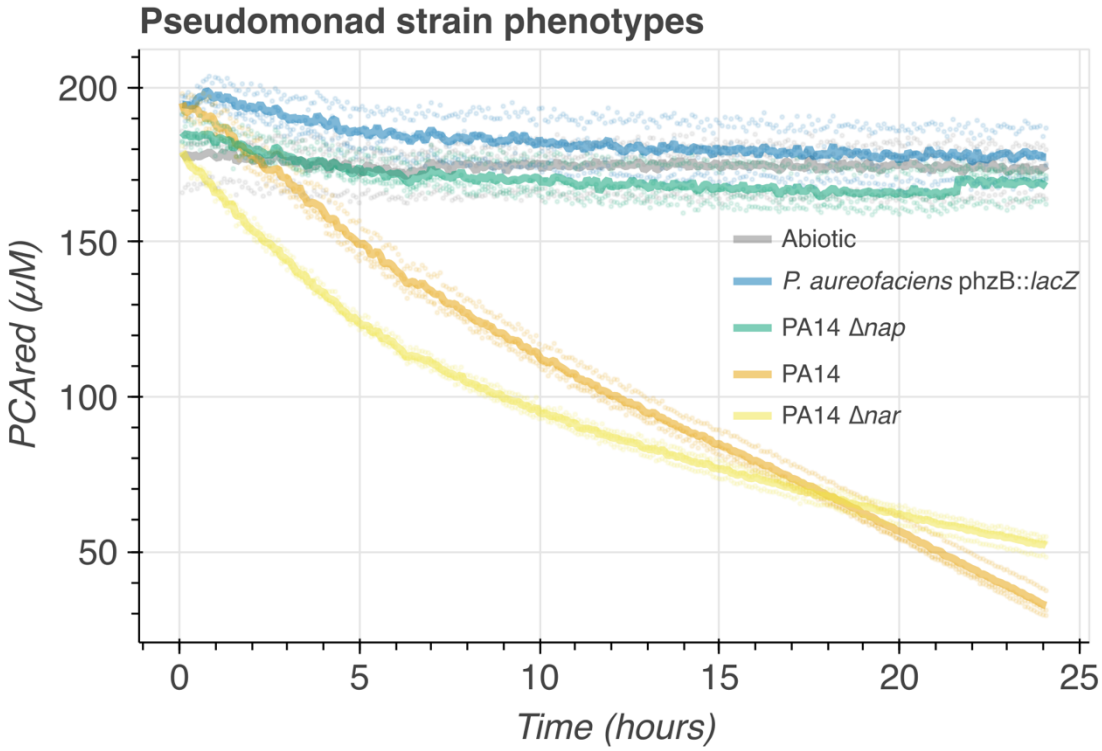

Figure 35. PCA oxidation phenotypes of pseudomonad strains. This graph shows the concentration of PCAred over time in a plate reader assay in which the wells were supplemented with 10 mM nitrate. The abiotic control is in grey, and it is overlayed by the data from PA14 Δ*nap* and *P. aureofaciens* phzB::*lacZ* strains. The wildtype PA14 trace is in orange, and the PA14 Δ*nar* trace is in yellow. Data points are of three technical replicates, with the bold lines representing their mean.

Next, to assess whether the apparent essentiality of Nap for nitrate-driven PCA oxidation by PA14 is real or due to gene regulation, I compared the three PA14 strains pre-grown shaking, standing with nitrate, or standing without a TEA additive (Figure 36). In this case, the cultures were pre-grown for 17 hours, and the pre-growth medium was 4.8 mL LB with 200 μL of the basal medium used in the plate reader assay.[12] Here, I saw that the Δ*nar* strain had no phenotype compared to the control when pre-grown shaking (Figure 36, top), and that the Δ*nap* strain had a partial loss of PCA activity under those conditions, as compared to the total loss in Figure 35.

[12] This was because the only stock of nitrate I had at the time was 1 M in that basal medium, so I added the same volume of basal medium to each pre-growth culture without nitrate.

However, when the cultures were pre-grown standing, with or without nitrate, the Δ*nar* phenotype was much more severe than the Δ*nap* one, which was very similar to the wildtype control.

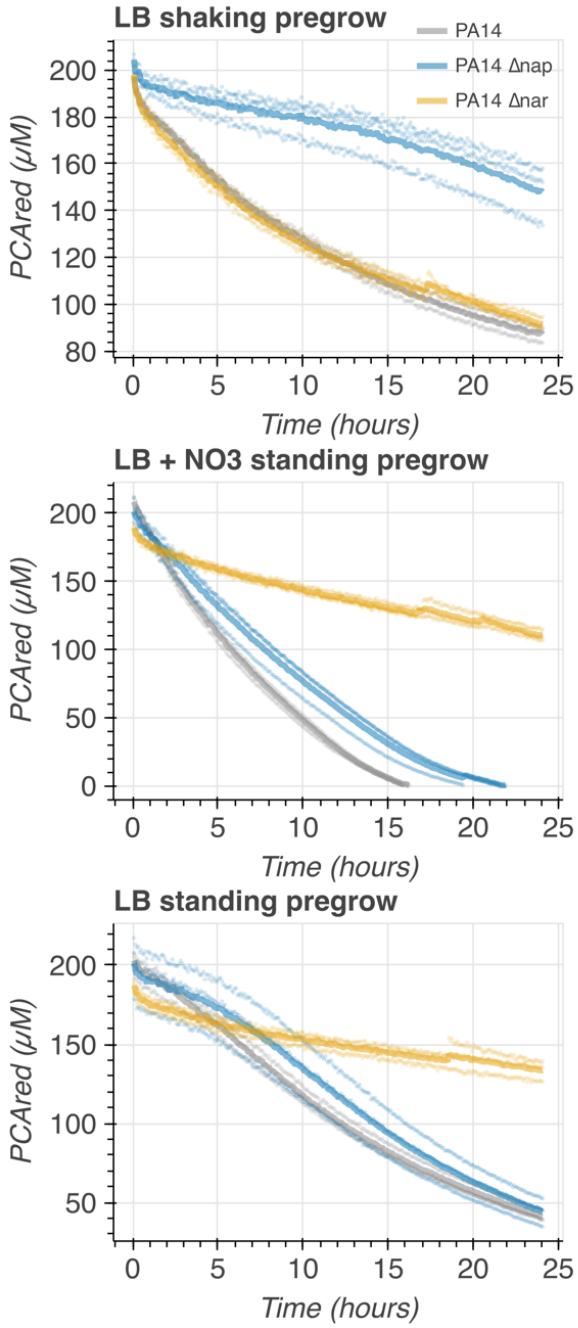

Figure 36. Pre-growth comparisons of PA14 phenotypes. Depending on the pre-growth condition, the dominant nitrate reductase driving PCA oxidation changes. When PA14 is pre-grown shaking (top), Δ*nar* has no phenotype and Δ*nap* loses PCA oxidation activity. When pre-grown standing with or without nitrate, practically the opposite is the case. Data points as in Figure 35.

DISCUSSION

The principal question underlying this chapter is whether PCA oxidation is mediated by direct electron transfer to a terminal reductase(s), regeneration of the quinol pool, or both. This question was motivated by the observation that seemingly any bacterium that I tested can respire anaerobically can drive PCA oxidation, which implies that there is either an elegant, shared mechanism for the process or extraordinary convergence of evolved mechanisms. In the experiments above, I was able to show that both are the case, depending on the exact context. Both of the homologs of the membrane-bound respiratory nitrate reductase, NarG and NarZ, are able to drive PCA oxidation without any available quinones (Figure 30). These two enzymes' amino acid sequences have 99.8% coverage and are 80% identical in sequence in *C. portucalensis* MBL[13], but have differing regulation regimes: the former is regulated by NarXL and Fnr, and the latter is regulated by RpoS, based on the promoter sequences and homology to *E. coli* (Blasco et al., 1990; Chang et al., 1999). As expected, which enzyme was dominant for contributing to PCA oxidation depended on the pre-growth conditions, which determined the gene regulation regime (Figures 26–28). However, since the catalytic NarG and NarZ subunits are actually in the cytosol and the other members of the complexes (NarHJI and NarYWV) are the proteins that interact with electron shuttles in the inner membrane and periplasm (Sparacino-Watkins et al., 2014), the mechanism for PCA oxidation likely lies within them and not the catalytic subunits.

The case of the periplasmic nitrate reductase NapA is interesting: the *narGnarZ* double knockout and the *menAubiCnarGnarZ* quadruple knockout both oxidize PCA (Figures 26 and 30). However, the pFE21-NapA vector does not complement the *napAnarZnarG* triple knockout. Potentially, this could be resolved by upping the induction—it is possible that, for whatever reason, NapA does not express very well from this plasmid. It is also possible that in this triple knockout background, the cell no longer transports NapA into the periplasm, rendering it inactive. It is also possible that, being in the periplasm, its nitrite-producing activity is somehow more auto-

[13] As aligned by MUSCLE 3.6.

inhibitory than that of NarG or NarZ, though this seems unlikely given that the *menAubiC-narGnarZ* quadruple knockout had a higher activity than the *menAubiC* parental strain (Figure 30).

For fumarate-, DMSO-, and TMAO-driven PCA oxidation, the picture is similar. Knocking out an active terminal reductase reduces or abolishes the PCA oxidation activity, and complementing the terminal reductase recovers some or all the activity (Figures 28, 32, 33, and 34). I was not able to fully knock out TMAO-driven PCA oxidation due to either a cryptic TMAO reductase or promiscuity with a different terminal reductase: *dmsA* gives the strongest phenotype, but *torA* only increases the rate of PCA oxidation. *C. portucalensis* MBL has a second Tor operon, but its homolog of the TorA catalytic subunit is truncated (Tsypin et al., 2020b), so I do not think it can be active. In the *menAubiC* strain, fumarate still drives PCA oxidation (Figure 30), which implies that either the fumrate reductase or succinate dehydrogenase complex can drive PCA oxidation without quinones. I did not attempt to knock out the succinate dehydrogenase, so I did not investigate this further.

While knocking out the terminal reductases was an effective strategy for abolishing PCA oxidation, knocking out quinones also substantively decreased the rate and extent of PCA oxidation for all forms of anaerobic respiration tested. The *ubiC* knockout alone, which retains the (demethyl-)menaquinones, has no effect on PCA oxidation in the case of fumarate-driven PCA oxidation, and even *increases* the rate (relative to wildtype) when provided DMSO, TMAO, or nitrate (Figure 30). The *menA* knockout causes a modest decrease in the extent and maximum PCA oxidation rate, but the *menAubiC* double knockout always has a more severe phenotype (Figure 30). I interpret this to mean that when (demethyl-)menaquinones are available, PCA only reduces them, but ubiquinone can potentially step in if the other quinones are absent. The MenA complementation is sufficient to rescue all or some of the PCA oxidation activity in the *menAubiC* background when given fumarate, DMSO, or TMAO, but not nitrate. The UbiC complementation gives a very slight improvement of PCA oxidation when given fumarate, DMSO, or TMAO, evident only in the time it took cultures to reach 75% of the maximum PCAred concentration. Like the MenA complementation, the UbiC complementation has no effect when provided nitrate. It is possible that by increasing the induction of MenA or UbiC, there would

be more of a complementation during nitrate-driven PCA oxidation, but it may also be the case that, because the nitrate reductases are sufficient to drive the activity themselves, other elements of the quinone biosynthesis pathways are downregulated under these conditions.

Altogether, these data suggest that:

1) PCA oxidation can be driven both by electron flux through the quinone-quinone pool and by terminal reductases (nitrate and fumarate (or succinate dehydrogenase)) more directly;

2) When flux is going through the quinone-quinol pool, this is primarily through menaquinone and demethylmenaquinones;

3) It is not possible to say whether menaquinone or demethylmenaquinone is the more important contributor.

This means that any organism with an anaerobic electron transport chain may be able to oxidize PCA. All that would be necessary is flux through a quinone-quinol pool, but some organisms may also have terminal reductases that react with PCAred more directly. Notably, *P. aeruginosa* does not have (demethyl-)menaquinones, but it still actively oxidizes PCA, as seen in Chapters 2 and 3. It cannot ferment nearly as well as *C. portucalensis* MBL, so it is probably not possible to derive a quinone knockout in *P. aeruginosa*, which means that it would be difficult to determine whether its PCA oxidation mechanism depends on ubiquinone or just the terminal reductases. However, John Ciemniecki has found that ubiquinone rapidly oxidizes PCA in solution, so it is entirely possible that PCA oxidation in *P. aeruginosa* also comprises quinol regeneration and terminal reductase interaction.

Furthermore, Figures 35 and 36 show that in *P. aeruginosa* UCBPP-PA14 either Nap or Nar can be the dominant driver of PCA oxidation, depending on the pre-growth conditions. As with *C. portucalensis* MBL, I interpret this to mean that the driving terminal reductase is determined by the gene regulatory state of the cell. The observation that deleting Nap can abolish PCA oxidation activity under certain conditions is in accordance with Alexa Price-Whelan's observation in her PhD thesis. She noticed that a transposon insertion in *NapA* results in more oxidized pyocyanin in LB cultures supplemented with nitrate, as compared to the wildtype (Price-Whelan,

2009). This was evident from the blue color of anaerobic cultures: pyocyanin is blue when oxidized and colorless when reduced. The fact that anaerobic LB cultures with nitrate stopped being blue in the *napA* transposon insertion implied that knocking out *NapA* stopped a pyocyanin oxidation process. Thus, we have the generalizable PCA oxidation mechanism in *C. portucalensis* MBL, my reproduction of the genetic dynamics in *P. aeruginosa* UCBPP-PA14, and the apparent extension of PCA oxidation to pyocyanin from Alexa Price-Whelan's dissertation. I feel confident in making the bold claim that you can take any bacterium under any anaerobic respiration conditions and observe PCA oxidation.

CHAPTER 5: CONCLUDING REMARKS

It is not your duty to finish the work,
but neither are you at liberty to neglect it.
—Pirkei Avot 2:16

The term "microbial infallibility" is dramatic. It invites pontification. And I indulged in it in Chapter 1, talking about sophistry and other nonsense. My undergraduate advisor, Aaron Turkewitz, once cautioned during a group meeting that when you say something, you start believing it to be true. This was in the context of a lab member interpreting some data that they were presenting, but this general idea has stayed with me since. Through saying things, we come to believe them, and they eventually become common sense. This is particularly true of evocative metaphors, such as microbial infallibility. Common sense is remarkably difficult to critically examine or rigorously support.

Underlying microbial infallibility is the general microbiologist's experience that microbes are everywhere and that they do everything, in the sense that we have not been able to imagine a biochemical process that they cannot or do not perform. This makes it very easy to rely on assumptions. These assumptions span from inferring activities from metagenomic (or—the horror—16S rRNA) sequences to trying to cultivate various and sundry microbes in the same media and in isolation from their neighbors. It is very rare to imagine a new biological process, discover it in nature, and figure out how it works, even in broad strokes.

PCA oxidation is not just abstractly interesting as a novel biological process: PCA is an ecologically important molecule, and its oxidation is the first example of a naturally-produced electron shuttle being oxidized by cells. PCA is produced everywhere there are plant roots, and its differential toxicity structures plant-associated microbial communities (Dahlstrom and Newman, 2022; Dar et al., 2020; Thomashow, 2013; Thomashow and Weller, 1988). PCA reduction supports survival under reductive stress and liberates recalcitrant nutrients (Glasser et al., 2014; McRose and Newman, 2021). PCA toxicity is one of the first and only examples of antibiotic activity in nature (Thomashow and Weller, 1988). And yet, in all of these examples, microbes are reducing PCA. What may we discover, then, knowing now that microbes readily oxidize it, too, whenever a terminal electron acceptor for respiration is around?

My work is not the first example of biological oxidation of a redox-active molecule, but it is the first example (to my knowledge) of biological oxidation of a naturally produced (not anthropogenic) and widespread redox-active metabolite.[14] Some examples of biological oxidation of inorganic electron donors include molecular hydrogen (an edge-case, but still arguably correct) (Thauer et al., 1977; Unden and Bongaerts, 1997), sulfur (Schmidt et al., 1987), iron (Li et al., 2014)[15], manganese (Yu and Leadbetter, 2020), and ammonia (Kuenen, 2008). Examples of biological oxidation of anthropogenic organic electron shuttles include anthraquinone-2,6-disulfonate (AQDS) (Coates et al., 2002; Lovley et al., 1999) and neutral red, a synthetic phenazine (Harrington et al., 2015). AQDS has been used to mimic humic substances in soils, complex organic acids that can act as electron donors to cells but cannot really be reproduced in the lab. Neutral red has been used as an electron shuttle to supplement electrode-driven fermentation in bioelectric reactors. Interestingly, neutral red is reported to be oxidized via (demethyl-)menaquinones in *E. coli*, too, though that study did not go as far as knocking out ubiquinone or assessing the activities of the terminal reductases (Harrington et al., 2015). Given all the compounds that bacteria oxidize all these compounds, it is easy to assume that they would oxidize naturally produced electron shuttles, and I am proud that I was able to rigorously validate what might have remained an assumption for a while yet.

To answer questions of how PCA is biologically oxidized, I worked with a soil isolate. It proved to be a serendipitous one: *C. portucalensis* was first described the same year I started my PhD (Ribeiro et al., 2017); being an environmental isolate, I can earnestly assert that studying *C. portucalensis* MBL has a genuine environmental relevance, which is important to me; developing it into a genetically-tractable system was a matter of porting tools that had already be developed for *E. coli*, which proved to be as easy as I could have hoped for. With some minor modifications, my dissertation work could have been done 20 years ago, though it would have taken considerably longer and been much more expensive. As a narrative, my PhD is the story

---

[14] Alexa Price-Whelan's dissertation (also conducted in the Newman lab) includes an observation that the phenazine pyocyanin, which is a derivative of PCA, appears to be oxidized by *P. aeruginosa* when given nitrate, and that this activity is lost in the NapA knockout strain, but this was not followed up further (Price-Whelan, 2009).

[15] There are other examples of iron oxidizing bacteria, but I chose this reference because it's about a different *Citrobacter* isolate!

of taking five years to imagine a new biological process, find it in nature, prove that it is in fact biological, develop the tools necessary to study the process in the original environmentally relevant context, and arrive at mechanistic insights. Leaving aside the significance of anything to do with phenazines and redox-active metabolites, I think the very fact of this story is important. We, as microbiologists, have developed enough tools and enough of a knowledgebase to move beyond the standard lab approaches and model organisms: rather than force square pegs into round holes, we are equipped to answer our questions in their most relevant context. My greatest hope for my dissertation is that it helps someone go out into nature and find what they are looking for.

* * *

It is difficult to conceptualize all the possible ecological dynamics that bacterial PCA oxidation could mediate, especially without a clear sense of when it would provide a fitness advantage or disadvantage to cells. However, there are a couple questions to try to ask and inferences to try to make, which may lead to testable hypotheses. First, it is not clear whether organisms that are "obligate" respirers, such as *P. aeruginosa*, tend to have slower PCA oxidation rates than organisms that can ferment, such as *C. portucalensis*. This hypothesis is appealing because it would correspond to the idea that organisms like *P. aeruginosa* rely on phenazines as alternative terminal electron acceptors: if these bacteria were very efficient at oxidizing phenazines, this would interfere with the assumed ontology. It would make sense for this to be generally true, but Figure 16 shows that *P. aeruginosa* Δ*phz** oxidizes PCA with nitrate faster than *E. coli*. It may be the case that the relative rates of phenazine reduction and oxidation do not actually compete because the former is relevant only when no terminal electron acceptor is available, and the latter only occurs with a terminal electron acceptor is present. Given that the above reasoning is largely layered conjecture, the correlation between fermentation capability, phenazine biosynthesis capacity, and the rates of phenazine oxidation and reduction needs to be rigorously explored.

Second, the existence of PCA oxidation has many implications for the bulk redox-state of PCA in the environment, and consequently affects its properties such as toxicity (Dahlstrom and Newman, 2022). In other words, the presence of anaerobically respiring organisms, or the

relative activity of anaerobic respiration, may determine how effective PCA is as a biocontrol agent. Insofar as phenazines play a role in structuring microbial communities, surrounding anaerobic respiration will shape that role.

Third, PCA oxidizing organisms may stand in for minerals, such as iron oxides, for organisms that rely on abiotic phenazine oxidation. This would stand to benefit cells that only care about getting rid of electron waste and find themselves in mineral-poor soils and sediments. However, previous work in the Newman lab has shown that PCA-mediated electron transfer to minerals can liberate essential nutrients (McRose and Newman, 2021). Consequently, an organism like *C. portucalensis* could use its PCA-oxidizing activity to starve competing cells by intercepting the PCA before it can deliver its electrons to the mineral. Even if this provided no immediate fitness advantage to *C. portucalensis*, it could still help it push out other species and establish its niche.

Altogether, the discovery of biological oxidation leaves us with a new parameter to try to model when considering microbial chemical ecology, as well as a reminder that more such parameters may be relevant. I hope that this work will help researchers interested in all aspects of environmental microbiology—modelers, physiologists, geneticists, et al.—take the next step toward a comprehensive understanding of what microbes are doing out there in the wilds.

* * *

To the reader who turned to this dissertation for helpful insights, thank you for reading. I hope that you found what you sought, and that I was able to convey it clearly. At least, I hope I was able to point you in some helpful directions or even teach you something interesting. If you came to find some ideas for experiments and potential pitfalls, I will try to outline my thinking about the project and where it might go from here.

Should you be physiologically inclined, there is a lot to uncover about the benefits and harms that phenazine oxidation confers. The key will be to determine the conditions under which PCA oxidation would be beneficial or harmful. From my experiments, I think the most surefire way to do this is to lean into oxidative and reductive stress. Most likely, PCA oxidation

will be the most useful to cells that have been shaking aerobically without a carbon source for a long time. I did not include this in the dissertation, but I did a pilot experiment in which I grew *C. portucalensis* MBL in a defined citrate medium to late stationary phase, washed it into a fresh basal medium with no carbon source, and tracked CFUs for over a week. There was no decrease in viability. Apparently, if you buffer these cells, they are extremely robust. So maybe you should starve them for a week, two weeks, a month, and see whether oxidizing PCA helps them recover. And maybe it is not PCA oxidation that would benefit the cells the most: perhaps it would be pyocyanin or phenazine-1-carboxamide oxidation. I did a brief pilot experiment and saw that *C. portucalensis* MBL oxidizes them, too. Given that Alexa Price-Whelan noticed a pyocyanin oxidation phenotype in a transposon insertion mutant in *NapA (Price-Whelan, 2009)*, this is not a far leap.

If you are ecologically-inclined, the path is wide open for you to explore the interactions of phenazine oxidizing and reducing microbes and how these redox cycles structure microbial communities. I suggest trying to pair *C. portucalensis* MBL with its original enrichment partners (the two *P. nitroreducens* strains). I mentioned in Chapter 3 that *C. portucalensis* does not grow on acetate, which raises the question of how it persisted through many passages of the enrichment cultures when the only carbon source was acetate. At the same time, we know that PCA reduction helps pseudomonads survive on acetate (Glasser et al., 2014). More likely than not, with some clever microscopy, you will be able to discover direct phenazine redox-mediated interactions. I was really hoping to be able to get there during my PhD, but when the pandemic presented me with the choice of compromising on my ambitions or my time, I chose to compromise on my ambitions.

If you are genetically-inclined. There are loose ends and mysteries that remain. Something is up with TMAO. There must be some third TMAO reductase. But be careful: I found batch-to-batch variability in TMAO bottles, where some of them caused rapid PCA oxidation abiotically. Make sure to check your chemicals before getting too far into the weeds. There also remains the question of how menaquinone and demethylmenaquinone compare. You can get at this by knocking out UbiE, which disrupts ubiquinone and menaquinone synthesis but keeps demethylmenaquinone synthesis intact (Nitzschke and Bettenbrock, 2018; Sharma et

al., 2012). This will help iron out some more details about how the terminal reductases and quinone pools interface with PCA oxidation. The paper to compare to results to is probably this one: (Wissenbach et al., 1990). This work should provide enough information to begin to mathematically model the process, which would be a big step forward toward modeling phenazine redox reactions in the environment.

If you are looking for something weird and unconstrained, I do not think you need to look much farther than the spiral colony waves. There are questions of material properties/mechanics, collective behavior, and stress response that may be at play. I have no way of saying whether it is a big deal or not, but it was difficult for me to resist the siren song and re-focus on the PCA oxidation work.

Citrobacter portucalensis MBL is a joy to work with. I feel profoundly lucky: I got it out of a soil enrichment and can genuinely assert that it is environmentally relevant, *and* all the *E. coli* tools and functional inferences work. You can even make sure that your cultures are not contaminated with *E. coli* by growing them on citrate. I really do not think there is a better environmental isolate out there to work with, at least for the questions that are relevant for this project. If you do decide to pursue this work, please feel welcome to get in touch. I will help however I can. If nothing else, I will cheer you on.

APPENDIX I: DETAILED PROTOCOLS AS USED IN CHAPTERS 2–4

CHAPTER 2

Anoxic enrichment medium

- 45 mM sodium bicarbonate buffer
- 10 mM ammonium chloride as a nitrogen source
- 1 mM potassium phosphate as a phosphorus source
- 1 mM PCAred as a potential electron donor
- 100 μM sodium acetate as a carbon source and electron donor
- 10 mM sodium nitrate as an electron acceptor and nitrogen source
- 50 μM sodium sulfide as a sulfur source and reductant
- 1x freshwater salts (Table 1)
- 1x trace elements (Table 2)
- 1x vitamins (Table 3)

Agar isolation medium

- 1 mM sodium phosphate buffer (pH 7)
- 10 mM ammonium chloride
- 100 μM sodium acetate[16]
- 100 μM sodium sulfate
- 10 mM sodium nitrate
- 1x freshwater salts (Table 1)
- 1x SL-10 trace elements (MediaDive solution ID S4178)
- 1x vitamins (Table 3)
- 1.5% agar

Electrode chamber assay medium

- 1x freshwater salts (Table 1)
- 1x SL-10 trace elements (MediaDive solution ID S4178)
- 1x 13-vitamin solution (Table 3)
- 20 mM sodium phosphate buffer (pH 7)
- 10 mM ammonium chloride
- 100 μM sodium sulfate
- 100 μM sodium acetate

---

[16] Some of my old notes say 100 μM sodium acetate, and some say 1 mM sodium acetate. If anyone follows up on this work and this detail is important, please keep this in mind.

- 100 μM PCA
- 10 mM nitrate

Plate reader assay medium

- 1x freshwater salts (Table 1)
- 1x SL-10 trace elements (MediaDive solution ID S4178)
- 1x 13-vitamin solution (Table 3)
- 20 mM sodium phosphate buffer (pH 7)
- 10 mM ammonium chloride
- 100 μM sodium sulfate
- 1 mM sodium acetate
- 200 μM PCA
- ± 10 mM TEA (nitrate, nitrite, or fumarate)

Plate reader assay

1. Make sure all materials in the Coy chamber are anoxic by letting them stand in there for at least one day for glassware and at least three days for plasticware.
2. Two days before, streak frozen stock on LB agar plate, grow over night at 30 ºC; inoculate liquid cultures for next step with a mixed patch of cells.
3. Grow three 5 mL cultures of cells overnight, shaking at 250 rpm, slanted, aerobically at 30 ºC, in rich medium (TYEM for *Pseudogulbenkiania* MAI-1 and LB for others).
4. Wash entire volume into basal medium plate reader assay medium with no terminal electron acceptor and no PCA.
   - In 1 mL aliquots, wash 3x into basal medium by spinning for 2 min at 6000x(g), aspirating with vacuum trap, and resuspending by pipetting.
   - Measure OD_{600} and calculate how to normalize all cultures to OD_{600} = 0.125.
5. Bring cultures into the anaerobic chamber.
6. Wash volume of cells that is necessary for inoculation 3x into anoxic basal medium (no TEA or PCA), as above, aspirating supernatant with pipette.
7. Resuspend in anoxic plate reader assay medium at an OD_{600} = 0.125 in at least 4 mL final volume per culture.
8. Let stand for 1 hour. To test that this is fine, track parallel culture(s) with resazurin to see when it turns pink or clear.
9. Add PCA to each anoxic culture (the ones without resazurin) to a final concentration of 200 μM.
10. Add 198 μL of each culture to each appropriate well.
11. Add 2 μL of 1 M TEA (or anoxic plate reader assay medium as a control) to each appropriate well.

12. Seal plate with qPCR film.
13. Plate reader protocol:
    - Incubate at 30 ºC.
    - "Medium" shaking.
    - Measure absorbance at 440 and 600 nm (PCA and cells, respectively).
    - Measure fluorescence (360/40 ex and 528/20 em, sensitivity 100, if using filters on BioTek Synergy 4).

CHAPTER 3

Plate reader PCA oxidation assay medium

- 20 mM K-Phosphate buffer
- 10 mM NH_4Cl
- 1 mM Na_2SO_4
- 1x Trace Elements
- 1x Fresh Water salts
- 1x 13-vitamin solution
- 200 μM PCAred
- pH 7-7.1

Electrode chamber PCA oxidation assay medium

- 20 mM K-Phosphate buffer
- 10 mM NH_4Cl
- 1 mM Na_2SO_4
- 1x Trace Elements
- 1x Fresh Water salts
- 1x 13-vitamin solution
- ± 50 mM sodium acetate
- 100 μM PCA
- pH 7-7.1

Ion chromatography assay medium

- 0, 10, or 50 mM sodium acetate (from 1 M stock)
- 10 mM sodium nitrate (from 1 M stock)
- 20 mM K-Phosphate buffer pH 7
- 1 mM Na_2SO_4 (from 100 mM stock)
- 1x SL-10 trace elements (from 1000x stock)
- 1x 13-vitamin solution (from 1000x stock) (Table 3)
- 1x freshwater salts (from 100x stock) (Table 1)
- 0 or 200 μM PCA (reduced or oxidized)

Ion chromatography assay

1. Two days before, streak frozen stock on LB agar plate, grow over night at 30 ºC; inoculate liquid cultures for next step with a mixed patch of cells.
2. Grow three 5 mL cultures of cells overnight, shaking aerobically at 30 ºC, in LB.
3. Wash entire volume into basal medium with no terminal electron acceptor, no PCA, and no acetate (essentially just buffer and salts).
   - In 1 mL aliquots, wash 3x into basal medium by spinning for 2 min at 8000x(g) and resuspending by pipetting.
   - Pool entire volume after washing.
4. Measure OD_{600} and calculate the dilution for final OD_{600} = 0.125 in 25 mL.
5. Bring culture into the anaerobic chamber.
6. Wash volume of cells that is necessary for inoculation 3x into anoxic basal medium (no C or N), as above.
7. Let stand for 2 hours or until parallel culture turns resazurin pink.
8. Add basal medium to empty tubes to bring tubes to final volume, minus nutrients, PCA, and cells.
9. Add nitrate to desired concentration.
10. Add vitamins to 1x.
11. Add carbon source to desired concentration.
12. Add PCA (reduced or oxidized) to desired concentration.
13. Inoculate cells to OD_{600} = 0.125.
14. Mix by flicking or gentle shaking between thumb and forefinger.
15. At the designated timepoints:
    - Mix culture by flicking or gently shaking between thumb and forefinger.
    - Sample 550 μL into centrifugal 0.2 μm filter for analytical chemistry.
      - Freeze at -80 ºC before use.

Greiss colorimetry for nitrate and nitrite concentrations

1. Prepare Greiss reagent mixture:
   a. Prepare 2% sulfanilamide in 1.6 M HCl (SULF), store at 4 ºC.
   b. 0.1% N-(1-Naphthyl)ethylenediamine dihydrochloride (NEDD), store at 4 ºC.
   c. Prepare saturated vanadium (III) chloride by dissolving 400 mg in 1 M HCl, filtering undissolved particulates through a nylon filer, store the VCl_3 reagent and solution under anoxic conditions in the dark.

d. Immediately prior to analysis, prepare the Greiss reagent a 1:1 mixture of NEDD and SULF.

2. In a 96-well plate, prepare calibration points and samples: 100 μL each.
    a. Calibration points: 0 μM, 40, μM, 80 μM, 120 μM, 180 μM, 240 μM.
    b. Samples: 10^{-2} dilution of filtered samples.
3. For nitrite assay, add 20 μL Greiss reagent and 80 μL ultrapure water to each well.
4. For nitrate assay, add 20 μL Greiss reagent and 80 μL of the VCl_3 solution to each well.
5. Incubate at 37 ºC in the plate reader and measure absorbance every five minutes for 45 minutes at 540 nm.
6. Note: the presence of PCA seems to interfere a bit with the nitrate measurements, but the nitrite measurements lined up perfectly with ion chromatography results.

Electrode chamber assays

1. Prepare electrode chambers:
    a. Clean chambers with a methanol soak (at least 2 hours), potassium hydroxide soak (overnight), acid soak (overnight), and muffling (980 ºF for four hours). Wrap in aluminum foil and autoclave with stir bar sand o-rings set up in the main chambers.
    b. Maintaining sterile conditions, set up electrode chambers with a graphite working electrode (Alfa Aezar Cat. No. 14738) in the main chamber and a platinum mesh counter electrode in the sidearm.
        i. For the graphite working electrode, polish with a lint-free KimWipe until smooth and shiny; immerse in 70% ethanol to sterilize before mounting into electrode chamber..
        ii. For the platinum electrode, immerse in 70% ethanol to sterilize before mounting into electrode chamber
    c. Stopper remaining ports in the main chamber lid.
    d. Bring into mBraun anoxic glove box.
2. Prepare reference electrodes:
    a. Always store the reference electrodes (BASI Cat. No. MW-2030) in sterile 3 M NaCl solution after opening them for the first time.
    b. Always keep one electrode that is never used as a reference for the reference electrodes.
    c. Confirm that there is no potential difference between the reference electrode(s) you want to use for the experiment and the never-used electrode with a multimeter by dipping both electrodes into the same 3 M NaCl solution and attaching a lead to either electrode.
    d. Prepare a molten 1% ultrapure agarose in 3 M NaCl solution in a microwave.

e. Carefully fill 200 μL gel loading tip with molten agarose solution without introducing any bubbles.

f. Carefully insert tip of reference electrode into the filled gel loading tip without introducing any bubbles.

g. Stand gel loading tip with inserted reference electrode vertically and allow agarose to cure for 45 minutes.

h. Firmly and gently secure electrode in gel loading tip using Parafilm

   i. Cut a strip of Parafilm in half (two rectangles approximately 1 cm by 4 cm).

   ii. With the first half-strip, hold it against the top of the pipette tip with your thumb without applying any pressure to the electrode.

   iii. Stretch the Parafilm up over the top of the electrode, and then back down on to another area of the pipette tip, applying downward pressure on the electrode to further secure it in the tip.

   iv. Catch the Parafilm against the new area of the pipette tip with your thumb, rotating the tip in the process.

   v. Repeat until the length of the half-strip runs out and repeat again with the second half-strip.

i. Using a brand-new razor blade, cut off the end of the gel-loading tip to remove any bubbles that may have formed during curing, leaving as much of the tip intact as possible.

j. Dip the tip into 70% ethanol to sterilize.

k. Transfer the prepared electrodes into 50 mL conical tubes with either sterile medium that will be used in the assay or sterile 3 M NaCl.

l. Hermetically seal the conical tubes before bringing into the mBraun anoxic chamber (the vacuum cycle in the airlock would ruin the electrodes).

3. In the mBraun anoxic chamber, insert reference electrodes into the narrow ports of the electrode chambers.

4. Fill the main chambers to account for a 100 mL final volume with medium, and fill the side-arms with 7 mL of the medium.

5. Connect the Gamry potentiostat leads to the working, reference, and counter electrodes according to manufacturer instructions.

6. If a given chamber will have an electrode reducing PCA (using a -500 mV potential), start the reduction the night before the experiment to have the PCA fully reduced at the beginning of the experiment.

7. Prepare the cells:

   a. Grow overnight 5 mL LB cultures at 30 ºC, shaking slanted tubes at 250 rpm.

b. Measure OD_{600} of overnight cultures and inoculate 250 mL LB in a 1 L Erlenmeyer flask to an OD_{600} = ~0.06.

c. Grow the 250 mL LB cultures, shaking at 250 rpm at 30 ºC, until they reach OC_{600} = ~2.8 (approximately 4-6 hours).

d. Pellet all 250 mL in one bottle by spinning for 10 minutes at 6000 × g at room temperature.

e. Resuspend cell pellet in 25 mL of the medium used for electrode chamber experiments and transfer to 50 mL conical tube.

f. Twice more, pellet the cells by spinning for 8 minutes at 5500 × g at room temperature.

g. After the second spin, resuspend in 6 mL of the experiment medium

h. Measure OD_{600} and adjust to a final value of OD_{600} = 75..

i. Bring cell suspension into mBraun anoxic chamber

8. Commence the assay

a. Inoculate 1 mL of cell suspension into appropriate chamber.

b. Set stir bars to spin at setting 4.

c. Confirm that potentiostat settles and does not show any errors or overloads after the first five minutes.

d. Sample for ATP by dissolving 20 μL of culture in chamber in 180 μL 100% DMSO and then diluting with 800 μL 0.1 M HEPES pH 7.5.

e. Sample for nitrite by taking 100 μL of culture and spinning through a 0.2 μm centrifugal filter at maximum speed for two minutes.

f. Sample for CFUs by taking 100 μL of culture and plating a serial dilution series:

i. Newman lab drip plates™:

1. Prepare a serial dilution in 10-fold increments in a 96 well plate.

2. With a multichannel pipette, gently place 10 μL aliquots of dilution series (up to eight at a time) in a row at one end of a Petri plate with LB agar.

3. Tilt the plate vertically to allow the droplets to run down the length in parallel lanes.

4. Un-tilt the plate before the lanes reach the plastic.

5. If the lanes are still runny, you can tilt the plate in the other direction and let them run back to the original spot.

6. This protocol requires plates that are sufficiently dry, which I achieve by pouring 12-15 mL plates, letting them cure in upright stacks on my bench for a day, then letting them stand in upside

down stacks on my bench for a day, and then sealing them in sleeves and storing at room temperature or 4 ºC until use.

CHAPTER 4

PCA oxidation assay basal medium

- 20 mM K-Phosphate buffer
- 10 mM NH_4Cl
- 1 mM Na_2SO_4
- 1x Fresh Water salts
- pH 7-7.1

*Preparation of electrocompetent cells for electroporating plasmids (*E. coli *and* C. portucalensis *MBL)*

1) For a large batch:
    a. Prepare 100 mL LB in a 500 mL Erlenmeyer flask.
    b. Prepare ice-cold 10 % glycerol and ultrapure water.
    c. Two days prior to electroporation, streak out strain on LB agar and grow at 30 ºC.
    d. One day prior to electroporation, inoculate a 5 mL LB liquid culture with a patch of cells from the overnight streak and incubate slanted, shaking at 250 rpm at 30 ºC overnight.
    e. Day of the electroporation, inoculate 1 mL of the overnight culture into the 100 mL LB flask and grow to OD_{600} = 0.4, shaking at 250 rpm at 30 ºC.
    f. Chill flask on ice for 20 minutes.
    g. Wash two the culture two times into ice-cold water (5000 × g for 10 minutes at 4 ºC; I typically divide the 100 mL volume into four 50 mL conical tubes, washing with 25 mL volumes).
    h. Combine pellets and spin final time.
    i. Resuspend in 2 mL ice-cold 10% glycerol.
    j. Aliquot 50 μL volumes into ice-cold microcentrifuge tubes and flash-freeze in liquid nitrogen.
    k. Store at -80 ºC or use immediately.
2) For a small batch:
    a. Two days prior, streak out strain as above.
    b. One day prior, grow 5 mL LB culture overnight as above.
    c. Day of, inoculate 50 μL overnight culture into 5 mL LB and incubate slanted, shaking at 250 rpm at 30 ºC until OD_{600} = 0.3.

d. Chill on ice for 10 minutes.

e. Wash three times into ice-cold water, final resuspension of combined pellets 50 μL (can also spin full 5 mL culture in conical tube directly).

Designing and implementing translational knockouts

3) Design the oligo for mutagenesis (Table 7), which I name with the tag "MAGE" because this protocol is based on one for Multiplexed Automated Genome Engineering:

   a. Identify where the gene of interest is on the chromosome relative to the origin of replication and determine which strand of DNA will be the lagging strand (the mutating oligo needs to be complementary to the lagging strand in order to stand in for an Okazaki fragment).

   b. Design the mutating oligo to introduce a minimal number of single nucleotide substitutions to change three consecutive codons into the three different stop codons (TAA, TGA, TAG) within the first third of the coding sequence.

   c. Convenient codons to look out for are tyrosine, lysine, and glutamine for converting to TAA or TAG; tryptophan or cysteine for converting to TGA; leucine, proline, or arginine, depending on the synonym of the original codon in the gene.

   d. The substitutions should take place near the middle of the oligo, which should be 90 nucleotides long, and the folding energy of the oligo should be more positive that -12.5 kcal mol^{-1}.

   e. If the folding energy is too negative, you can try sliding the oligo sequence to move the nucleotide substitutions toward the 5' end, but you may need to design a different oligo at a different locus.

   f. When ordering the MAGE oligo, add phosphorothioated bonds between the first two nucleotides at the 5' end to stabilize the oligo.

4) Design the oligos for screening the candidate mutants (Table 7). I named these primers with the tag "MASC" because my protocol is based on one for Multiplex Allele-Specific Colony PCR.

   a. Design one primer that matches the substituted nucleotides at its 3' end (the mut primer) and one that matches the wildtype nucleotides at its 3' end (the wt primer) to both have an annealing temperature of ~60 ºC. If the genotype is wildtype, only the wt primer will anneal; if the genotype is mutated, only the mut primer will anneal; if the cell has mismatched DNA or there is a mixed culture of mut and wt cells, both may anneal.

   b. Design a primer that is reverse to both the wt and mut primers above that would give an amplicon of 200-400 bp. Design it such that it also anneals at ~60 ºC and does not dimerize with either the mut or wt primers with an energy more negative than -10 kcal mol^{-1}. Tag the name with the expected amplicon length.

c. Benchmark primers by testing, for example, Fmut/R200 and Fwt/R200 on a strain that is wildtype for the gene of interest. Only Fwt/R200 should amplify by PCR.

    i. I use GoTaq Green (2x Master Mix) for this, with the following example reaction composition (can be scaled down):

        a. 25 μL 2x GoTaq Green.

        b. 1.25 μL 10 μM primerF.

        c. 1.25 μL 10 μM primerR.

        d. 0.5 μL 100% DMSO.

        e. 21 μL nuclease-free water.

        f. 1 μL colony resuspension in 20 μL sterile water (touch pipette tip to colony to get a minimal, but visible amount of cells and pipette up and down to resuspend in 20 μL).

    ii. PCR protocol:

        a. 95 ºC for five minutes.

        b. 95 ºC for 30 seconds.

        c. 60 ºC for 30 seconds.

        d. 72 ºC for 30 seconds.

        e. Go to (b) 24 times.

        f. 72 ºC for five minutes.

        g. End (hold at 22 ºC in thermocycler and freeze or refrigerate after removing from thermocycler).

d. Design one or two primers (names tagged with Seq) for amplifying and sequencing the region: if designing just one primer pair it with the reverse primer above.

5) Electroporate helper plasmid into the strain:

a. In the genetic background that you want to mutate, preprare electrocompetent cells as above to electroporate in the pHelper plasmid.

b. Electroporate:

    i. Add 10-60 ng plasmid to 50 μL electrocompetent aliquot on ice (plasmid should be in ultrapure water, and you should aim to add no more than 1 μL to the cells).

    ii. Gently mix the DNA and cells by tapping the tube a couple times.

    iii. Transfer to ice-cold electroporation cuvette.

    iv. Zap: 2.5 kV, 200 Ω, 25 μF if using 2 mm gap cuvette; 1.25 kV, 200 Ω, 25 μF if using 1 mm gap cuvette.

v. Pulse length should be approximately 5 ms.

c. Recover electroporated cells in LB:

i. Recover in a total of 1 mL LB by adding 950 μL to the cuvette, mixing, and transferring as much volume as possible to a microcentrifuge tube.

ii. Incubate shaking horizontally at 30 ºC for one hour.

iii. Plate serial dilution on selective LB agar (selective for whatever marker is appropriate to the electroporated plasmid.

d. Once the plasmid-bearing strain is attained, grow overnight in 5 mL LB under selection and prepare a -80 ºC freezer stock in 35% glycerol.

6) Induce the helper plasmid and electroporate in the MAGE oligo:

a. Two days before, streak frozen stock carrying pHelper on LB/agar gentamicin (15 μg/mL) plate, grow over night at 37 ºC.

b. One day before, inoculate patch of struck cells into 5 mL culture overnight, shaking at 250 rpm, slanted, aerobically at 37 ºC, in LB + gentamicin (15 μg/mL).

c. Day of electroporation: inoculate 1 mL of overnight culture into 100 mL flask (this protocol can be scaled up or down according the how many reactions you want), add gentamicin to 15 μg/mL, grow shaking at 250 rpm at 37 ºC for ~2 hours until OD_{600} = 0.3. Check OD every 30 minutes starting at the 1-hour mark.

d. When culture reaches OD_{600} = 0.3, induce with 1 mM m-toluic acid (100 μL of 1 M solution or 125 μL of 800 mM solution), continuing to shake at 37 ºC for 30 minutes.

e. After induction, chill on ice for 10 minutes.

f. Split culture into two 50 mL conical tubes (pre-chilled), balance, and wash three times by spinning 10 minutes at 5000x(g) at 4C, using slow deceleration. After first spin, resuspend each pellet in 10 mL ice-cold NanoPure water and combine in one conical tube. After the second spin, resuspend in 10 mL ice-cold 10% glycerol and then add another 10 mL. After the third spin, resuspend with ice-cold 10% glycerol to a final volume of 1 mL (depending on how well you decant, this will take 500-750 uL). All resuspensions are done by gentle tapping and pi-petting.

g. Aliquot 81 μL volumes of induced, electrocompetent cells into ice-cold micro-centrifuge tubes.

h. For aliquots that are to be transformed immediately, add 9 μL of transformation oligo and mix by gently tapping.

i. Transfer to prechilled electroporation cuvette(s) and make sure that the culture fully spans the cuvette gap.

j. Zap: 2.5 kV, 200 Ω, and 25 μF in 2 mm cuvette (should give a ~5 ms pulse) (1.25 - 1.8 kV in 1 mm cuvettes might work, but I have not really tested this).

k. Add 900 μL LB to cuvette(s), mix by pipetting, and transfer as much as possible to an Eppendorf(s).

l. Flash-freeze unused aliquots in liquid nitrogen and store in -80 ºC freezer (can start at step (h) if thawing previously frozen induced, electrocompetent aliquots).

m. Rescue transformants, shaking horizontally at 250 rpm at 37 ºC for 1 hour.

n. Transfer the ~1 mL rescue cultures to 4 mL LB with 1.25x gentamicin for a final volume of 5 mL with 1x gentamicin (15 μg/mL) and outgrow (slanted, shaking, 37 ºC) for another 3 hours.

o. Plate serial dilution series on LB/agar + gentamicin, expect good separation of colonies at ~10^{-5} dilution.

p. Incubate at 37 ºC overnight.

7) Screen candidate mutants:

a. Pick at least eight colonies for a given desired genotype.

b. PCR amplify with the wildtype and mutant primer combinations (MASC primers) described above in separate tubes.

c. Select colonies that give only mutant bands.

d. If you have colonies that give both wildtype and mutant bands, you can restreak them and screen individual colonies from the restruck plate.

e. If you have a lot of PCRs to run, a more efficient approach is often to PCR first with only the mutant primer pair and then confirm that positive colonies do not give a wildtype band, rather than screening each colony with two primer pairs from the outset.

8) Cure mutant strains of helper plasmid:

a. Inoculate selected mutant strain into 5 mL LB with no antibiotics and grow overnight at 30 ºC in slanted tubes shaking at 30 ºC.

b. Serially dilute the overnight culture and plate on no-salt, 5% sucrose LB agar.

c. Grow overnight at 30 ºC.

d. Rescreen a couple colonies by PCR with the wt and mut MASC primers.

e. In parallel, patch mutant colonies onto non-selective and gentamicin LB agar and inoculate into 5 mL non-selective LB.

f. Incubate plates at liquid cultures at 30 ºC, shaking the liquid cultures at 250 rpm in slanted tubes.

g. If the patch test shows that the mutants lost gentamicin resistance and the PCR screen shows only mutant bands, prepare 35% glycerol -80 ºC freezer stocks of the mutants.

h. If you need the mutant strain to still carry the pHelper plasmid for adding more mutations into the same background, you can include a gentamicin LB liquid culture in step (e) and prepare a -80 ºC freezer stock from it directly.

Gene deletions via homologous recombination

1) Amplify the resistance cassette for knocking out a genetic region of interest using primer pairs from Table 8. Use a high-fidelity polymerase, such as Q5, KAPA, or Phusion according to manufacturer instructions.
    a. Design primers with 36 bp homology upstream to/downstream from region you want to knock out.
    b. Append GTGTAGGCTGGAGCTGCTTC to 3' end of upstream primer.
    c. Append CATATGAATATCCTCCTTAG to 3' end of downstream primer.
    d. Use pKD4 for KanR cassette template.
    e. Using Phusion: use approx. 15 ng plasmid template for PCR:
        i. 98 ºC 30 sec.
        ii. 98 ºC 5 sec.
        iii. 55 ºC 30 sec.
        iv. 72 ºC 54 sec.
        v. Go to (ii) 24 times.
        vi. 72 ºC 5 min.
        vii. 22 ºC hold until freezing or refrigeration.
    f. Purify PCR products using NEB PCR cleanup kit (Cat. No. T1030) after gel verification.
2) Deletion of genomic region:
    a. Two days prior, streak out MBL/pKD46 on 50 μg/mL ampicillin (Amp) or carbenicillin (Carb) LB agar at 30 ºC.
    b. One day prior, grow overnight culture in 5 mL LB with 50 μg/mL Amp/Carb.
    c. Morning of, inoculate 2 mL overnight culture into 100 mL (25 mL per transformation) LB with 50 μg/mL Amp/Carb and 0.2% L-arabinose.
    d. Grow at 30C to OD_{600} approx. 0.6-0.8 (around 2 hours).
    e. Wash at 2000 × g (slow deceleration) at 4 ºC into ice-cold 10% glycerol three times, combining final aliquot in one tube during last wash.
    f. Resuspend into 400 μL final vol 10% glycerol (assuming four reactions--100 μL per reaction).
    g. Aliquot 100 μL reaction volumes into ice-cold microcentrifuge tubes.

h. Add approximately 100 ng resistance cassette to cell aliquot and gently mix by tapping.

i. Electroporate in ice-cold cuvettes using 2.5 kV, 250 Ω, and 25 μF (confirm approx. 5 ms pulse for each), assuming 2 mm gap cuvettes.

j. Add 500 μL LB to each cuvette.

k. Transfer cell suspension to microcentrifuge tube and recover at 37 ºC shaking horizontally for an hour.

l. Plate 300 μL of recovered cell suspension on LB + 50 μg/mL kanamycin and grow at 37C. Leave remaining cells standing overnight and plate the next day of nothing grows from the first attempt.

3) Cure pKD46 plasmid and confirm deletion:

a. Pick a couple individual colonies for each transformation and re-streak on non-selective LB to grow at 42 ºC overnight.

b. From each re-streak, pick a single colony to patch onto non-selective LB, LB/Kan, and LB/Carb or Amp. Grow at 30 ºC.

c. Check for colonies that are kanamycin-resistant and carbenicillin/ampicillin-sensitive.

d. PCR verify correct insertion of kanamycin resistance cassette (forward primer in KanR (Table 8, KanR_arbF) and reverse downstream from knocked out region (e.g., Δnap_check_F) and loss of λRed (primers in λRed gene on pKD46, Table 8 λRed_F and λRed_R).

e. Prepare -80C stocks for good strains in 35% glycerol from overnight cultures grown in LB + 50 μg/mL kanamycin.

4) FLP out resistance cassette:

a. Electroporate pCP20 (AmpR, ts-origin) into deletion strains using plasmid electroporation protocol.

b. Recover in LB at 30 ºC.

c. Grow overnight on LB/Carb or Amp plate at 30 ºC.

d. Streak several colonies on non-selective LB and grow at 42 ºC overnight.

e. Screen for loss of all antibiotic resistance by patching on non-selective and selective LB plates.

f. Confirm FRT scar by PCR using primers in flanking regions (e.g., Δnap_check_F and Δnap_check_R) and sequencing.

Cloning complementation vectors

1. Amplify the backbone and wildtype genes:

a. Using pZ/FE_backbone_F and _R primers, amplify the pFE21 backbone with a Q5 polymerase:

i. 50 μL 2x NEB Q5 High-Fidelity master mix.
ii. 5 μL 10 μM primer F.
iii. 5 μL 10 μM primer R.
iv. 3 μL 100% DMSO.
v. 36 μL nuclease-free water.
vi. 1 μL (~50 ng) plasmid.

b. PCR protocol:
i. 98 ºC 30 sec.
ii. 98 ºC 10 sec.
iii. 69 ºC 30 sec.
iv. 72 ºC 1.5 min.
v. Got to (ii) 35 times.
vi. 18 ºC 5 min.
vii. Hold at 22 ºC until freezing or refrigeration.

2. Mix together 5 μL of 2x Gibson master mix with a 3:1 ratio of insert to vector backbone in a total volume of 10 μL.
3. Incubate for two hours at 50 ºC.
4. Transform into chemically competent DH10β *E. coli* (courtesy of Steven Wilbert):
   a. Thaw chemically competent cells on ice.
   b. Add entire Gibson reaction to cells and mix by gently tapping.
   c. Heat shock at 42 ºC for 45 seconds.
   d. Incubate on ice for 2 minutes.
   e. Add 400 μL LB to cells.
   f. Recover at 37 ºC shaking horizontally for 1 hour.
   g. Plate entire volume on LB + 50 μg/mL kanamycin agar.
   h. Incubate overnight at 37 ºC.
5. Verify plasmids by amplifying the insert region with pZ/FE_screen_F2 and _R2 primers (Table 8) and check for expected size.
6. Pick several correct colonies to grow overnight in LB + 50 μg/mL kanamycin liquid culture overnight.
7. Prepare -80 ºC freezer stocks of overnight cultures.
8. Miniprep the plasmid and send for Primordium sequencing (whole-plasmid sequencing via Oxford Nanopore technology).

Plate reader PCA oxidation assay

1. Two days before, streak frozen stock on LB agar plate, grow over night at 30 ºC; inoculate liquid cultures for next step with a mixed patch of cells.
2. Grow 5 mL cultures of cells overnight at 30 ºC in LB for 17 hours ± 10 minutes.
    - Depending on the experiment, tubes are either slanted shaking at 250 rpm; standing non-shaking with caps sealed with Parafilm; or standing non-shaking with 40 mM nitrate added to the LB and with caps sealed with Parafilm.
3. Wash entire volume into basal medium with no terminal electron acceptor and no PCA (essentially just buffer and salts):
    - In 1 mL aliquots, wash 3x into basal medium by spinning for 2 min at 6000x(g), aspirating with vacuum trap, and resuspending by pipetting.
    - Measure OD_{600} and normalize all cultures to OD_{600} = 0.2-1, target OD_{600} = 0.5.
        - For slow growing cultures, like *menAubiC*, this amounts to spinning down 1 mL of the overnight culture and resuspending it in 250 μL, then adjusting the volume.
        - May need to scale up if inoculating a lot of wells.
4. Bring cultures into the anaerobic chamber.
5. Transfer washed cultures to anoxic microcentrifuge tubes.
6. Let stand for at least 1 hour. To test that this is fine, can track parallel culture with resazurin to see when it turns pink or clear.
7. During incubation, set up plate:
    - For PCA_{red} calibration:
        - prepare 500 μM solution by diluting PCA_{red} stock in basal medium.
        - In one row of the plate, prepare calibration (in μM): 250, 200, 175, 150, 125, 100, 75, 50, 25, 10, 5, 0.
        - This corresponds to the following volumes of the 500 μM PCA_{red} per well (in μL): 100, 80, 70, 60, 50, 40, 30, 20, 10, 4, 2, 0.
        - Bring total volume in each well to 200 μL.
    - Desired concentration of PCA in PCA wells is 200 μM (40 μL of 1 mM stock).
    - Desired concentration of cells is 50 μL of OD_{600} = 0.5 culture for a target of OD_{600} = 0.1 in the wells.
    - Other components depend on the experiment: e.g., 2 μL of 1 M sodium nitrate for a 10 mM experimental concentration.
        - Note: all solutions prepared in the same basal medium.
    - Final volume in each well is 200 μL.

   - Order of preparing wells (except calibration): basal medium, then PCA, then TEA, then cells (always last).

8. Plate reader protocol, using either BioTek Synergy 4 or Synergy HTX:
   - Incubate at 30 ºC
   - "Medium" shaking
   - Measure absorbance at 440 and 600 nm (PCA and cells, respectively)
   - Measure fluorescence (360/40 ex and 528/20 em), sensitivity depends on instrument and how good the optics are, but it does not really matter so long as the calibration curve spans the dynamic range

COMPUTATIONAL ANALYSES

All my analyses were done using Python, various python libraries, and several command line packages, mostly for genome sequencing and annotation. When this thesis is deposited to the Caltech library, it will include a repository with all the data and analyses, and I will do my darndest to make my code clear and reproducible. On GitHub, you can find the code and data at https://github.com/ltsypin/PhD_Thesis.

APPENDIX II: BLUE SOYMILK SIDE PROJECT

I was scrolling through Twitter one day during the height of the COVID-19 pandemic, and I saw that a fellow graduate student, Marina De León, working in Jonathan Eisen's lab at UC Davis, published the genome of a bacterium that turns soymilk and tofu blue (De León et al., 2021). The causative bacterium is a strain of *Pseudomonas carnis*, and I was immediately intrigued: was the pigment a phenazine, like pyocyanin? Was the blue color redox-state dependent? This observation appealed to me because I saw parallels in both the isolation- and metabolite-driven aspects of the project. I reached out to Marina, and she sent me her strains.

In Marina's hands, the soymilk turned blue only after refrigerated incubation, and she had not yet developed a solid medium for studying the process. My only real contribution to the project was that I decided to just buy Silk-brand soymilk, autoclave it with 1.5% agar, and try out the plates. They worked beautifully (Figure 37). The soymilk curdles after autoclaving, but the solid particulate settles to the bottom in molten agar, so the plates have a perfect, solid surface. I found that the bacteria produce the blue pigment in a density-dependent manner, regardless of whether they are incubated at room temperature or refrigerated after pre-growth (Figure 37, left and middle plates). In a stroke of luck, I one day got a spontaneous mutant that did not turn blue (Figure 37, right)! Presumably, if someone (you, perhaps?) were to sequence the genomes of the spontaneous mutant and parental strain, you could figure out the necessary gene(s).

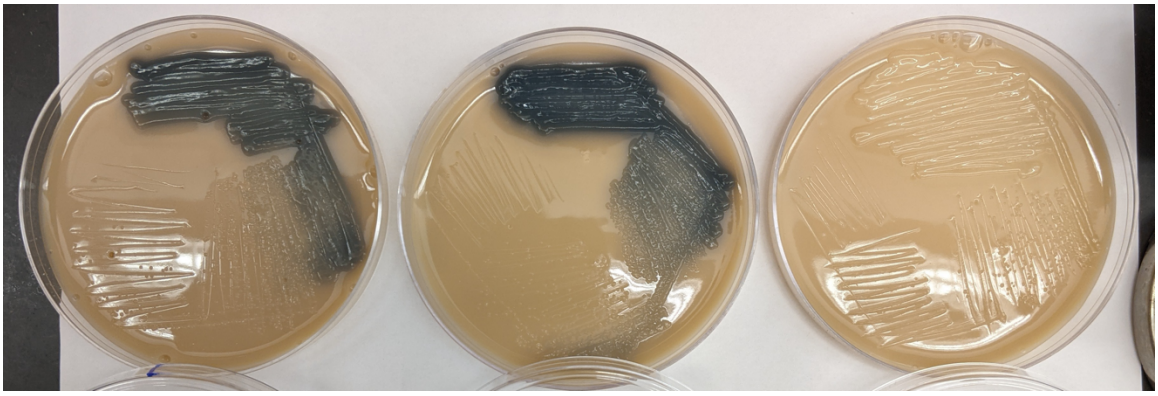

Figure 37. Blue soymilk strains and a spontaneous colorless mutant. Left and middle: two re-streaks of the original isolates. Right: spontaneous mutant that no longer turns blue.

The project did not go much further than this: I had to focus on my main dissertation work when I was not managing various personal crises. But I think there is something really interesting

here. Blue is a very rare color in nature. Any opportunity to find a new blue is one that we should collectively jump to explore. In terms of the likely things that are going on, one possibility is that this pigment is a tryptophan-derivative, such as indigo-like compounds (Andreani et al., 2015; Heumann et al., 1968). In addition to protein, soymilk is also very rich in phytoestrogens, which are redox-active isoflavone metabolites (Mahesha et al., 2007). In soymilk, these isoflavones are largely coupled to sugar moieties (Figure 38).

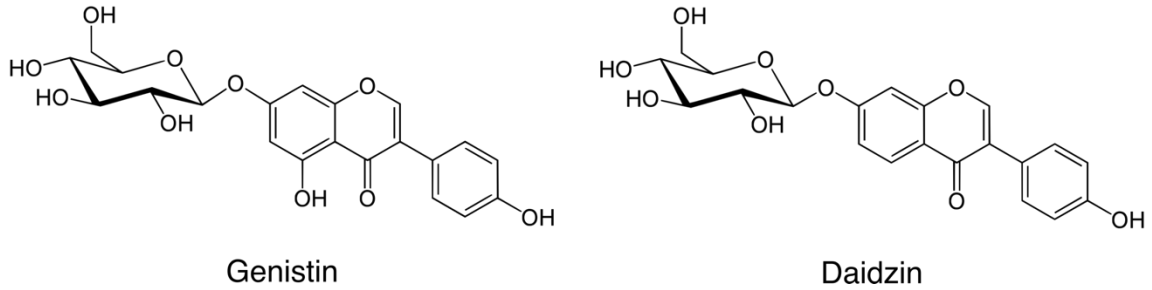

Figure 38. **Soymilk phytoestrogens.** Soymilk contains two dominant phytoestrogens, which are in the form of isoflavones coupled to sugar moieties. The difference between genistin (left) and daidzin (right) is the hydroxyl group on the first ring of the isoflavone.

To the redox-active metabolite trained eye, the structures of these molecules are very suggestive of pigments. The phenomenon of soymilk turning blue, is also reminiscent of chromogenic media, such as CHROMagar™ (Merlino et al., 1996). In these media, chromogens are covalently bonded to various sugars, which prevents them from absorbing light. When bacteria digest the sugars, acidify the medium, etc., the released chromogens attain their colors. It is plausible that soymilk acts as a chromogenic medium for a blue pigment, such as a modified isoflavone, and that *P. carnis* just so happens to be a bacterium that can liberate or convert the chromogen into its colorful form.

I was not able to take this side-project as far as I would have wanted to (though I have some more notes that I could share), but I think that it is in a good place for a starting-out graduate student, summer students, or part-time undergrads to take on. It has avenues into genomics, genetics, and basic bacterial physiology, which you could take as far as your curiosity goes. The strains are in our freezer, and I plan to send the spontaneous colorless mutant back to the Eisen lab in case they want to work with it. In addition to the biology itself, this project is a good opportunity for a fun inter-university collaboration.

BIBLIOGRAPHY

Abou-Jaoudé, A., Chippaux, M., Pascal, M.-C., 1979. Formate-nitrite reduction in *Escherichia coli* K12. Eur. J. Biochem. 95, 309–314. https://doi.org/10.1111/j.1432-1033.1979.tb12966.x

Andreani, N.A., Carraro, L., Martino, M.E., Fondi, M., Fasolato, L., Miotto, G., Magro, M., Vianello, F., Cardazzo, B., 2015. A genomic and transcriptomic approach to investigate the blue pigment phenotype in Pseudomonas fluorescens. Int. J. Food Microbiol., Special Issue: FoodMicro 2014, 24th International ICFMH Conference, From single cells to functions of consortia in food microbiology, 1 - 4 September, 2014, Nantes, France. 213, 88–98. https://doi.org/10.1016/j.ijfoodmicro.2015.05.024

Bankevich, A., Nurk, S., Antipov, D., Gurevich, A.A., Dvorkin, M., Kulikov, A.S., Lesin, V.M., Nikolenko, S.I., Pham, S., Prjibelski, A.D., Pyshkin, A.V., Sirotkin, A.V., Vyahhi, N., Tesler, G., Alekseyev, M.A., Pevzner, P.A., 2012. SPAdes: a new genome assembly algorithm and its applications to single-cell sequencing. J. Comput. Biol. 19, 455–477. https://doi.org/10.1089/cmb.2012.0021

Baron, S.S., Terranova, G., Rowe, J.J., 1989. Molecular mechanism of the antimicrobial action of pyocyanin. Curr. Microbiol. 18, 223–230. https://doi.org/10.1007/BF01570296

Bergkessel, M., 2021. Bacterial transcription during growth arrest. Transcription 12, 232–249. https://doi.org/10.1080/21541264.2021.1968761

Bergkessel, M., Basta, D.W., Newman, D.K., 2016. The physiology of growth arrest: uniting molecular and environmental microbiology. Nat. Rev. Microbiol. 14, 549–562. https://doi.org/10.1038/nrmicro.2016.107

Blankenfeldt, W., Parsons, J.F., 2014. The structural biology of phenazine biosynthesis. Curr. Opin. Struct. Biol. 29, 26–33. https://doi.org/10.1016/j.sbi.2014.08.013

Blasco, F., Iobbi, C., Ratouchniak, J., Bonnefoy, V., Chippaux, M., 1990. Nitrate reductases of *Escherichia coli*: sequence of the second nitrate reductase and comparison with that encoded by the narGHJI operon. Mol. Gen. Genet. MGG 222, 104–111. https://doi.org/10.1007/BF00283030

Boedicker, J.Q., Vincent, M.E., Ismagilov, R.F., 2009. Microfluidic confinement of single cells of bacteria in small volumes initiates high-density behavior of quorum sensing and growth and reveals its variability. Angew. Chem. Int. Ed. 48, 5908–5911. https://doi.org/10.1002/anie.200901550

Boetius, A., Ravenschlag, K., Schubert, C.J., Rickert, D., Widdel, F., Gieseke, A., Amann, R., Jørgensen, B.B., Witte, U., Pfannkuche, O., 2000. A marine microbial consortium apparently mediating anaerobic oxidation of methane. Nature 407, 623–626. https://doi.org/10.1038/35036572

Bolger, A.M., Lohse, M., Usadel, B., 2014. Trimmomatic: a flexible trimmer for Illumina sequence data. Bioinformatics 30, 2114–2120. https://doi.org/10.1093/bioinformatics/btu170

Borenshtein, D., Schauer, D.B., 2006. The Genus Citrobacter, in: Dworkin, M., Falkow, S., Rosenberg, E., Schleifer, K.-H., Stackebrandt, E. (Eds.), The Prokaryotes. Springer New York, New York, NY, pp. 90–98. https://doi.org/10.1007/0-387-30746-X_5

Bosi, E., Donati, B., Galardini, M., Brunetti, S., Sagot, M.-F., Lió, P., Crescenzi, P., Fani, R., Fondi, M., 2015. MeDuSa: a multi-draft based scaffolder. Bioinformatics 31, 2443–2451. https://doi.org/10.1093/bioinformatics/btv171

Brisbane, P.G., Janik, L.J., Tate, M.E., Warren, R.F., 1987. Revised structure for the phenazine antibiotic from Pseudomonas fluorescens 2-79 (NRRL B-15132). Antimicrob. Agents Chemother. 31, 1967–1971. https://doi.org/10.1128/AAC.31.12.1967

Brown, J., Pirrung, M., McCue, L.A., 2017. FQC Dashboard: integrates FastQC results into a web-based, interactive, and extensible FASTQ quality control tool. Bioinformatics 33, 3137–3139. https://doi.org/10.1093/bioinformatics/btx373

Chang, L., Wei, L.I., Audia, J.P., Morton, R.A., Schellhorn, H.E., 1999. Expression of the *Escherichia coli* NRZ nitrate reductase is highly growth phase dependent and is controlled by RpoS, the alternative vegetative sigma factor. Mol. Microbiol. 34, 756–766. https://doi.org/10.1046/j.1365-2958.1999.01637.x

Clark, D.P., 1989. The fermentation pathways of *Escherichia coli*. FEMS Microbiol. Rev. 5, 223–234. https://doi.org/10.1111/j.1574-6968.1989.tb03398.x

Coates, J.D., Cole, K.A., Chakraborty, R., O'Connor, S.M., Achenbach, L.A., 2002. Diversity and ubiquity of bacteria capable of utilizing humic substances as electron donors for anaerobic respiration. Appl. Environ. Microbiol. 68, 2445–2452. https://doi.org/10.1128/aem.68.5.2445-2452.2002

Dahlstrom, K.M., Newman, D.K., 2022. Soil bacteria protect fungi from phenazines by acting as toxin sponges. Curr. Biol. 32, 275-288.e5. https://doi.org/10.1016/j.cub.2021.11.002

Dar, D., Thomashow, L.S., Weller, D.M., Newman, D.K., 2020. Global landscape of phenazine biosynthesis and biodegradation reveals species-specific colonization patterns in agricultural soils and crop microbiomes. eLife 9, e59726. https://doi.org/10.7554/eLife.59726

Datsenko, K.A., Wanner, B.L., 2000. One-step inactivation of chromosomal genes in *Escherichia coli* K-12 using PCR products. Proc. Natl. Acad. Sci. 97, 6640–6645. https://doi.org/10.1073/pnas.120163297

De León, M.E., Wilson, H.S., Jospin, G., Eisen, J.A., 2021. Draft Genome Sequences and Genomic Analysis for Pigment Production in Bacteria Isolated from Blue Discolored Soymilk and Tofu. J. Genomics 9, 55–67. https://doi.org/10.7150/jgen.65500

Dietrich, L.E.P., Kiley, P.J., 2011. A shared mechanism of SoxR activation by redox-cycling compounds. Mol. Microbiol. 79, 1119–1122. https://doi.org/10.1111/j.1365-2958.2011.07552.x

Dietrich, L.E.P., Okegbe, C., Price-Whelan, A., Sakhtah, H., Hunter, R.C., Newman, D.K., 2013. Bacterial community morphogenesis is intimately linked to the intracellular redox state. J. Bacteriol. 195, 1371–1380. https://doi.org/10.1128/JB.02273-12

Dietrich, L.E.P., Price-Whelan, A., Petersen, A., Whiteley, M., Newman, D.K., 2006. The phenazine pyocyanin is a terminal signalling factor in the quorum sensing network of *Pseudomonas aeruginosa*. Mol. Microbiol. 61, 1308–1321. https://doi.org/10.1111/j.1365-2958.2006.05306.x

Edgar, R.C., 2004. MUSCLE: a multiple sequence alignment method with reduced time and space complexity. BMC Bioinformatics 5, 113. https://doi.org/10.1186/1471-2105-5-113

Eren, A.M., Esen, Ö.C., Quince, C., Vineis, J.H., Morrison, H.G., Sogin, M.L., Delmont, T.O., 2015. Anvi'o: an advanced analysis and visualization platform for 'omics data. PeerJ 3, e1319. https://doi.org/10.7717/peerj.1319

Flamholz, A.I., Dugan, E., Blikstad, C., Gleizer, S., Ben-Nissan, R., Amram, S., Antonovsky, N., Ravishankar, S., Noor, E., Bar-Even, A., Milo, R., Savage, D.F., 2020. Functional reconstitution of a bacterial CO2 concentrating mechanism in *Escherichia coli*. eLife 9, e59882. https://doi.org/10.7554/eLife.59882

Friedheim, E., Michaelis, L., 1931. Potentiometric study of pyocyanine. J. Biol. Chem. 91, 355–368. https://doi.org/10.1016/S0021-9258(18)76619-2

Gale, E.F. (Ernest F., 1951. The chemical activities of bacteria. New York, Academic Press.

Glasser, N.R., Kern, S.E., Newman, D.K., 2014. Phenazine redox cycling enhances anaerobic survival in *P seudomonas aeruginosa* by facilitating generation of ATP and a proton-motive force: Phenazines facilitate energy generation. Mol. Microbiol. 92, 399–412. https://doi.org/10.1111/mmi.12566

Goris, J., Konstantinidis, K.T., Klappenbach, J.A., Coenye, T., Vandamme, P., Tiedje, J.M., 2007. DNA-DNA hybridization values and their relationship to whole-genome sequence similarities. Int. J. Syst. Evol. Microbiol. 57, 81–91. https://doi.org/10.1099/ijs.0.64483-0

Gu, M., Imlay, J.A., 2011. The SoxRS response of *Escherichia coli* is directly activated by redox-cycling drugs rather than by superoxide. Mol. Microbiol. 79, 1136–1150. https://doi.org/10.1111/j.1365-2958.2010.07520.x

Gurevich, A., Saveliev, V., Vyahhi, N., Tesler, G., 2013. QUAST: quality assessment tool for genome assemblies. Bioinformatics 29, 1072–1075. https://doi.org/10.1093/bioinformatics/btt086

Haft, D.H., DiCuccio, M., Badretdin, A., Brover, V., Chetvernin, V., O'Neill, K., Li, W., Chitsaz, F., Derbyshire, M.K., Gonzales, N.R., Gwadz, M., Lu, F., Marchler, G.H., Song, J.S., Thanki, N., Yamashita, R.A., Zheng, C., Thibaud-Nissen, F., Geer, L.Y., Marchler-Bauer, A., Pruitt, K.D., 2018. RefSeq: an update on prokaryotic genome annotation and curation. Nucleic Acids Res. 46, D851–D860. https://doi.org/10.1093/nar/gkx1068

Harrington, T.D., Tran, V.N., Mohamed, A., Renslow, R., Biria, S., Orfe, L., Call, D.R., Beyenal, H., 2015. The mechanism of neutral red-mediated microbial electrosynthesis in *Escherichia coli*: menaquinone reduction. Bioresour. Technol. 192, 689–695. https://doi.org/10.1016/j.biortech.2015.06.037

Hernandez, M.E., Kappler, A., Newman, D.K., 2004. Phenazines and other redox-active antibiotics promote microbial mineral reduction. Appl. Environ. Microbiol. 70, 921–928. https://doi.org/10.1128/AEM.70.2.921-928.2004

Heumann, W., Young, D., Gottlich, C., 1968. Leucoindigoidine formation by an Arthrobacter species and its oxidation to indigoidine by other micro-organisms. Biochim. Biophys. Acta BBA - Gen. Subj. 156, 429–431. https://doi.org/10.1016/0304-4165(68)90280-8

Johnson, M., Zaretskaya, I., Raytselis, Y., Merezhuk, Y., McGinnis, S., Madden, T.L., 2008. NCBI BLAST: a better web interface. Nucleic Acids Res. 36, W5–W9. https://doi.org/10.1093/nar/gkn201

Koren, S., Walenz, B.P., Berlin, K., Miller, J.R., Bergman, N.H., Phillippy, A.M., 2017. Canu: scalable and accurate long-read assembly via adaptive k-mer weighting and repeat separation. Genome Res. 27, 722–736. https://doi.org/10.1101/gr.215087.116

Kuenen, J.G., 2008. Anammox bacteria: from discovery to application. Nat. Rev. Microbiol. 6, 320–326. https://doi.org/10.1038/nrmicro1857

Kurtz, S., Phillippy, A., Delcher, A.L., Smoot, M., Shumway, M., Antonescu, C., Salzberg, S.L., 2004. Versatile and open software for comparing large genomes. Genome Biol. 5, R12. https://doi.org/10.1186/gb-2004-5-2-r12

Li, B., Tian, C., Zhang, D., Pan, X., 2014. Anaerobic Nitrate-Dependent Iron (II) Oxidation by a Novel Autotrophic Bacterium, *Citrobacter freundii* Strain PXL1. Geomicrobiol. J. 31, 138–144. https://doi.org/10.1080/01490451.2013.816393

Lin, E.C.C., Iuchi, S., 1991. Regulation of gene expression in fermentative and respiratory systems in *Escherichia coli* and related bacteria. Annu. Rev. Genet. 25, 361–387. https://doi.org/10.1146/annurev.ge.25.120191.002045

Louca, S., Mazel, F., Doebeli, M., Parfrey, L.W., 2019. A census-based estimate of Earth's bacterial and archaeal diversity. PLOS Biol. 17, e3000106. https://doi.org/10.1371/journal.pbio.3000106

Lovley, D.R., Fraga, J.L., Coates, J.D., Blunt-Harris, E.L., 1999. Humics as an electron donor for anaerobic respiration. Environ. Microbiol. 1, 89–98. https://doi.org/10.1046/j.1462-2920.1999.00009.x

Mahesha, H.G., Singh, S.A., Rao, A.G.A., 2007. Inhibition of lipoxygenase by soy isoflavones: Evidence of isoflavones as redox inhibitors. Arch. Biochem. Biophys. 461, 176–185. https://doi.org/10.1016/j.abb.2007.02.013

Mathee, K., 2018. Forensic investigation into the origin of *Pseudomonas aeruginosa* PA14 — old but not lost. J. Med. Microbiol. 67, 1019–1021. https://doi.org/10.1099/jmm.0.000778

McRose, D.L., Newman, D.K., 2021. Redox-active antibiotics enhance phosphorus bioavailability. Science 371, 1033–1037. https://doi.org/10.1126/science.abd1515

Meirelles, L.A., Newman, D.K., 2018. Both toxic and beneficial effects of pyocyanin contribute to the lifecycle of *Pseudomonas aeruginosa*. Mol. Microbiol. 110, 995–1010. https://doi.org/10.1111/mmi.14132

Meirelles, L.A., Perry, E.K., Bergkessel, M., Newman, D.K., 2021. Bacterial defenses against a natural antibiotic promote collateral resilience to clinical antibiotics. PLOS Biol. 19, e3001093. https://doi.org/10.1371/journal.pbio.3001093

Merlino, J., Siarakas, S., Robertson, G.J., Funnell, G.R., Gottlieb, T., Bradbury, R., 1996. Evaluation of CHROMagar Orientation for differentiation and presumptive identification of gram-negative bacilli and Enterococcus species. J. Clin. Microbiol. 34, 1788–1793. https://doi.org/10.1128/jcm.34.7.1788-1793.1996

Miller, M.A., Pfeiffer, W., Schwartz, T., 2010. Creating the CIPRES Science Gateway for inference of large phylogenetic trees, in: 2010 Gateway Computing Environments Workshop (GCE). Presented at the 2010 Gateway Computing Environments Workshop (GCE), IEEE, pp. 1–8. https://doi.org/10.1109/GCE.2010.5676129

Miranda, K.M., Espey, M.G., Wink, D.A., 2001. A rapid, simple spectrophotometric method for simultaneous detection of nitrate and nitrite. Nitric Oxide 5, 62–71. https://doi.org/10.1006/niox.2000.0319

Morello, J.E., Pierson, E.A., Pierson, L.S., 2004. Negative cross-communication among wheat rhizosphere bacteria: effect on antibiotic production by the biological control bacterium pseudomonas aureofaciens 30-84. Appl. Environ. Microbiol. 70, 3103–3109. https://doi.org/10.1128/AEM.70.5.3103-3109.2004

Nitzschke, A., Bettenbrock, K., 2018. All three quinone species play distinct roles in ensuring optimal growth under aerobic and fermentative conditions in *E. coli* K12. Plos One 13, e0194699. https://doi.org/10.1371/journal.pone.0194699

O'Malley, M.A., Walsh, D.A., 2021. Rethinking microbial infallibility in the metagenomics era. FEMS Microbiol. Ecol. 97, fiab092. https://doi.org/10.1093/femsec/fiab092

Page, R., Peti, W., 2016. Toxin-antitoxin systems in bacterial growth arrest and persistence. Nat. Chem. Biol. 12, 208–214. https://doi.org/10.1038/nchembio.2044

Popov, F.A., Kozlova, L.M., Noskova, E.N., 2018. Improving of oat cultivation technology under conditions of Kirov region. Agrar. Nauka Evro-Sev.-Vostoka 63, 64–68. https://doi.org/10.30766/2072-9081.2018.63.2.64-68

Price-Whelan, A.M., 2009. Physiology and mechanisms of pyocyanin reduction in *Pseudomonas aeruginosa*. California Institute of Technology.

Remali, J., Sarmin, N. 'Izzah M., Ng, C.L., Tiong, J.J.L., Aizat, W.M., Keong, L.K., Zin, N.M., 2017. Genomic characterization of a new endophytic *Streptomyces kebangsaanensis* identifies biosynthetic pathway gene clusters for novel phenazine antibiotic production. PeerJ 5, e3738. https://doi.org/10.7717/peerj.3738

Ribeiro, T.G., Gonçalves, B.R., da Silva, M.S., Novais, Â., Machado, E., Carriço, J.A., Peixe, L., 2017. *Citrobacter portucalensis* sp. nov., isolated from an aquatic sample. Int. J. Syst. Evol. Microbiol. 67, 3513–3517. https://doi.org/10.1099/ijsem.0.002154

Richter, M., Rosselló-Móra, R., 2009. Shifting the genomic gold standard for the prokaryotic species definition. Proc. Natl. Acad. Sci. U. S. A. 106, 19126–19131. https://doi.org/10.1073/pnas.0906412106

Richter, M., Rosselló-Móra, R., Oliver Glöckner, F., Peplies, J., 2016. JSpeciesWS: a web server for prokaryotic species circumscription based on pairwise genome comparison. Bioinformatics 32, 929–931. https://doi.org/10.1093/bioinformatics/btv681

Ronquist, F., Huelsenbeck, J.P., 2003. MrBayes 3: Bayesian phylogenetic inference under mixed models. Bioinformatics 19, 1572–1574. https://doi.org/10.1093/bioinformatics/btg180

Rothberger, C., 1898. Differential diagnostische Untersuchungen mit gefarbten Nahrboden. Cent. Für Bakteriol. Parasitenkd. Infekt. 24, 513–518.

Saunders, S.H., 2020. Mechanisms of phenazine-mediated extracellular electron transfer by *Pseudomonas aeruginosa* (PhD). California Institute of Technology. https://doi.org/10.7907/P4Z5-5445

Saunders, S.H., Tse, E.C.M., Yates, M.D., Otero, F.J., Trammell, S.A., Stemp, E.D.A., Barton, J.K., Tender, L.M., Newman, D.K., 2020. Extracellular DNA promotes efficient extracellular electron transfer by pyocyanin in *Pseudomonas aeruginosa* biofilms. Cell 182, 919-932.e19. https://doi.org/10.1016/j.cell.2020.07.006

Schmidt, T.M., Arieli, B., Cohen, Y., Padan, E., Strohl, W.R., 1987. Sulfur metabolism in *Beggiatoa alba*. J. Bacteriol. 169, 5466–5472. https://doi.org/10.1128/jb.169.12.5466-5472.1987

Sharma, P., Teixeira de Mattos, M.J., Hellingwerf, K.J., Bekker, M., 2012. On the function of the various quinone species in *Escherichia coli*. FEBS J. 279, 3364–3373. https://doi.org/10.1111/j.1742-4658.2012.08608.x

Sparacino-Watkins, C., Stolz, J.F., Basu, P., 2014. Nitrate and periplasmic nitrate reductases. Chem. Soc. Rev. 43, 676–706. https://doi.org/10.1039/c3cs60249d

Strous, M., Fuerst, J.A., Kramer, E.H.M., Logemann, S., Muyzer, G., van de Pas-Schoonen, K.T., Webb, R., Kuenen, J.G., Jetten, M.S.M., 1999. Missing lithotroph identified as new planctomycete. Nature 400, 446–449. https://doi.org/10.1038/22749

Sullivan, N.L., Tzeranis, D.S., Wang, Y., So, P.T.C., Newman, D., 2011. Quantifying the dynamics of bacterial secondary metabolites by spectral multiphoton microscopy. ACS Chem. Biol. 6, 893–899. https://doi.org/10.1021/cb200094w

Tatusova, T., DiCuccio, M., Badretdin, A., Chetvernin, V., Nawrocki, E.P., Zaslavsky, L., Lomsadze, A., Pruitt, K.D., Borodovsky, M., Ostell, J., 2016. NCBI prokaryotic genome annotation pipeline. Nucleic Acids Res. 44, 6614–6624. https://doi.org/10.1093/nar/gkw569

Teal, T.K., Lies, D.P., Wold, B.J., Newman, D.K., 2006. Spatiometabolic stratification of *Shewanella oneidensis* biofilms. Appl. Environ. Microbiol. 72, 7324–7330. https://doi.org/10.1128/AEM.01163-06

Teeling, H., Meyerdierks, A., Bauer, M., Amann, R., Glöckner, F.O., 2004. Application of tetranucleotide frequencies for the assignment of genomic fragments. Environ. Microbiol. 6, 938–947. https://doi.org/10.1111/j.1462-2920.2004.00624.x

Thauer, R.K., Jungermann, K., Decker, K., 1977. Energy conservation in chemotrophic anaerobic bacteria. Bacteriol. Rev. 41, 100–180.

Thomashow, L.S., 2013. Phenazines in the environment: microbes, habitats, and ecological relevance, in: Chincholkar, S., Thomashow, L. (Eds.), Microbial Phenazines: Biosynthesis, Agriculture and Health. Springer, Berlin, Heidelberg, pp. 199–216. https://doi.org/10.1007/978-3-642-40573-0_10

Thomashow, L.S., Weller, D.M., 1988. Role of a phenazine antibiotic from *Pseudomonas fluorescens* in biological control of Gaeumannomyces graminis var. tritici. J. Bacteriol. 170, 3499–3508. https://doi.org/10.1128/jb.170.8.3499-3508.1988

Tong, M., French, S., El Zahed, S.S., Ong, W. kit, Karp, P.D., Brown, E.D., 2020. Gene dispensability in *Escherichia coli* grown in thirty different carbon environments. mBio 11, e02259-20. https://doi.org/10.1128/mBio.02259-20

Tsypin, L.M., Bar-On, Y., Saunders, S.H., Leadbetter, J.R., Newman, D., 2020a. Phenzine oxidizer enrichment and isolation. protocols.io. http://dx.doi.org/10.17504/protocols.io.bh4tj8wn

Tsypin, L.M., Newman, D.K., 2021. Nitrate reduction stimulates and is stimulated by phenazine-1-carboxylic acid oxidation by *Citrobacter portucalensis* MBL. mBio 12, e02265-21. https://doi.org/10.1128/mBio.02265-21

Tsypin, L.M., Saunders, S.H., Bar-On, Y., Leadbetter, J.R., Newman, D.K., 2020b. Draft genome sequence of the redox-active enteric bacterium *Citrobacter portucalensis* strain MBL. Microbiol. Resour. Announc. 9, e00695-20. https://doi.org/10.1128/MRA.00695-20

Unden, G., Bongaerts, J., 1997. Alternative respiratory pathways of *Escherichia coli*: energetics and transcriptional regulation in response to electron acceptors. Biochim. Biophys. Acta BBA - Bioenerg. 1320, 217–234. https://doi.org/10.1016/S0005-2728(97)00034-0

Unden, G., Cole, S.T., 1983. Studies on the relatedness of bacterial fumarate reductases. FEMS Microbiol. Lett. 20, 181–185. https://doi.org/10.1111/j.1574-6968.1983.tb00113.x

Wang, Y., Kern, S.E., Newman, D.K., 2010. Endogenous Phenazine Antibiotics Promote Anaerobic Survival of *Pseudomonas aeruginosa* via Extracellular Electron Transfer. J. Bacteriol. 192, 365–369. https://doi.org/10.1128/JB.01188-09

Wang, Y., Newman, D.K., 2008. Redox reactions of phenazine antibiotics with ferric (hydr)oxides and molecular oxygen. Environ. Sci. Technol. 42, 2380–2386. https://doi.org/10.1021/es702290a

Wang, Y., Wilks, J.C., Danhorn, T., Ramos, I., Croal, L., Newman, D.K., 2011. Phenazine-1-carboxylic acid promotes bacterial biofilm development via ferrous iron acquisition. J. Bacteriol. 193, 3606–3617. https://doi.org/10.1128/JB.00396-11

Wannier, T.M., Nyerges, A., Kuchwara, H.M., Czikkely, M., Balogh, D., Filsinger, G.T., Borders, N.C., Gregg, C.J., Lajoie, M.J., Rios, X., Pál, C., Church, G.M., 2020. Improved bacterial recombineering by parallelized protein discovery. Proc. Natl. Acad. Sci. 117, 13689–13698. https://doi.org/10.1073/pnas.2001588117

Wilson, K., 2001. Preparation of genomic dna from bacteria. Curr. Protoc. Mol. Biol. 56, 2.4.1-2.4.5. https://doi.org/10.1002/0471142727.mb0204s56

Wissenbach, U., Kröger, A., Unden, G., 1990. The specific functions of menaquinone and demethylmenaquinone in anaerobic respiration with fumarate, dimethylsulfoxide, trimethylamine N-oxide and nitrate by *Escherichia coli*. Arch. Microbiol. 154, 60–66. https://doi.org/10.1007/BF00249179

Wolfe, A.J., 2005. The acetate switch. Microbiol. Mol. Biol. Rev. 69, 12–50. https://doi.org/10.1128/MMBR.69.1.12-50.2005

Yu, H., Leadbetter, J.R., 2020. Bacterial chemolithoautotrophy via manganese oxidation. Nature 583, 453–458. https://doi.org/10.1038/s41586-020-2468-5

Zhang, Z., Wang, Jianing, Wang, Jinlan, Wang, Jingjing, Li, Y., 2020. Estimate of the sequenced proportion of the global prokaryotic genome. Microbiome 8, 134. https://doi.org/10.1186/s40168-020-00903-z